

RHEOLOGICAL CHARACTERIZATION OF CHARGED
POLYACRYLAMIDES USED IN FRACTURING FLUIDS
WITH EMPHASIS ON SHALE – POLYACRYLAMIDE
INTERACTION

By

SAMYUKTA KOTEESWARAN

Bachelor of Technology in Chemical Engineering

Anna University

Chennai, Tamil Nadu, India

2008 – 2012

Submitted to the Faculty of Graduate College

of Oklahoma State University

in partial fulfillment of the requirements

for the degree of

DOCTOR OF PHILOSOPHY

March 2017

RHEOLOGICAL CHARACTERIZATION OF CHARGED
POLYACRYLAMIDES USED IN FRACTURING FLUIDS
WITH EMPHASIS ON SHALE – POLYACRYLAMIDE
INTERACTION

Dissertation Approved

Dr. Peter E. Clark

Dissertation Advisor

Dr. Jack C. Pashin

Dr. Geir Hareland

Dr. Clint P. Aichele

ACKNOWLEDGEMENTS

First and foremost, I want to thank my advisor Dr. Peter E. Clark, for his continuous support in the last 5 years. He has helped me mold my research and guide me in the right direction and for ensuring that I was funded during the duration of the program. His encouragement and support helped me gain holistic development here in Oklahoma State University.

I thank all my committee members Dr. Jack C. Pashin, Dr. Clint P. Aichele and Dr. Geir Hareland for their time and effort. I take this opportunity to thank Dr. Pashin and Dr. Jim Puckette for helping me obtain shale samples, mineralogy data for shale samples, help me analyze and interpret results and all other technical support. A big thank you to Department of Chemical engineering, HOD Dr. Rob Whiteley, Dr. Sundarajan V. Madihally and Dr. Heather Fahlenkamp, all the staff in our department, a special thanks to Ms. Eileen Nelson, Ms. Shelley Taylor, Ms. Carolyn Sanders, Ms. Shelley Potter and Ms. Paula Kendrick. The immense support and encouragement that I have received from Dr. R. Russell Rhinehart as the OSU Automation society advisor, as my mentor, professor has created a great impact in my graduate student life. I thank Dr. Rhinehart for all his time and encouragement that helped me in my career here in OSU. I would like to thank all my TA professor Dr. Martin High, Dr. Clint P. Aichele, Dr. R. Rhinehart, Mr. Mike Resatarits, Dr. Seok-Jhin Kim, Dr. Jindal Shah for believing in me and it was great pleasure working for them. It was a great learning experience for me.

I thank my parents K. Koteeswaran and S. Devika without whom any of this would not have been possible. I am grateful for the things that they have sacrificed to help me in chasing my dreams. My little sister Deekshi, for being a great companion in this journey. My grandparents, my cousins Nive, Shyam, Akash, my uncles and aunties who did their part in helping me finish my work here.

A special mention to my friend Yuvaraj who has been nothing less than my motivation, my strength and my pillar of support. My OSU friends Suresh, Ashwin, Minu, Bharat, Sandeep, Anand, Upasana, Viji, Alden, Brett, Trey, Swapneel for making my stay memorable, fun and lot of other technical support.

Last but not the least, I would like to say a big thanks to Ram Kumar, who has been by biggest support this entire time, my critic, my wall who keeps pushing me to pursue greater endeavors even the ones not within my reach. Thanks Ram for trusting me, understanding me and being there for me always.

Acknowledgements reflect the views of the author and are not endorsed by committee members of Oklahoma State University

Name: Samyukta Koteeswaran

Date of Degree: March 2017

Title of Study: RHEOLOGICAL CHARACTERIZATION OF CHARGED
POLYACRYLAMIDES USED IN FRACTURING FLUIDS WITH EMPHASIS ON SHALE –
POLYACRYLAMIDE INTERACTION

Major Field: Chemical Engineering

Abstract:

Interaction of polymer containing injected fluids with shale is a widely studied phenomenon, but much is still unknown about the interaction of charged polyacrylamides such as anionic and cationic polyacrylamides with shale. The nature of interaction of charged polyacrylamides with shale is not well understood, especially from the perspective of assessing the potential for polyacrylamides to cause formation damage. Zeta potential and rheological measurements were made for Chattanooga and Pride Mountain shales suspended in polyacrylamide solutions with and without inorganic salts and tetramethyl ammonium chloride (TMAC). The change in zeta potential and viscosity with time is recorded. The magnitude of decrease in the absolute value of zeta potential with time is indicative of adsorption of polymer on the surface of shale and serves as a measure of the extent of polymer interaction with shale. The salts that were used in this study are potassium chloride (KCl), sodium chloride (NaCl). This study quantifies the interaction of anionic and cationic polyacrylamide with different shales from North American region. From the experimental results, it was determined that the polyacrylamides interact strongly with shale particularly the cationic polyacrylamide. The objective of this study was to determine the extent of interaction of anionic and cationic polyacrylamide with each shale sample in the presence of additives such as salts. Additionally, this work presents qualitative techniques for evaluating shale-fluid interaction. A simple desktop test method, such as immersion testing, can help production engineers choose the appropriate shale inhibitors such as salt, Tetramethyl ammonium chloride and polymers that can effectively reduce the impact of oilfield fluids invading shale and causing it to swell or disperse. The swelling tendency of shale is highly dependent on clay mineralogy and other properties, such as porosity and permeability. A series of immersions tests was performed to study the combined and isolated effects of salt, TMAC, and polyacrylamide on preventing shale from becoming unstable. The merit of each fluid system in shale inhibition is probed for Woodford, Chattanooga and Pride Mountain shale. Rheology of bentonite slurries are studied with different salts and TMAC to probe their efficiency in preventing the swelling of bentonite clay.

TABLE OF CONTENTS

CHAPTER I.....	1
1. Introduction.....	1
1.1 Shale-fluid interaction mechanism.....	2
1.1.1 Darcy Flow.....	2
1.1.2 Diffusive flow	2
1.1.3 Osmotic flow.....	4
1.2 Shale Stability in presence of additives.....	6
1.2.1 Salts.....	6
1.2.2 Synthetic Polymers	7
1.3 Research Objectives	8
1.3.1 Rheological characterize shale-fluid interaction.....	8
1.3.2 Semi – Quantify shale-fluid interaction using zeta potential tests.....	8
1.3.3 Use simple methods such as immersion tests and correlate test results with rheological studies	9
1.4 Structure of dissertation	9
CHAPTER II.....	11
2. Quantitative Characterization of Polyacrylamide-Shale Interaction under Various Saline Conditions	11
2.1 Introduction	11

2.2	Materials and Methods	15
2.2.1	Polyacrylamides	15
2.2.2	Shale Samples	15
2.2.3	Sample Information	16
2.2.4	Characterization of shale.....	16
2.2.5	Equipment	17
2.2.6	Zeta Potential Analyzer.....	19
2.2.7	Analysis.....	21
2.3	Results and Discussion.....	23
2.3.1	Characterizing polymer-shale interaction through zeta potential measurements.....	23
2.3.2	Rheological Study of Polymer-Shale Interaction	34
CHAPTER III		39
3.	Characterization of Shale-Fluid Interaction through a Series of Immersion Tests and Rheological Studies	39
3.1	Introduction	39
3.2	Materials and Methods	42
3.2.1	Experimental Methods	42
3.2.2	Shale Samples	42
3.2.3	Shale Characterization	43

3.3	Formulation of Fluid Phase	47
3.3.1	Fluid Design.....	47
3.3.2	Equipment.....	48
3.3.3	Immersion Tests.....	49
3.4	Results and Discussion.....	49
3.4.1	Rheological Studies	63
CHAPTER IV		67
4.	Studying the Effect of Stripping Lighter Hydrocarbons from Shale Oil by Probing the Rheology of a Model Oil System.....	67
4.1	Introduction	67
4.2	Materials and Methods	71
4.2.1	Rheometer	71
4.2.2	Rheometer Geometry	72
4.2.3	Rheological measurements	73
4.2.4	Microscopy	73
4.3	Results and Discussion.....	74
4.3.1	Yield stress measurements.....	74
4.3.2	Small Amplitude Oscillatory Measurements	77
4.3.3	Creep and recovery of gels with varying cooling rates.....	84

4.3.4	Effect of cooling rate on morphology and particle size distribution of wax crystal	87
4.3.5	Effect of lighter hydrocarbons on WAT and total volume fraction of wax-oil system	89
Chapter V		94
5.	Conclusion and Recommendations	94
5.1	Quantitative Characterization of Polyacrylamide – Shale Interaction	94
5.2	Characterization of Shale-Fluid Interaction through a Series of Immersion Tests and Rheological Studies.....	95
5.3	Studying the Effect of Stripping Lighter Hydrocarbons from Shale Oil	96
5.4	Recommendations for Future Work.....	96
6.	REFERENCE.....	98

LIST OF TABLES

Table 1: Whole rock mineralogy of shale samples determined by XRD	17
Table 2: TOC, effective porosity and pressure decay permeability.....	17
Table 3: Compositions of different suspension media used in the study.....	21
Table 4: Shale characterization methods	43
Table 5: Whole rock mineralogy of shale samples from different formations	44
Table 6: TOC, Effective Porosity, Pressure decay permeability and % Water Saturation	45
Table 7: Composition of different fluid mixture used in the study.....	48
Table 8: Qualitative description of Woodford shale samples after immersion tests	57
Table 9: Qualitative description of Chattanooga shale samples after immersion tests.....	59
Table 10: Qualitative description of Pride Mountain Formation shale samples after immersion tests	60
Table 11: Application of KCl based fluids for the shales under study	61
Table 12: Application of NaCl based fluids for studied shale formations.....	62
Table 13: Application of TMAC-based fluids for the studied shale samples.....	62
Table 14: WAT for all the model oil samples used	71
Table 15: Pour point of all the wax - model oil samples used.....	79
Table 16: WAT measured as an effect of solvent concentration	92

LIST OF FIGURES

Figure 1: Schematic representation of downhole forces acting on a shale system (Van Oort, 2003).....	3
Figure 2: Schematic representation of an osmotic pressure cell (Talal M. Al-Bazali, 2011)...	6
Figure 3: Schematic representation of polymer interaction with clay (Lu, 1988)	7
Figure 4: (a) DHR-3 Rheometer (b) Vane Geometry (c) Cone and plate geometry.....	19
Figure 5: Histogram of particle size distribution of shale particles used in the study	20
Figure 6: Carreau Model logarithmic fit for viscosity vs. shear rate.....	35
Figure 7: Change in Zeta Potential of shales in cationic polyacrylamide with salts and TMAC	37
Figure 8: Change in Zeta Potential of shales in anionic polyacrylamide with salts and TMAC.....	25
Figure 9: Zeta potential vs. time for anionic polyacrylamide	26
Figure 11: Zeta potential of Chattanooga shale incubated w/ anionic polyacrylamide under various conditions	28
Figure 12: Zeta potential of Chattanooga shale incubated w/ cationic polyacrylamide under various conditions.....	28
Figure 13: Zeta potential of Pride Mountain shale incubated w/ anionic polyacrylamide under various conditions	29

Figure 14: Zeta potential of Pride Mountain shale incubated w/ cationic polyacrylamide under various conditions	29
Figure 15: Increase in zeta potential for shale in anionic polyacrylamide with salt and TMAC	32
Figure 16: Flocculation of Pride Mountain shale in presence of cationic polyacrylamide measured by dynamic light scattering.....	33
Figure 17: C* and C** for anionic polyacrylamide.....	35
Figure 18: C* and C** for cationic polyacrylamide.....	35
Figure 19: Change in zero shear rate viscosity with increasing anionic polyacrylamide concentration for Chattanooga and Pride Mountain shale	36
Figure 20: Change in zero shear rate viscosity with time of Chattanooga and Pride Mountain shale in anionic polyacrylamide	38
Figure 21: SEM images of Woodford Shale in Rother (10372.1 ft). Images A and B contain abundant randomly oriented clay platelets.....	46
Figure 22: SEM images of pyrite in the Gorgas #1 well, Pride Mountain Formation (2864.4 ft) (A) Poorly aligned and folded clay platelets. (B) Clusters of pyrite crystals forming of spherical to oblate framboids.....	46
Figure 23: SEM images of Chattanooga Shale in Lamb 1 - 3 #1 well (9173.5 ft). (A) Randomly oriented clay platelets (B) Pyrite framboids in matrix of platy illite	47
Figure 24: Percent expansion or shrinkage of Woodford Shale after immersion test	51

Figure 25: Percent expansion or shrinkage of Woodford Shale after immersion test	51
Figure 26: Percent expansion or shrinkage of Woodford Shale after immersion test	52
Figure 27: Percent weight gain of Woodford Shale after immersion test.....	52
Figure 28: Percent weight gain of Woodford Shale after immersion test.....	53
Figure 29: Percent weight gain of Woodford Shale after immersion test.....	53
Figure 30: Surface of Woodford shale immersed in Bentonite + NaCl + Anionic Polyacrylamide.....	55
Figure 31: Surface of Woodford shale immersed in Bentonite + TMAC + Cationic Polyacrylamide.....	55
Figure 32: Surface of Woodford shale immersed in Bentonite + KCl + Cationic Polyacrylamide.....	55
Figure 33: Surface of Woodford shale immersed in Bentonite + NaCl + Cationic Polyacrylamide.....	55
Figure 34: Percent weight gain of Chattanooga shale after immersion test	58
Figure 35: Percent weight gain or loss of Chattanooga shale after immersion test	58
Figure 36: Percent weight gain of Pride Mountain Formation shale after immersion test	59
Figure 37: Percent weight gain of Pride Mountain Formation shale after immersion test	60
Figure 38: Change in apparent viscosity of an anionic polyacrylamide system with shear rate.....	64

Figure 39: Change in apparent viscosity of a cationic polyacrylamide system with shear rate.....	64
Figure 40: Change in zero shear-rate viscosity of a bentonite salt system with shear rate.....	65
Figure 41: DHR-3 Rheometer.....	72
Figure 41:(a) Vane geometry (b) Bob geometry.....	87
Figure 43: Olympus microscope and the linkam stage.....	74
Figure 44: Static yield stress and dynamic yield stress measured using stress sweep experiment.....	75
Figure 45: Effect of cooling rate on yield stress of (a) straight chain alkanes (b) cyclic alkane	77
Figure 46: G' and G'' change with temperature.....	78
Figure 47: Storage Modulus vs. Oscillation stress for different cooling rate (a) wax in model oil system (b) wax in model oil with solvent hexane (c) wax in model oil with solvent pentane (c) wax in model oil with solvent heptane	81
Figure 48: Storage modulus as a function of time for different cooling rates for wax in model oil system with heptane in solvent.....	82
Figure 49: The storage modulus as a function of oscillation strain showing the LVR for wax model oil system at 10 °C and 20 °C	83
Figure 50: (a) Storage modulus vs. oscillation strain at different temperatures (b) Loss modulus vs. oscillation strain at different temperatures	84

Figure 51: Creep and recovery experiments at various cooling rates for (a) wax in model oil (b) wax in model oil with hexane in solvent.....	86
Figure 52: Images of wax crystal is in wax model oil system at 5 C after cooling at different rates (a) 0.5 °C/min (b) 1 °C/min (c) 2.5 °C/min (d) 5 °C/min.....	88
Figure 53: Particle size distribution at different cooling rates for wax in model oil system at 5 °C	89
Figure 54: Volume fraction vs. the shear stress for wax in model oil system with different solvents	90
Figure 55: Effect of solvent concentration on WAT	92
Figure 56: Average particle size for the wax in model oil in presence of solvents measured at different cooling rates.	93

CHAPTER I

1. Introduction

Recent developments in horizontal drilling and hydraulic fracturing have increased the production of shale oil and shale gas to record highs. These technologies have been modified and improved over the years that now with increased area of contact with shale reservoirs have led to an increase in production due and more economic. Shales make up over 75% of the drilled formations and over 70% of the wellbore instability problems are caused by shales (Lal, 1999). The reason for this is shales are rich in clays and are relatively weak rock. Shale is a fine-grained sedimentary rock, rich in clay minerals and with low permeability. During hydraulic fracturing, the shale is in continuous contact with water-based fluids such as fracturing, drilling, completion fluid and so on. The presence of reactive clays in the shale makes them prone to swelling and dispersion. Swelling is caused when the shale absorbs water from the contacting fluid between its clay layers and weakens the bonding between clay which leads to reduction in shale strength (Junhao Zhou, Jung, Pedlow, Chenevert, & Sharma, 2013). This causes an imbalance between the in-situ rock stresses and the rock strength as a hole is drilled, replacing shale with injection fluid. Common problems that lead to wellbore stability are fluid loss, lost circulation, tight hole, stuck pipe, borehole collapse, bit balling and so on (Labenski, Reid, & Santos, 2003).

Hence, it is important to study shale-fluid interactions in detail and quantify those interactions, to help us understand and regulate the use of appropriate additives in water based fluids.

1.1 Shale-fluid interaction mechanism

Many theories and methods have been studied in detail explaining shale-fluid interactions. Several interactions occur between the shale and the fluids. The common mechanisms of shale fluid interactions are

1.1.1 Darcy Flow

Convective Darcy flow is driven by hydraulic gradient, where the water is driven from the wellbore into the shale, when the wellbore pressure is greater than the shale pore pressure (Ewy & Stankovich, 2002; Van Oort, 2003).

1.1.2 Diffusive flow

In diffusive flow there is transfer of solutes from the fluid to the shale due to chemical potential gradient between the fluid and the shale and osmotic forces. The movement of solute can be from or to the shale and this direction is governed by the activity of the fluid the shale is in contact with. Fluids with higher activity drive the water out of the shale which leads to an increase in pore pressure. The ion movement between the shale and fluid is influenced by the cation exchange capacity of shale, relative concentration of ionic species such as K^+ , Na^+ , Ca^{2+} etc. in the fluid, interactions between the H_2O ions and clay. In studies done by (Van Oort, Hale, & Mody, 1995; van Oort, Hale, Mody, &

Roy, 1996), the proved that shale acts as leaky membrane as opposed to previous belief that shale acted as a perfect semi-permeable membrane.

In shales with low permeability diffusion is a more prominent and faster process than hydraulic flow (Van Oort, 2003). This diffusion is controlled by using additives commonly termed as ‘shale inhibitors’ that alters the membrane efficiency of shales. Inorganic salts such as potassium chloride (KCl) and sodium chloride (NaCl) are commonly used shale inhibitors. The ions from the fluid exchange with the more swellable ions at the clay sites thereby altering the swelling of shales. Contrary to the popular belief, there is swelling pressure always existent in shale and is not created by the fluid coming in contact with the shale (Van Oort, 2003). However, magnitude of the swelling pressure can be altered by the ion movements into the shale matrix. Van Oort presented a conceptual model of the forces acting on clay fabric as shown in Figure 1 (Van Oort, 2003)

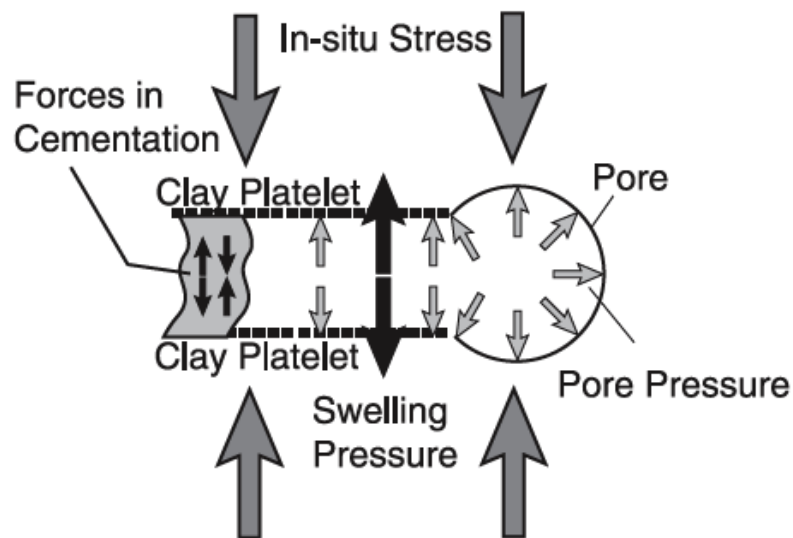


Figure 1: Schematic representation of downhole forces acting on a shale system (Van Oort, 2003)

The short-range forces that exist between the clay particles are Van der Waals attraction and Born repulsion. These repulsive forces between the charged particles are described by the DLVO theory. The DLVO theory states that the electrostatic forces between the clay particles in dispersion are assumed to be repulsive at all interparticle separations, yet state is aggregation is the most favorable and thermodynamically stable (McBride, 1997; Van Oss, Giese, & Costanzo, 1990). The balance between these forces has to be kept intact to maintain stability in the clay matrix (McBride, 1997; Van Oort, 2003). Swelling is caused when an ion with higher hydration radius causes repulsion between the clay platelets. Swelling can be reduced by incorporating less swellable K⁺ ions in the fluid, to exchange with the ions in shale. Even using shale inhibitors swelling can only be minimized and cannot be diminished completely.

1.1.3 Osmotic flow

When the water activity of the shale is higher than the surrounding fluid, the chemical potential difference will drive out the water from the shale. This method has been widely used for shale strengthening and as a way to prevent from shales swelling. But the concept of osmosis strictly applies only to ideal semi-permeable membrane where only water is allowed to flow from region of low salt concentration to high salt concentration, but since shale acts as a leaky membrane and lets solute pass through it acting as a non-ideal semi-permeable membrane, this non-ideality is expressed as membrane efficiency (Talal M. Al-Bazali, 2011).

$$\sigma = \frac{\Delta P}{\Delta \pi}$$

Where σ is the membrane efficiency, ΔP is pressure drop of the system and $\Delta\pi$ is the osmotic potential. Where $\Delta\pi$ can be found using the following equation

$$\Delta\pi = \left(\frac{RT}{V}\right) \ln\left(\frac{a_{w2}}{a_{w1}}\right)$$

Where R is the universal gas constant, T is the absolute temperature, v is the partial molar volume of water and a_w is the water activity. The water activity can be related to chemical potential using the following equation

$$\mu = \mu_{i0} + RT \ln a_i$$

Where μ_{i0} is the chemical potential of pure component at standard conditions.

For an ideal semi-permeable membrane, σ will be 1. Values less than 1 indicate the extent to which solutes can pass through the membrane. Experimentally measured σ values for shale are in the range of 0.03 to 0.1. The water activity of injection fluids can be reduced by adding salts, creating an osmotic potential that will drive water out of the shales. But the type and amount of salts should be strictly monitored, because excessive dehydration can cause the shale to weaken. In addition, the ionic imbalance can cause diffusion of ions into the shale pore fluid causing damage to shale cementing and cohesion degradation (Talal Mohammad Al-Bazali, 2005). Figure 2 (Talal M. Al-Bazali, 2011) shows the schematic representation of an osmotic pressure cell.

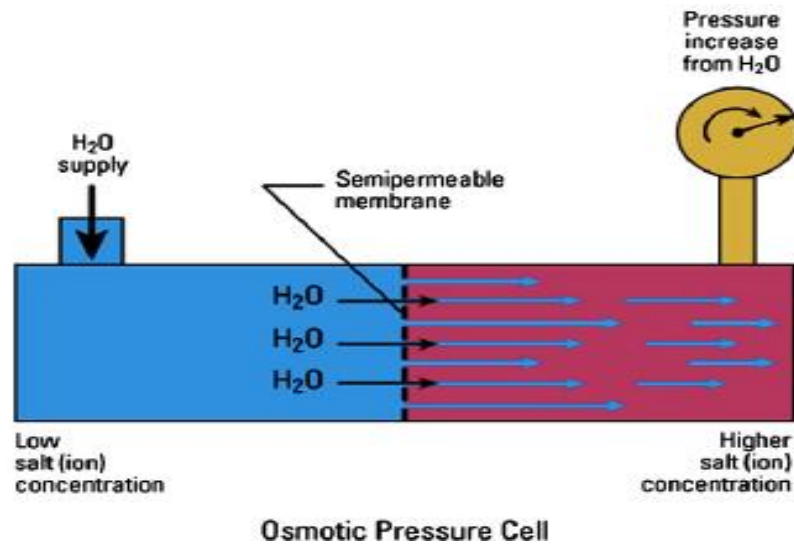


Figure 2: Schematic representation of an osmotic pressure cell (Talal M. Al-Bazali, 2011)

1.2 Shale Stability in presence of additives

There are many readily available commercial shale stabilizers used widely in industries. In this work, we have studied the effect of salts, tetramethyl ammonium chloride and polyacrylamides as shale inhibitors.

1.2.1 Salts

KCl (Potassium Chloride) is most widely used shale inhibitor in the industry. The smaller hydration radius of the K^+ causes low degree of repulsion. KCl is especially effective for shales that are rich in expandable clays such as smectites and montmorillonites. KCl has also been proven to have lower membrane efficiencies and do not cause changes to shale permeability that might lead to formation damage. However, when KCl is used along with polyacrylamides, the viscosity reduction is high which leads to fluid losses during fracturing applications. On the other hand, NaCl (Sodium Chloride)

is not as inhibitive as KCl, especially for shales rich in expandable clays. But with NaCl the viscosity reduction is not as drastic as with KCl.

1.2.2 Synthetic Polymers

Synthetic polymers such as charged partially hydrolyzed polyacrylamides are better alternatives to inorganic salts. Unlike K^+ , the polymers attach to multiple sites on the clay and bridge the clay platelets and preventing the water and solutes from entering the shales. The polymers can adsorb onto the surface of the shale particle, and the adsorption rate is controlled by the polymer concentration and diffusivity (Lu, 1988). Also, with stricter environmental regulations, it is discouraged to use high salinity water. But the disadvantage of using polyacrylamides is some of these have been associated to cause formation damage and alter the permeability of the shale. Polyacrylamides along with KCl has proven to provide good shale inhibition for wide range of shales. Figure 3 (Lu, 1988) Shows the schematic representation of polymeric bridging by shale particles

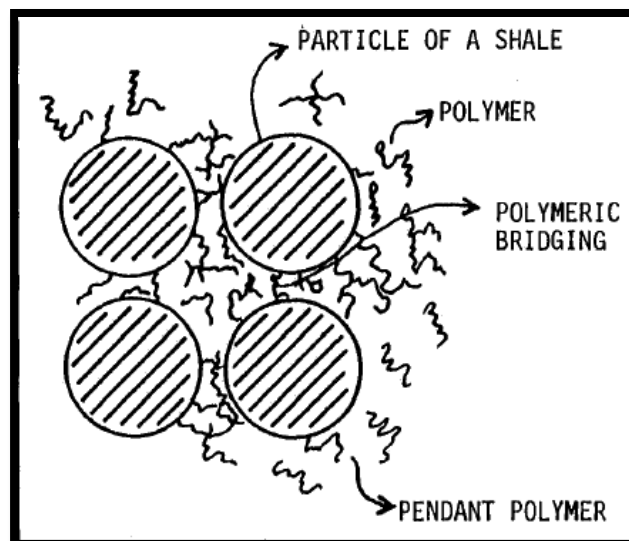


Figure 3: Schematic representation of polymer interaction with clay (Lu, 1988)

1.3 Research Objectives

Shale – fluid interaction has been studied extensively over the decades and many new techniques are being used to study the same. But a lot of these methods are either time consuming, tedious, or cannot be easily and readily used. The simpler methods such as the swelling and dispersion tests alter the shale clay matrix and water content by grinding and reconstituting the sample, thereby not giving a true representation of shale – fluid interaction. Hence, simpler and more reproducible methods have been devised to help understand and semi – quantify shale fluid interaction. The objectives of this study is broadly divided into 3 categories

1.3.1 Rheological characterize shale-fluid interaction

Rheological methods have been used to characterize interaction of pure clays such as bentonite with water and drilling fluids. In this study, shale interaction with polyacrylamides, salts is probed using series of flow ramp and yield stress measurements. Additionally, the additives used such as polyacrylamides with salts, bentonite with and without salts is characterized.

1.3.2 Semi – Quantify shale-fluid interaction using zeta potential tests

Rheological measurements can be used to qualitatively assess shale-fluid interaction. There is a need to use methods that will give quantitative data and yet are simple in nature. One such method that was proposed is to use zeta potential measurements for studying the shale interactions with different fluids. Zeta potential methods are proven effective for clay stability studies and the same principle is applied in this work to study the extent of shale interaction with polyacrylamides in presence and absence of additives. The use of zeta potential tests is studied in detail and the interpretation of results is discussed.

1.3.3 Use simple methods such as immersion tests and correlate test results with rheological studies

Immersion tests have been used in the past to study shale compatibility with different water based drilling muds. In an immersion test, the shale samples are simply immersed in the test fluid and the change in shale properties are measured through visual and tactile inspections. The immersion tests are used in this work to study the effect of polyacrylamides, salt on effectiveness in preventing swelling and dispersion. Additionally, surface of the shale was probed to see the extent of additives modifying the shale surface. These results were correlated to the rheological results and a brief summary of correlation between mineralogy of shale and effective shale inhibition is given.

1.4 Structure of dissertation

The dissertation has five chapters in the following order and is divided into two parts. The first part is focused on characterizing shale – fluid interaction. The first chapter gives a brief introduction about shale – fluid interaction, various mechanisms associated with shale – fluid interaction and the significance of it in current work. The second chapter discusses the use of zeta potential and rheological techniques to quantify shale-fluid interaction, with focus on ability of polyacrylamides to cause potential formation damage. The third chapter elaborates the use of simple laboratory techniques such as immersion tests, and study the effect of bentonite, salts, and polyacrylamides on altering the surface properties of shale using imaging techniques. The results are correlated to the mineralogy of the shale samples and validated with rheological measurements. Fourth chapter will be Part II of the dissertation, a different study focused on rheologically studying the effect of stripping lighter hydrocarbons from shale and crude oil using a simple model – oil system. Additionally, the effect of cooling rate on the rheological properties of wax – model oil system is studied. The final

chapter discusses the conclusions drawn from all the studies and future recommendations for continuing the work and the research gaps that can be addressed.

CHAPTER II

2. Quantitative Characterization of Polyacrylamide-Shale Interaction under Various Saline Conditions

2.1 Introduction

Interaction of injected fluids such as drilling, fracturing and completion fluids with shale has been a problem for many decades in the oil field, and shale constitutes 75% of all the formations drilled by the oil and gas industry (Khodja et al., 2010). Over the years, many studies have been performed to quantify shale-fluid interaction and also to minimize this interaction. Interactions between shale and injected fluids are of concern for a variety of reasons. The interaction of injected fluids with shale leads to wellbore instability (Muniz, Fontoura, & Lomba, 2005; Tan, Richards, & Rahman, 1996; Yu, Chenevert, & Sharma, 2003). The productivity of the well decreases due to this instability, which also increases the drilling cost (Lal, 1999; Mahto & Sharma, 2004). Water-based mud (WBM) is the most commonly used type of drilling fluid, and shale is highly sensitive to the additives and the clays present in the WBM (Friedheim, Guo, Young, & Gomez, 2011; Gomez & He, 2012; He, Gomez, Leonard, & Li, 2014). The common additives used in WBM are friction reducers, acids, gellants, crosslinkers, clay controlling agents and other polymers (Aften & Watson, 2009; Harris, 1988). It is important to use all the necessary

additives in injected fluids, but it is also equally important to use additives that do not potentially weaken the shale.

The way shale interacts with the injected fluid depends on shale properties, such as mineralogy, rock mechanical properties, porosity, clay composition and permeability, as well as the properties of injected fluids such as ionic strength and salt concentration (Gomez & He; Horsrud, Bostrom, Sonstebo, & Holt, 1998; Lal). Clay in shale has a great influence on the chemical and mechanical properties of shale. Clay minerals have a tendency to absorb water and cause an increase in the swelling pressure—a phenomenon called hydration, and this is attributed to the hydrophilic surface of the clay (Lu, 1988). The clay minerals present in shale are mostly classified into 5 categories: montmorillonite, illite, smectite, kaolinite and attapulgite (Luckham & Rossi, 1999; Van Olphen, 1977). The presence of clay minerals in abundance changes the interaction properties of the shale with injected fluids, and the composition of the clay affects reactivity, with montmorillonitic clay being highly prone to swelling and highly crystalline illite being less prone.

Much research is being done to study the rock mechanics to understand the interaction of shale with fluids. Conventional techniques such as the dispersion test and the swelling test do not fully reveal the effects of polymer-shale interaction. Tests such as pressure transmission tests are done to measure the effect of anions, cations and salts present in injected fluid that affects shale-fluid interaction (Ghassemi & Diek, 2003; Van Oort et al., 1995; van Oort et al., 1996). The presence of charged ions, in injected fluid alters the membrane efficiency of shale, thereby influencing ion transport from the fluid to the shale that causes the shale to swell/disperse (Talal Mohammad Al-Bazali, 2005; Mody & Hale, 1993; Van Oort, 2003; Zhang, Al-Bazali, Chenevert, & Sharma).

High molecular weight polyacrylamides are commonly used friction reducers in hydraulic fracturing of shale formations. The large volumes of friction reducers (liquid volumes can be as high as four million gallons for one well), especially synthetic polymers such as polyacrylamides that are difficult to break and are proven to form membrane over shales are used, that are associated with causing fracture and formation damage (Carman & Cawiezel, 2007). Formation damage is caused by the adsorption of polyacrylamides on the shale surface alter the surface properties. In this paper, the shale-polyacrylamide interaction studies were focused on the extent to which polyacrylamides adhere to the shale, which can potentially cause formation damage.

Some of the commonly used methods such as swelling tests and dispersion tests do not give a true representation of the shale-fluid interaction and are qualitative in nature. Other sophisticated methods such as the autonomous triaxial test and high pressure triaxial tests are tedious and intensive processes which give a good quantitative measure of shale-fluid interaction by measuring the axial load, sample deformation, cell and pore pressures (Mody, Tare, Tan, Drummond, & Wu, 2002). Hence, a simple testing method was devised that produces reproducible semi-quantitative data, that will aid in understanding the interaction of different fluids and its components with shale better.

One such method that was devised to probe the polymer - shale interaction is by rheologically measuring the interactions. The rheology of shale slurries suspended in the polymer was analyzed. The factors that affect the rheology of the particle suspension are concentration, particle shape, interactions among particles, and interaction between particles and the bulk fluid (Mueller, Llewellyn, & Mader, 2010). Characterizing the interaction between the particle and the bulk fluid is key to the research. When shale particles interact strongly with the bulk fluid, viscosity

increases with increasing polymer concentration. This is used as a measure of the interaction of bulk fluid with shale particles. Additionally, the polymer tends to adsorb on the surface of the shale. Rheological methods were used to assess the interaction of anionic and cationic polyacrylamide with samples of North American shale, including Pride Mountain shale and the Devonian-age Chattanooga shale. The interaction of shale with anionic and cationic polyacrylamide was studied rheologically by a series of flow ramp tests.

The second method used zeta potential measurements made over time to quantify polymer – shale interaction. The zeta potential is an electric potential developed at the solid-liquid interface due to the relative movement of solid particles in water (Vane & Zang, 1997). Zeta potential at solid-liquid interface is an indirect measure of solid-liquid interactions (Menon & Wasan, 1987b; Petersen & Saykally, 2008; Werner, Zimmermann, & Kratzmüller, 2001). The electro kinetic measurements made at the solid-liquid interface are a relative measure of surface charge and adsorption (Delgado, González-Caballero, Hunter, Koopal, & Lyklema, 2007; Hunter, 2013). Zeta potential measurements have long been used to measure the stability of colloidal systems (Heurtault, Saulnier, Pech, Proust, & Benoit, 2003; Hunter, 2013; Jiang, Gao, & Sun, 2003). The colloidal system in the present study is shale dispersed in polyacrylamide. By measuring the stability of the shale system as a function of zeta potential over time, we will be able to quantify polymer - shale interaction. A comparison is made between different salt-polymer solutions (also called as shale inhibitors) for their role in preventing polymer adsorption on shale. Salts such as KCl and NaCl are widely used for shale inhibition (Gholizadeh-Doonechaly, Tahmasbi, & Davani; Lee, Patel, & Stamatakis, 2001; Patel, 2009). In the past, amines were widely used for this purpose (He et al., 2014). In this work, TMAC is compared with KCl and NaCl as an additive to anionic and cationic polyacrylamide systems for shale inhibition.

In this work, the impact of anionic and cationic polyacrylamide in injected fluids on the alteration of the surface properties of shale is studied. Using zeta potential and rheological measurements to quantify shale- polymer interaction is a novel technique and is extensively researched and studied in this work.

2.2 *Materials and Methods*

2.2.1 *Polyacrylamides*

Anionic polyacrylamide and cationic polyacrylamide of average molecular weight 10^7 g/gmol were obtained from Kemira Supplies. The polyacrylamides are highly water absorbent and form soft gels even at low concentration. The anionic and cationic polyacrylamide samples were measured by weight and added to deionized water slowly and was mixed in a shaker table for 15 minutes at a speed of 200 RPM. The time and speed of mixing the sample was chosen carefully so that the shear damage in polyacrylamide samples was kept minimum before the experiments. The samples were left to hydrate for 24 h. All of the solutions were tested within 36 hours of preparation.

2.2.2 *Shale Samples*

Pride Mountain and Chattanooga shale samples were prepared using a mortar and pestle. They were ground using Bel-Art mixer to obtain smaller particles, and the sample was sieved to obtain fairly homogenous particles, with particle size smaller than 75 μm . The particles were small enough to remain suspended in the polymer solution and big enough to make accurate rheological

measurements of slurry. The shale was kept at a constant concentration of 0.5 lb/bbl (pounds/barrel) for all of the rheology and zeta potential experiments.

2.2.3 Sample Information

The Chattanooga shale sample is from an exploratory well in southwestern Tuscaloosa County, Alabama and is typical of Devonian shale reservoir rock in the eastern United States. The Pride Mountain sample is from the Gorgas #1 borehole, which was drilled to explore the CO₂ storage potential at a large coal-fired power facility in the Black Warrior Basin, Walker County, Alabama. The Pride Mountain sample is more representative of a sealing formation and is rich in expandable mixed-layer clay - wellbore stability was a significant problem during the drilling of this zone.

2.2.4 Characterization of shale

The shale samples were analyzed for clay and non-clay content by X-ray diffraction (XRD) (Clark et al., 2012). Other parameters such as total organic carbon (TOC), Pressure decay permeability, and effective porosity were determined for both shale samples (Clark et al., 2012).

Table 1: Whole rock mineralogy of shale samples determined by XRD

Analysis	Chattanooga	Pride Mountain
Depth (ft)	9167	2863
Clay Content (Wt.%)		
Smectite	0	1
Illite/Smectite	5	16
Illite+Mica	24	37
Kaolinite	0	12
Chlorite	0	4
Non Clay Mineral Content (Wt.%)		
Quartz	41	21
K Feldspar	16	3
Plagiocase	2	2
Calcite	0	1
Ankerite/Fe Dolomite	0	1
Dolomite	5	0
Pyrite	5	1
Fluorapatite	0	0
Barite	1	1
Siderite	0	1
Magnetite	0	0

Table 2: TOC, effective porosity and pressure decay permeability

Parameters	Chattanooga	Pride Mountain
TOC (Wt. %)	3.33	0.80
Effective Porosity (% of BV)	2.32	12.30
Pressure Decay Permeability (mD)	0.00032	0.00048

2.2.5 Equipment

A Discover DHR-3 stress controlled rheometer was used to make rheological measurements. Vane geometry was used for the polymer - shale samples. Vane geometry helps prevent wall slippage at higher shear rates, helps disrupt flow inhomogeneity while shearing, and also works well for samples with suspended solids (Goh, Leong, & Lehane, 2011). A cone-and-plate geometry was used for polymer solutions. Cone-and-plate is useful for solutions that have low

viscosity and that do not have any dispersions with suspended solids larger than 64 μm . Cone-and-plate geometry (diameter: 60 mm and cone angle 2°) provides homogenous shear, shear rate, and stress in the geometry gap when used to measure the rheological properties of a solution. All the experiments were performed at a temperature of 25 °C \pm 0.03°C. The polymer-shale sample was pre-sheared at 200 s⁻¹ before the start of each experiment to prevent the shale particles from settling to the bottom of the geometry during the experiment.

Since the cationic polyacrylamide form agglomerates with shale, it is not possible to quantify the polymer -shale interaction rheologically. Due to agglomeration or in other words due to the flocculation of the shale particles in the solution accurate rheological measurements cannot be made. The shale particles have to be suspended in the solution and have minimal settling velocity in order to perform rheological studies. In cationic polyacrylamide medium, flocculation resulted in excessive gravitational settling of the agglomerated shale particles. Hence, only the anionic polyacrylamide was used to rheologically quantify polymer - shale interaction. However, both cationic and anionic polyacrylamide were used to quantify polymer - shale zeta potential. The anionic polyacrylamide concentration was 0.1 to 0.2 Wt. %, such that the concentration is well above C* (critical overlap concentration) and below C** (critical entanglement concentration). The concentration of shale was kept constant at 0.5 lb/bbl, and the concentration of anionic polyacrylamide was varied from 0.1 to 0.2 Wt. %.

Figure 4 shows the experimental setup, including the cone-and-plate and vane geometry.

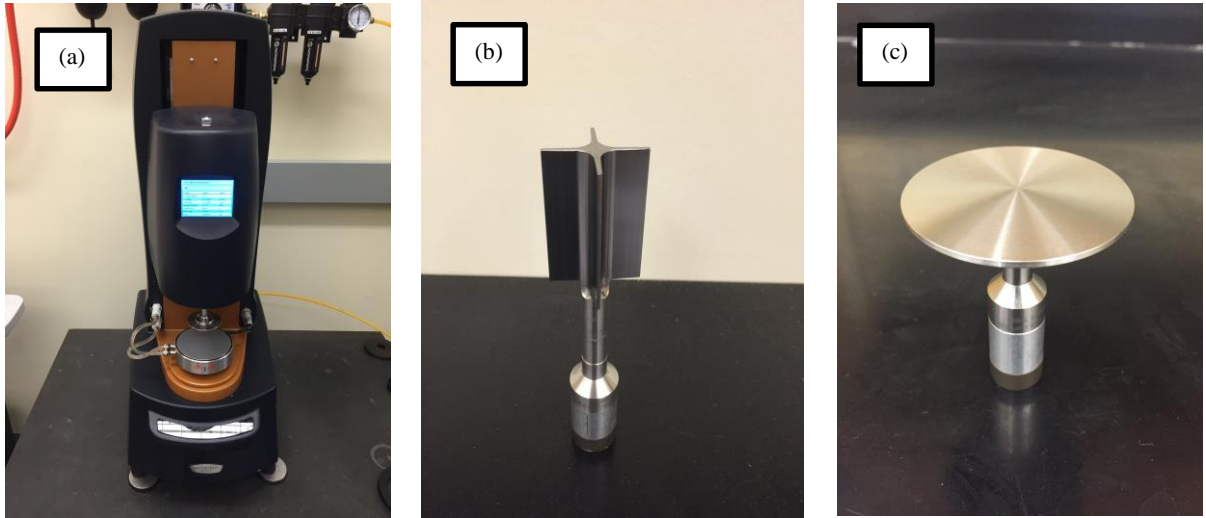


Figure 4: (a) DHR-3 Rheometer (b) Vane Geometry (c) Cone and plate geometry

2.2.6 Zeta Potential Analyzer

A Phase Analysis Light-Scattering Technique (PALS) is used to measure the zeta potential of polyacrylamide - shale interfaces. A Zeta PALS measurement system manufactured by Brookhaven Instruments Corporation (Holtsville, NY) was used. The experiments were conducted at 25°C and were performed in triplicate. A platinum electrode and H-Ne laser light source were used to measure the electrophoretic mobility of colloidal suspensions. The polyacrylamide - shale sample was prepared by adding polyacrylamide to Deionized (DI) water, and it was kept in a shaker table at a speed of 200 RPM for 15 minutes. The shale sample was weighed and added to DI water. Both samples were left to hydrate at room temperature for 24 hours. The shale particles were filtered using a 1 μm syringe filter and added to the polyacrylamide sample. The solution was shaken and added to the cuvette using a pipette. The size of the shale particles is in the colloidal range (1×10^{-9} m), in which physiochemical forces such as Van der Waals attractive forces and double layer repulsive forces are stronger than

gravitational forces (Kaya, Oren, & Yukselen, 2003). Figure 5 shows the particle size distribution of shale particles before filtering it to get particle sizes lesser than 1 μm .

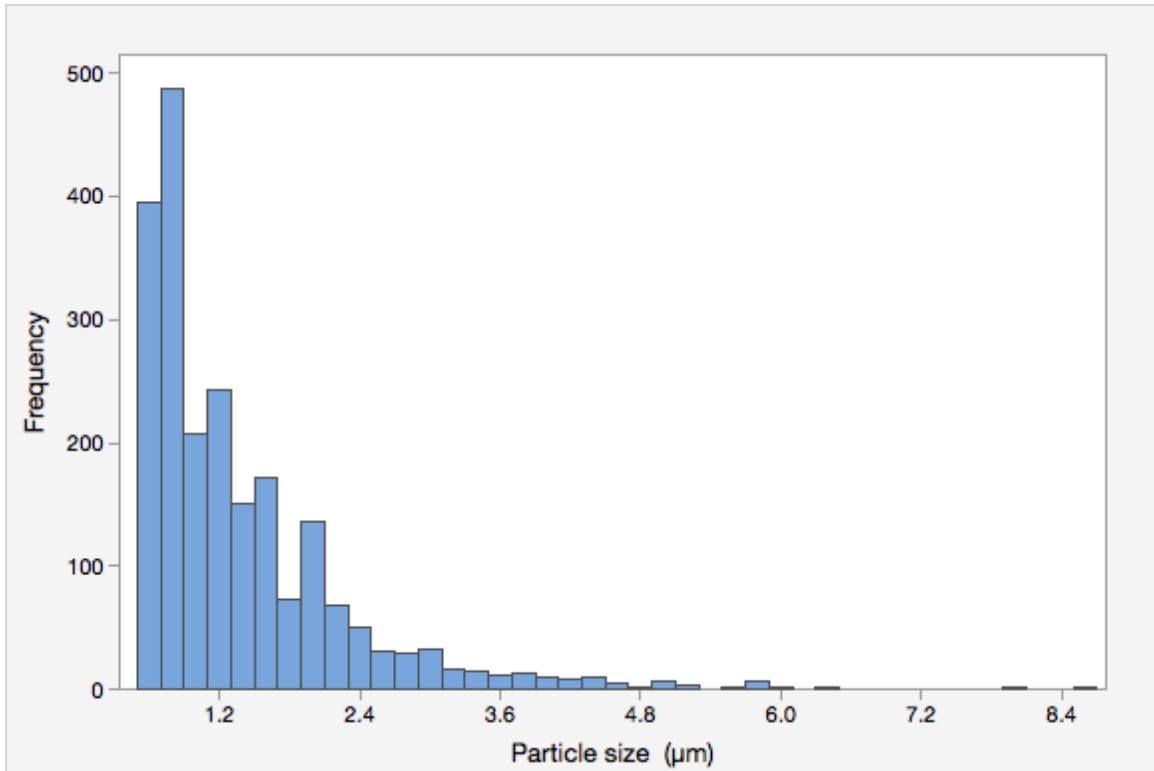


Figure 5: Histogram of particle size distribution of shale particles used in the study

One cm^3 of sample was used for all the measurements, and the tip of the cuvette was immersed in the sample to prevent formation of air bubbles. The Pt electrode was then placed in the cuvette, and the zeta potential measurements were recorded. In order to study the influence of salt on polymer - shale interaction, salt solutions of KCl, NaCl and TMAC were used. To study the increase in average particle size with time, dynamic light scattering using the Zeta PALS is used. A 0.45 μm syringe filter was used to filter dust from the samples before loading the sample to the Zeta PALS. A zeta potential measurement was recorded every 20 minutes and for each data point, ten readings were taken, and the average effective diameter and the associated standard error

were plotted vs. time. The compositions of the various suspensions used are given in Table III. The compositions of the suspension was chosen such that the salt concentration met the Zeta PALS instrument specification, and the polyacrylamide concentration was chosen that was just enough to keep the shale suspended in the polyacrylamide.

Table 3: Compositions of different suspension media used in the study

Sample	Medium
1.	0.05 Wt. % anionic polyacrylamide
2.	0.05 Wt.% cationic polyacrylamide
3.	0.05 Wt.% anionic polyacrylamide + 0.05 Wt. % KCl
4.	0.05 Wt.% cationic polyacrylamide + 0.05 Wt. % KCl
5.	0.05 Wt.% anionic polyacrylamide + 0.05 Wt. % NaCl
6.	0.05 Wt.% cationic polyacrylamide + 0.05 Wt. % NaCl
7.	0.05 Wt.% anionic polyacrylamide + 0.05 Wt. % TMAC
8.	0.05 Wt.% cationic polyacrylamide + 0.05 Wt. % TMAC

2.2.7 Analysis

2.2.7.1 Carreau Model

In order to determine the zero shear rate viscosity of the fluid, the Carreau model was used. The Carreau model describes a wide range of non-Newtonian behavior by curve fitting within the Newtonian and the shear thinning non-Newtonian regions (Rao, 2014). This model can be applied over a wide range of shear rates. The Carreau model is a variant of the Cross model and is used for logarithmic data sets.

This viscosity model allows data to be fitted to the following model,

$$\frac{\eta - \eta_{\infty}}{\eta_0 - \eta_{\infty}} = \frac{1}{(1 + (\lambda\dot{\gamma})^2)^{n/2}}$$

where η_0 the Newtonian viscosity, η_∞ the infinite viscosity, $\dot{\gamma}$ the shear rate, λ the relaxation time, and n the power law index.

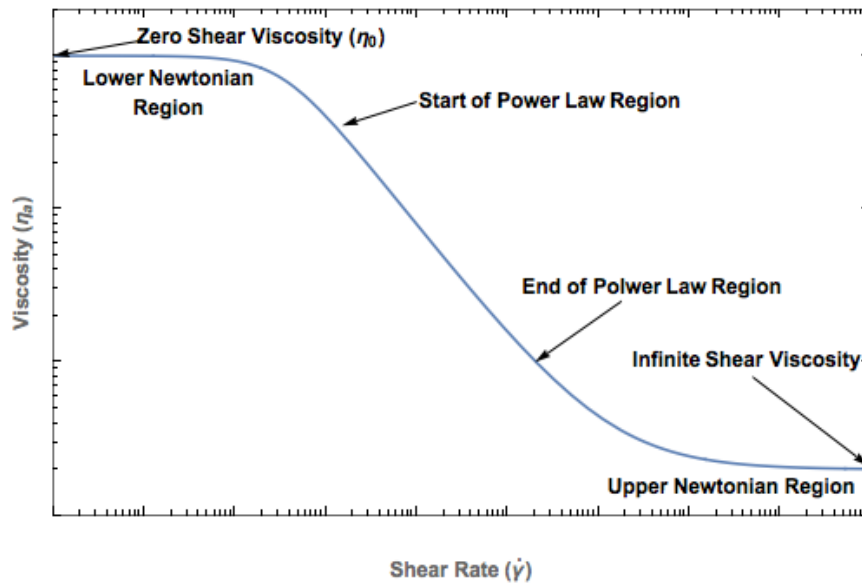


Figure 6: Carreau Model logarithmic fit for viscosity vs. shear rate

Figure 6 shows the plot of apparent viscosity vs. shear rate for a shear thinning Carreau fluid identifying three separate regions. The zero shear viscosity represents the lower Newtonian region at lower shear rates, the infinite shear viscosity captures the higher shear rate, which is the upper Newtonian region, the power law region is characterized by the power law index and the relaxation time which gives the time estimate at which the lower Newtonian region ends.

2.3 Results and Discussion

2.3.1 Characterizing polymer-shale interaction through zeta potential measurements

Zeta potential measurements were made for Pride Mountain and Chattanooga shale samples in different suspending media to quantify the polyacrylamide - shale interaction. The measured zeta potential is a function of the surface charge of the suspended particle, any adsorbed layer at the particle-liquid interface, and the nature and composition of surrounding medium (Jia & Williams, 1990). For the same experimental conditions, the change in zeta potential over time is indicative of polymer adsorption on shale. The higher the absolute values of negative zeta potential, the bigger the double layer thickness of the shale particle. Higher negative zeta potential value is also indicative of swelling and dispersion of clay (Zhong, Qiu, Huang, & Cao, 2011). The zeta potential values measured for just the shale samples, was ~ -24 mV for both Chattanooga and Pride Mountain shale.

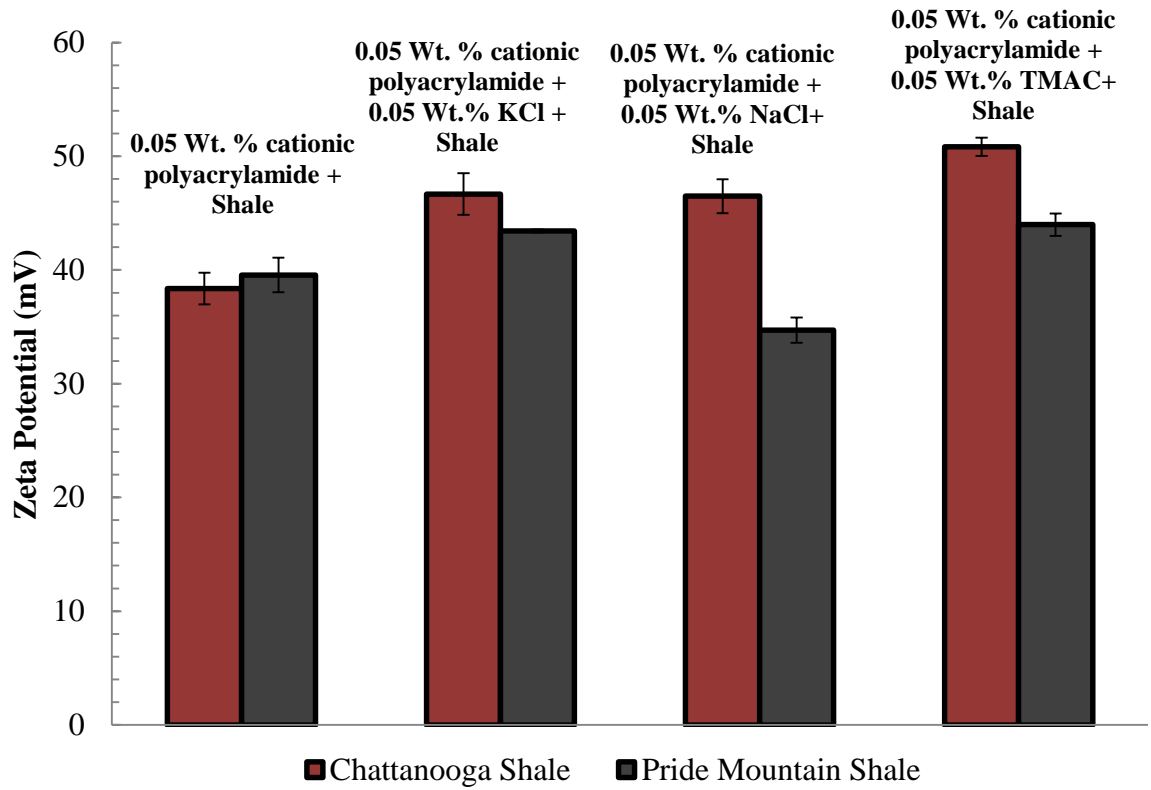


Figure 7: Change in Zeta Potential of shales in cationic polyacrylamide with salts and TMAC

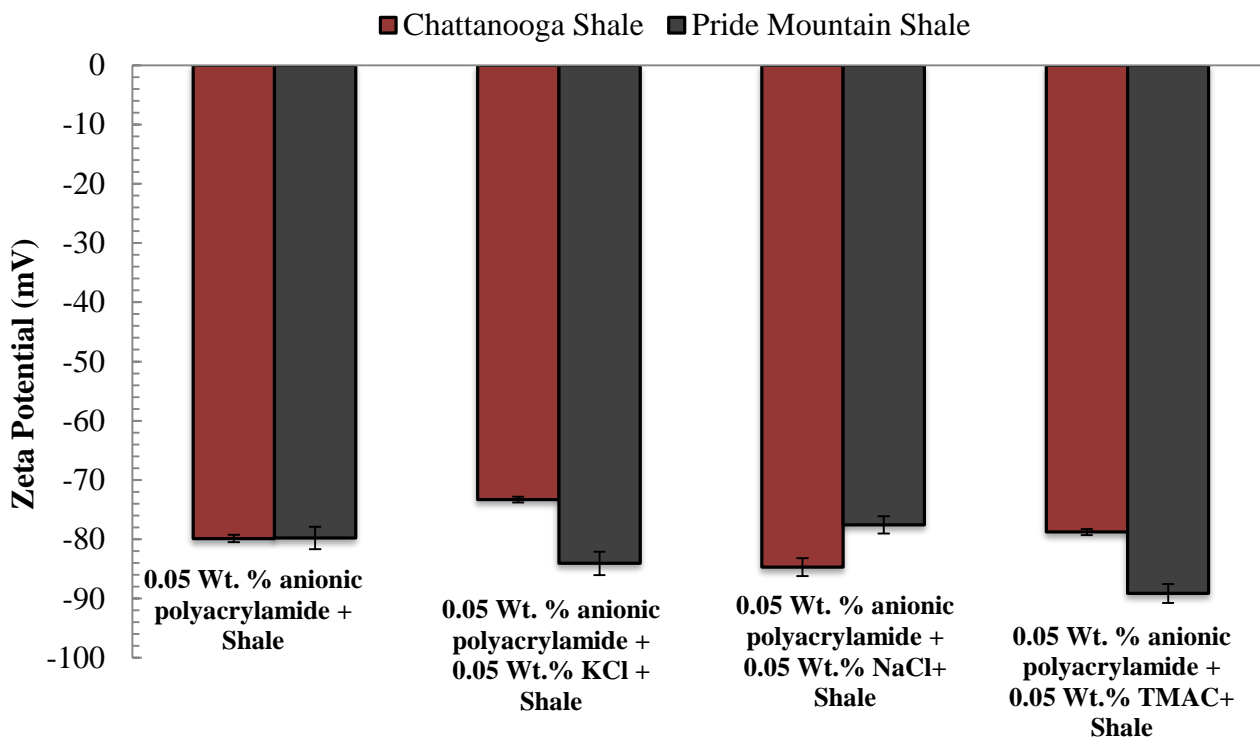


Figure 8: Change in Zeta Potential of shales in anionic polyacrylamide with salts and TMAC

Zeta potential of cationic and anionic polyacrylamide with Chattanooga and Pride Mountain shale was measured immediately after adding the sample to the polyacrylamide sample. In cationic polyacrylamide (with no salts) there is not a significant difference in zeta potential values for both the shales. Whereas in presence of salts (KCl and NaCl) and TMAC (Figure 7) Chattanooga shale has higher zeta potential values which is indicative of higher adsorption density. Similarly in anionic polyacrylamide, Pride Mountain shale has higher absolute zeta potential values in presence of KCl and TMAC indicative of higher adsorption density (Figure 8). The change in zeta potential with time for the same system will be discussed in the following sections.

In order to determine the influence of polymer adsorption on shale the change in zeta potential with time is measured, it is important to measure the zeta potential of the shale free polymer

solution as a control. Polyacrylamides are stable for 48 hours from preparation of the sample. Figure 9 and Figure 10 show zeta potential measured over time for anionic and cationic polyacrylamide with no shale.

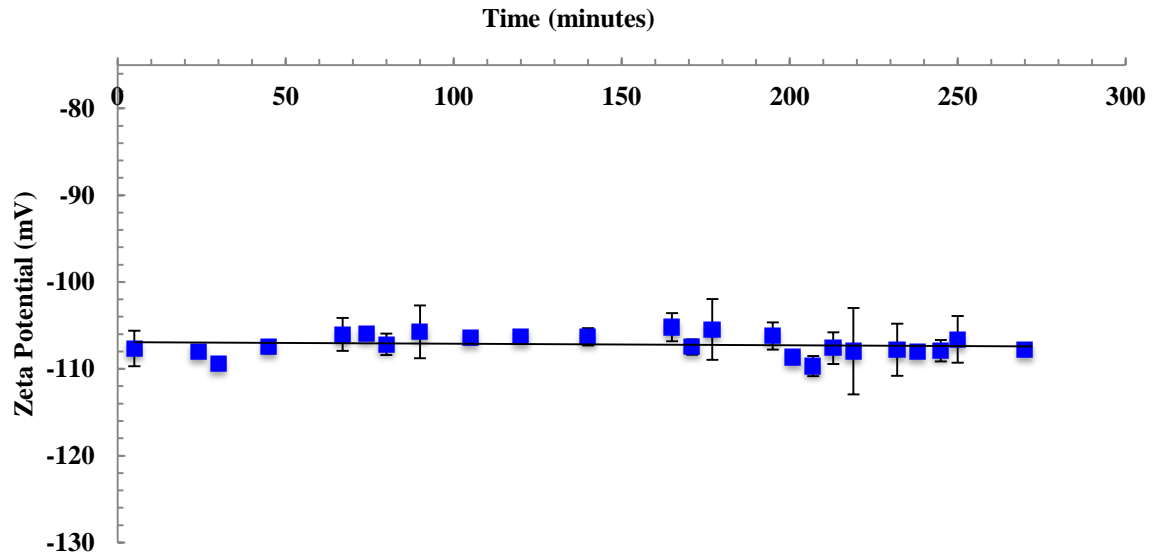


Figure 9: Zeta potential vs. time for anionic polyacrylamide

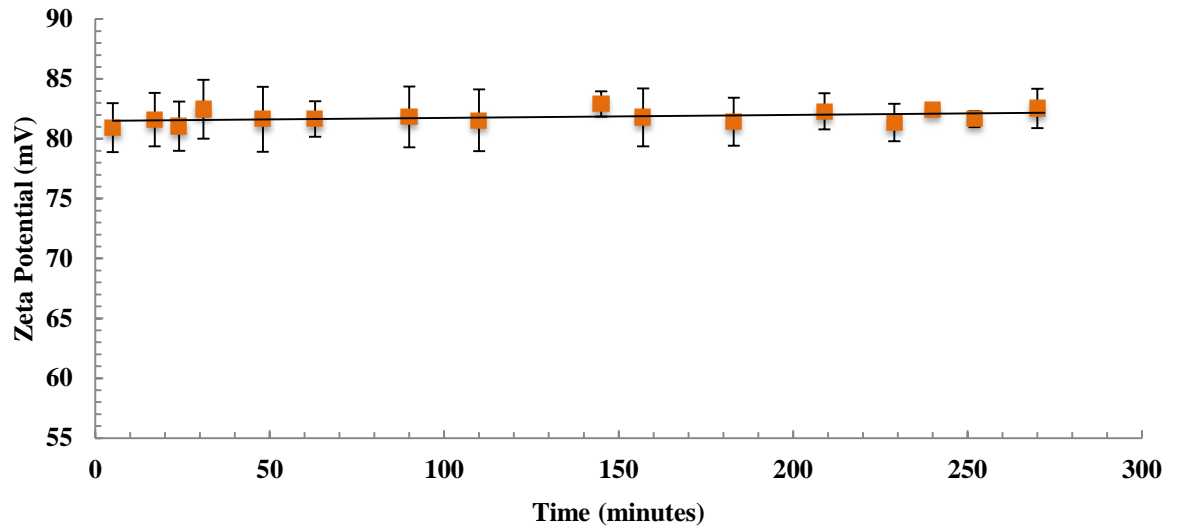


Figure 10: Zeta potential vs. time for cationic polyacrylamide

The zeta potential remains effectively constant over time. This proves that the polyacrylamide remains stable during the time of experiment and the change in zeta potential after adding shale to the polymer is solely because of changes in the surface properties of shale when in contact with polyacrylamide.

Figure 11 and Figure 12 show the change in zeta potential with time for Chattanooga shale incubated different media containing anionic and cationic polyacrylamide, respectively. The zeta potential change with time is plotted as a series plot. A dotted line is drawn at 20 mV (Figure 12 and Figure 14) to show the point below which the colloidal system is unstable due to flocculation.

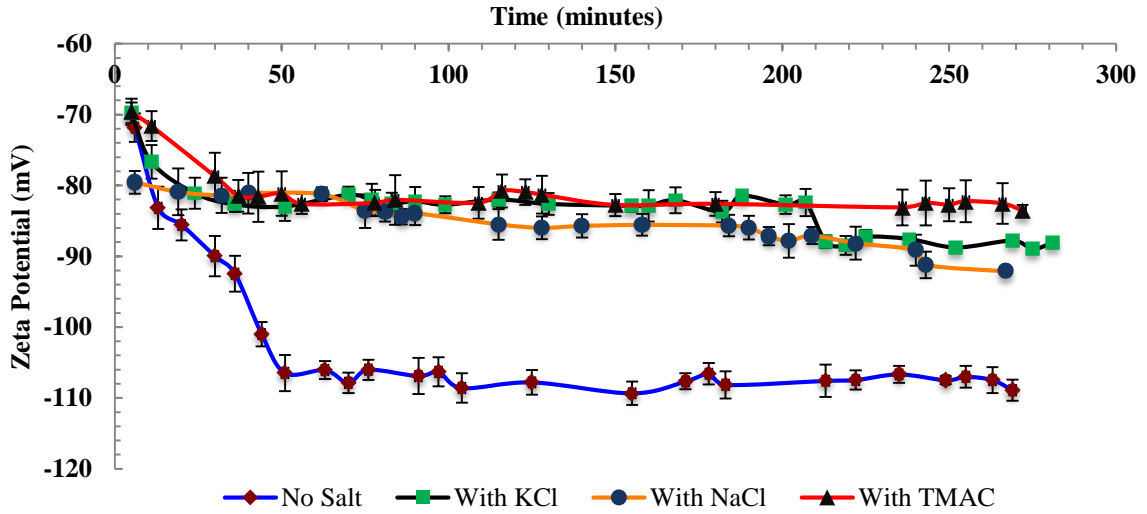


Figure 11: Zeta potential of Chattanooga shale incubated w/ anionic polyacrylamide under various conditions

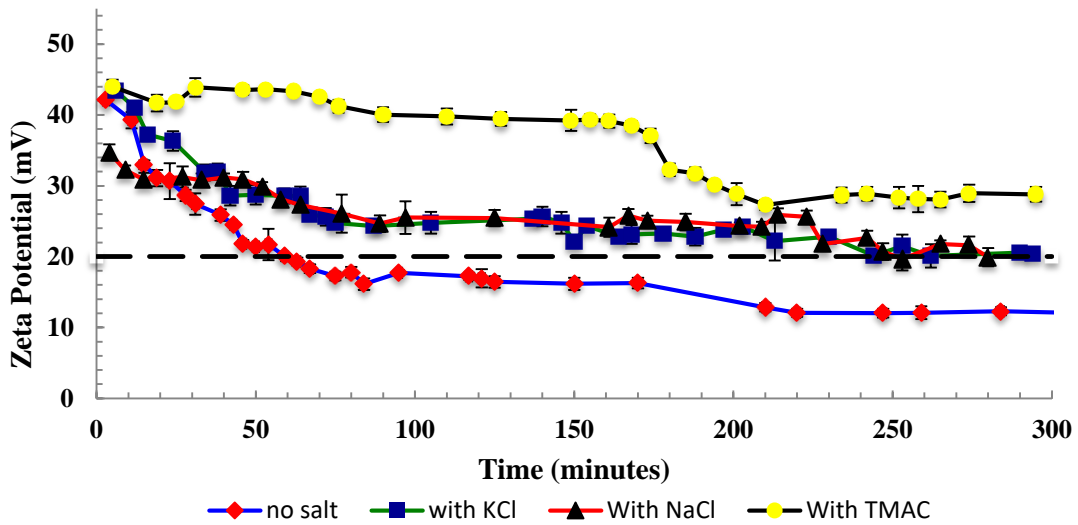


Figure 12: Zeta potential of Chattanooga shale incubated w/ cationic polyacrylamide under various conditions

Figure 13 and Figure 14 shows the change in zeta potential with time for Pride Mountain shale in different media of anionic and cationic polyacrylamide, respectively.

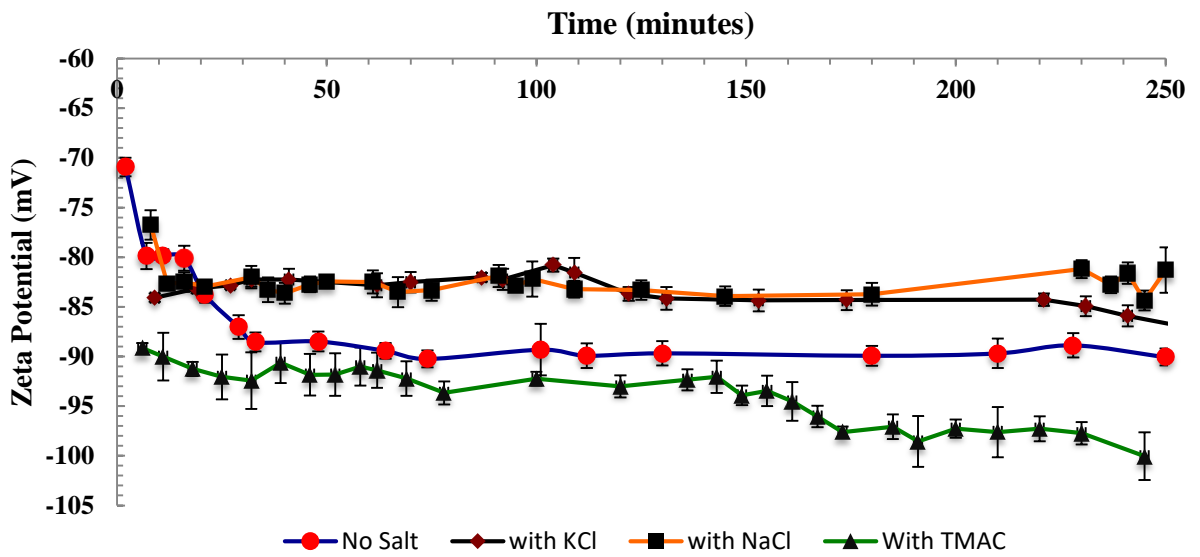


Figure 13: Zeta potential of Pride Mountain shale incubated w/ anionic polyacrylamide under various conditions

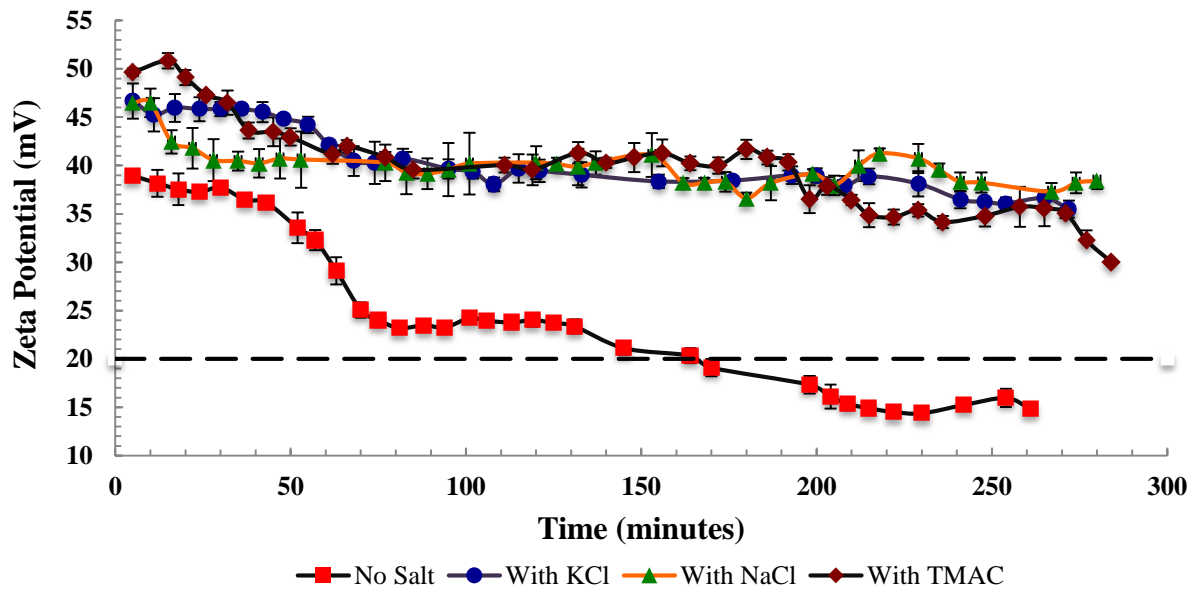


Figure 14: Zeta potential of Pride Mountain shale incubated w/ cationic polyacrylamide under various conditions

In the absence of salt, the overall magnitude (i.e. absolute value) of the zeta potential increased for both shale samples in anionic polyacrylamide and decreased in cationic polyacrylamide (Figure 11, 12, 13 and 14). In cationic polyacrylamide, the decrease in zeta potential with polymer adsorption is due either to a decrease in charge density or a shift in the shear plane. Zeta potential also decreases more rapidly when the double layer is compressed at high ionic strength (Brooks & Seaman, 1973; Vane & Zang, 1997). The hydrophilic ends of the cationic polyacrylamide attach themselves to the positively charged edges of clay particles and cause bridging of clay particles. This creates clusters of large particles that resist flow which leads to decrease in mobility and zeta potential (Yalçın, Alemdar, Ece, & Güngör, 2002). Addition of salts increases the net positive charge of the medium, leading to the increase in zeta potential. Zeta potential values between -20 mV and 20 mV have an effective charge low enough that flocculation occurs (Johnson et al., 2010)

Colloidal particles in suspension either flocculate or deflocculate according to which force predominates, the van der Waals attractive force or the double layer repulsive force (Street & Wang, 1966). In the absence of salt, cationic polyacrylamide causes flocculation of shale particles with time because the attractive forces predominate. Since there is rapid flocculation as the shale comes in contact with cationic polyacrylamide, it is difficult to determine if adsorption density is increasing with time. Additional studies will need to be performed with cationic polyacrylamide and shale to determine the effect of adsorption on zeta potential. The observed flocculation is however a sign of strong interaction of polymer with shale, and the addition of salt inhibits flocculation.

In the anionic polyacrylamide system for Chattanooga and Pride Mountain shale, there is an increase in absolute value of zeta potential with time. This is indicative of the increase in the

double layer thickness, which, in turn, is due to increasing adsorption density of polyacrylamide. In Chattanooga shale, the absence of salt causes the absolute value of zeta potential to increase to a point and then level off. Salt helps to decrease the ionic nature of clay and thus leaves fewer sites remaining for the polymer to adsorb (Kulshrestha, Giese, & Aga, 2004; Menon & Wasan, 1987b). In previous work, it has been shown that salts such as KCl minimize clay hydration and swelling, thereby minimizing the interaction of shale with fluid (Anderson et al., 2010; Lane & Aderibigbe, 2013; Patel, 2009; Patel, Stamatakis, & Davis, 2001; Van Oort, 1994; Van Oort, 2003). Whereas in Pride Mountain shale, the zeta potential values are higher in the presence of TMAC. This is attributed to both the shale and the polyacrylamide having predominantly negative surface charge, which leads to an overall increase in charge of the system and also the pride mountain being rich in smectites has higher exchangeable sodium ions. Ammonium ions from TMAC exchanges with smaller sodium ions, ammonium with its larger hydration radius increases the swelling leading to an increase in zeta potential values.

The zeta potential of Chattanooga shale and Pride Mountain is measured in different saline media before adding the anionic and cationic polyacrylamide. Figure 15 shows the increase in absolute value of zeta potential after adding the anionic polyacrylamide to the shale - salt solution (i.e., the difference in the value of zeta potential before and after adding anionic polyacrylamide). In anionic polyacrylamide, KCl is the most effective shale inhibitor followed by TMAC and NaCl for Chattanooga shale. For Pride Mountain shale, KCl also is the most effective shale inhibitor, but NaCl is slightly more effective than TMAC. The reason for KCl providing better inhibition is because, potassium ions have smaller hydration radius and can easily exchange with the more swellable sodium ions on shale surface and due to their small hydration radius they reduce swelling and provide better shale inhibition.

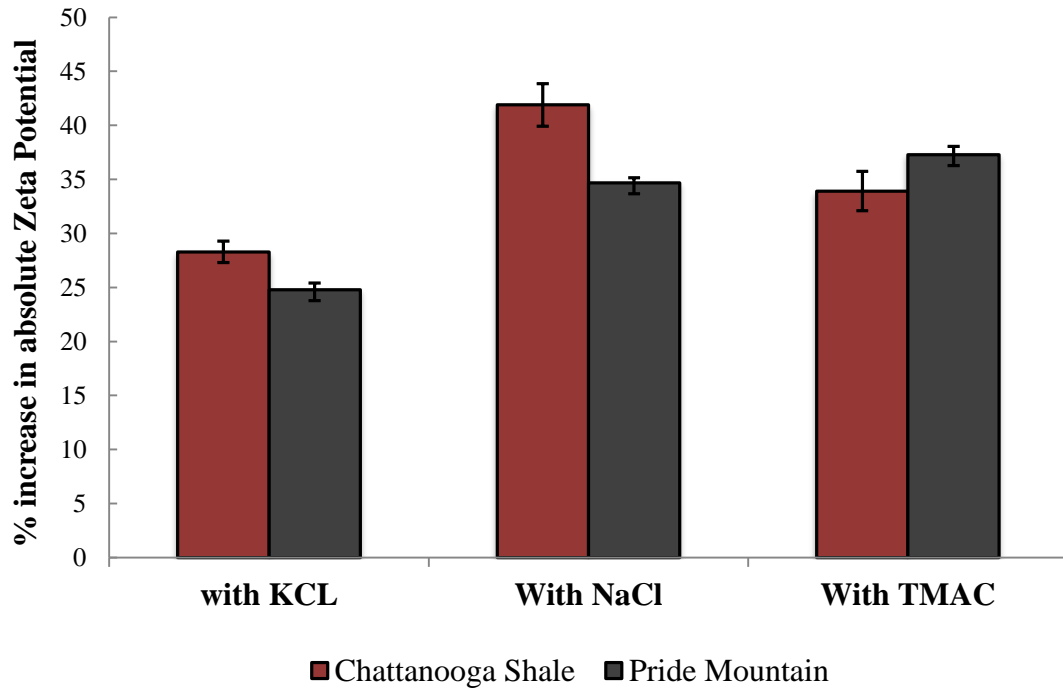


Figure 15: Increase in zeta potential for shale in anionic polyacrylamide with salt and TMAC

In order to observe flocculation of shale with cationic polyacrylamide, particle size measurements were made with time for the Pride Mountain shale-cationic polyacrylamide system. Figure 16 shows the increase in effective diameter of the shale particles with time. The system became unstable after 120 minutes because of flocculation and particle settling.

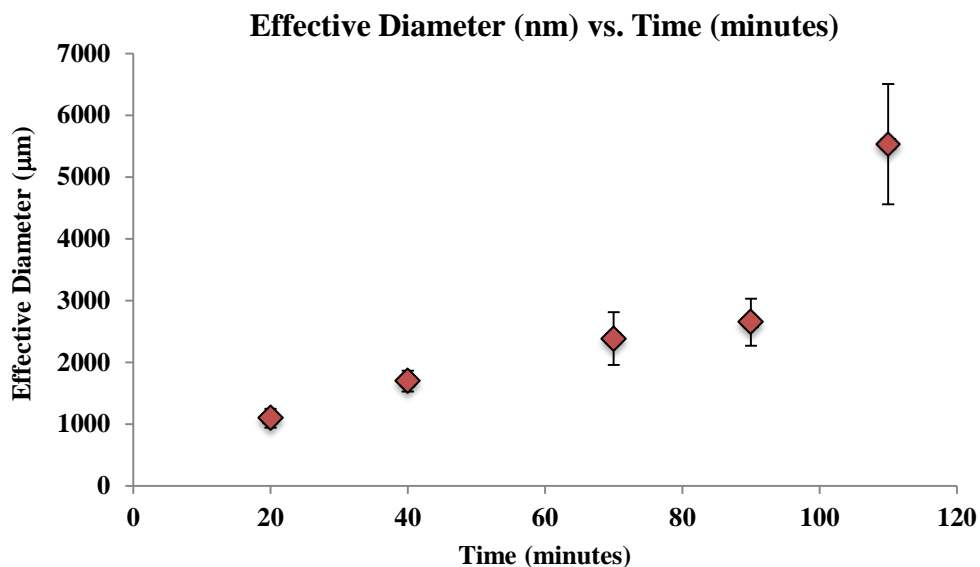


Figure 16: Flocculation of Pride Mountain shale in presence of cationic polyacrylamide as measured by dynamic light scattering

As shown in Figure 16, the effective diameter increased with time indicative of flocculation.

The results are in agreement with previous work on the effect of adsorption density on zeta potential. As adsorption density increases, the zeta potential of the shale polyacrylamide complex increases and levels off when the adsorption density approaches capacity (Menon & Wasan, 1987a, 1987b). In presence of cationic polyacrylamide, by contrast, the absolute value of zeta potential decreases due to flocculation. In summary, salt tends to decrease the adsorption density of polymer on clay surfaces and leaves fewer active sites on the clay surfaces for the polyacrylamides to interact.

2.3.2 Rheological Study of Polymer-Shale Interaction

Before characterizing the polymer - shale interaction, the critical overlap concentration (C^*) and critical entanglement concentration (C^{**}) of the polyacrylamides used in this study is determined. C^* is the concentration at which there is a significant degree of overlapping between the polymer molecules but not large enough to cause onset of entanglement. C^{**} indicates distinct onset of chain entanglements in the polymer solution (Gupta, Elkins, Long, & Wilkes, 2005). The polyacrylamide concentration was chosen such that, it was above C^* and well below C^{**} . Figure 17 and 18 below shows the C^* and C^{**} for anionic and cationic polyacrylamides. Cationic polyacrylamides tend to have higher hydrodynamic volume due to higher chain lengths and caused the C^{**} to be higher than that of anionic polyacrylamide.

The specific viscosity is determined using the following equation

$$\eta_{\text{specific viscosity}} = \frac{\eta_{\text{solution}} - \eta_{\text{solvent}}}{\eta_{\text{solvent}}}$$

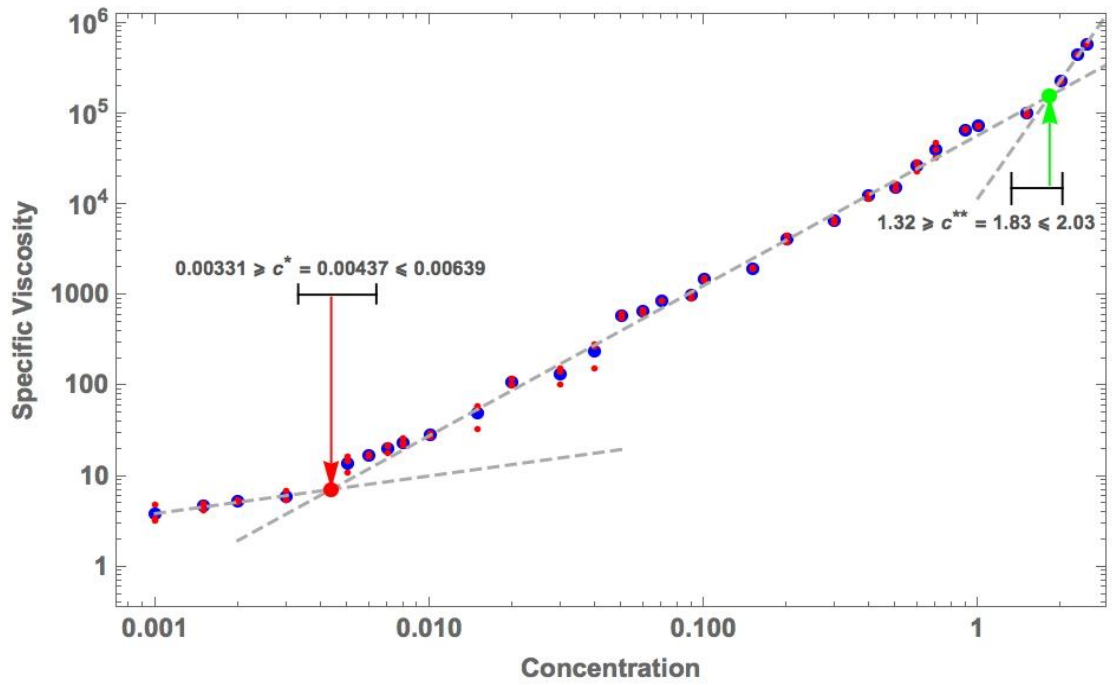


Figure 17: C^* and C^{**} for anionic polyacrylamide

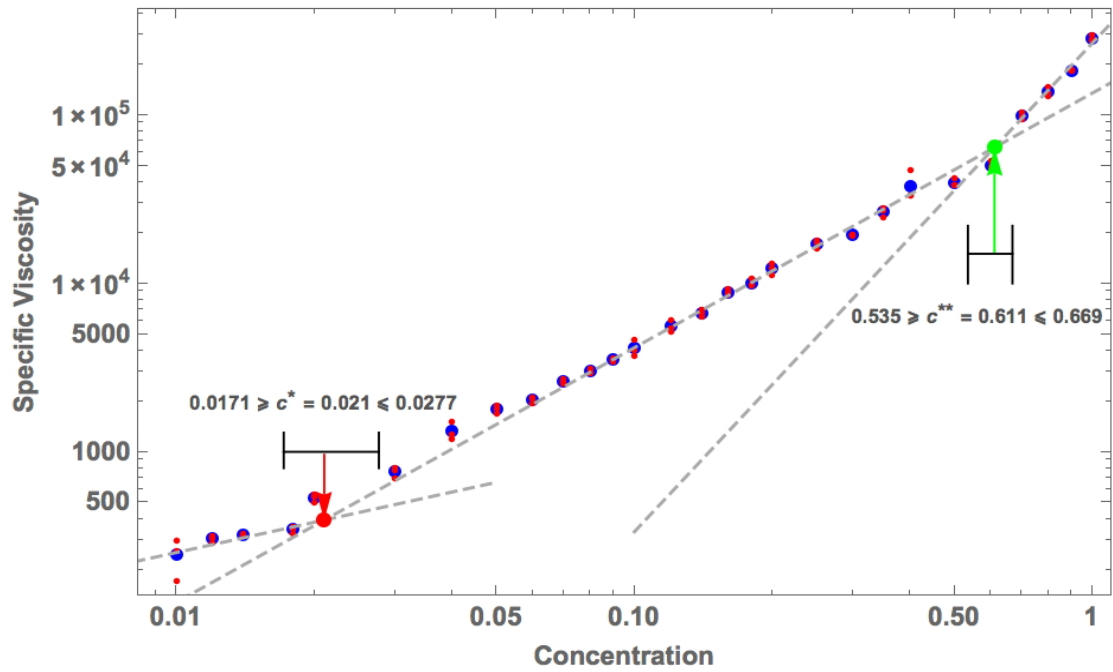


Figure 18: C^* and C^{**} for cationic polyacrylamide

In this section we discuss the rheology of the anionic and cationic polyacrylamide before and after adding the ground shale particles. The interaction of anionic polyacrylamide with the different shale samples was plotted as a function of anionic polyacrylamide concentration. The concentration of shale was kept constant at 0.5 lb/bbl, and the concentration of anionic polyacrylamide was varied from 0.1 to 0.2 Wt. %. The change in zero shear rate viscosity for the change in anionic polyacrylamide concentration is shown in Figure 19.

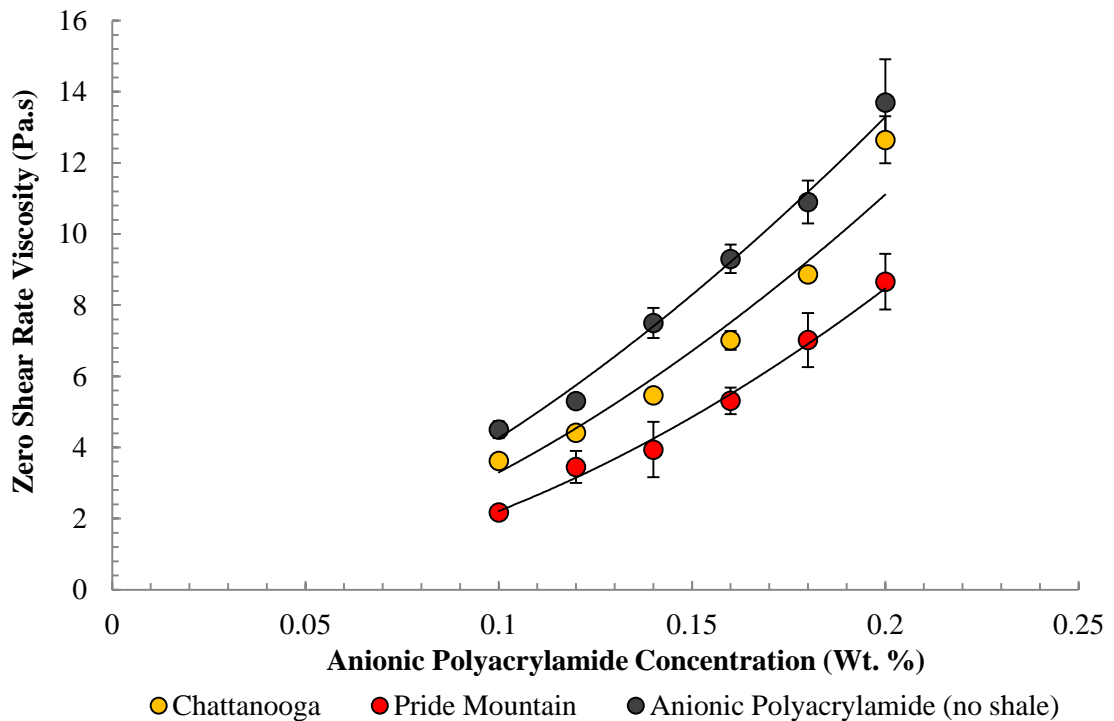


Figure 19: Change in zero shear rate viscosity with increasing anionic polyacrylamide concentration for Chattanooga and Pride Mountain shale

Figure 19 demonstrates that each shale interacts differently with anionic polyacrylamide. The Chattanooga shale sample has the highest viscosity in a given polyacrylamide concentration, and

the Pride Mountain sample has the lowest viscosity. Usually the sample with highest viscosity is considered to have strong interaction of the bulk fluid with the shale particles, but in this case the viscosity decreases after adding the shale to the polyacrylamide i.e. polyacrylamides without shale has higher viscosity values at a given polyacrylamide concentration. This is indicative of polyacrylamides adsorbing onto the shale and leaving the solution that is causing the decrease in the viscosity. Hence, Pride Mountain shale has stronger interactions with anionic polyacrylamide.

In order to determine the change in viscosity of the shale-polymer samples with time, flow ramp tests were conducted on the samples for 5 days at equal intervals. The concentration of the anionic polyacrylamide and shale was kept constant at 0.16 Wt. % and 0.5 lb/bbl respectively. After taking the first reading, the sample was left undisturbed in the geometry for few hours before the next reading. The sample is manually stirred in order to suspend the shale particles in the anionic polyacrylamide sample before starting the experiment. Figure 20 shows the change in viscosity of the shale-polymer sample with time.

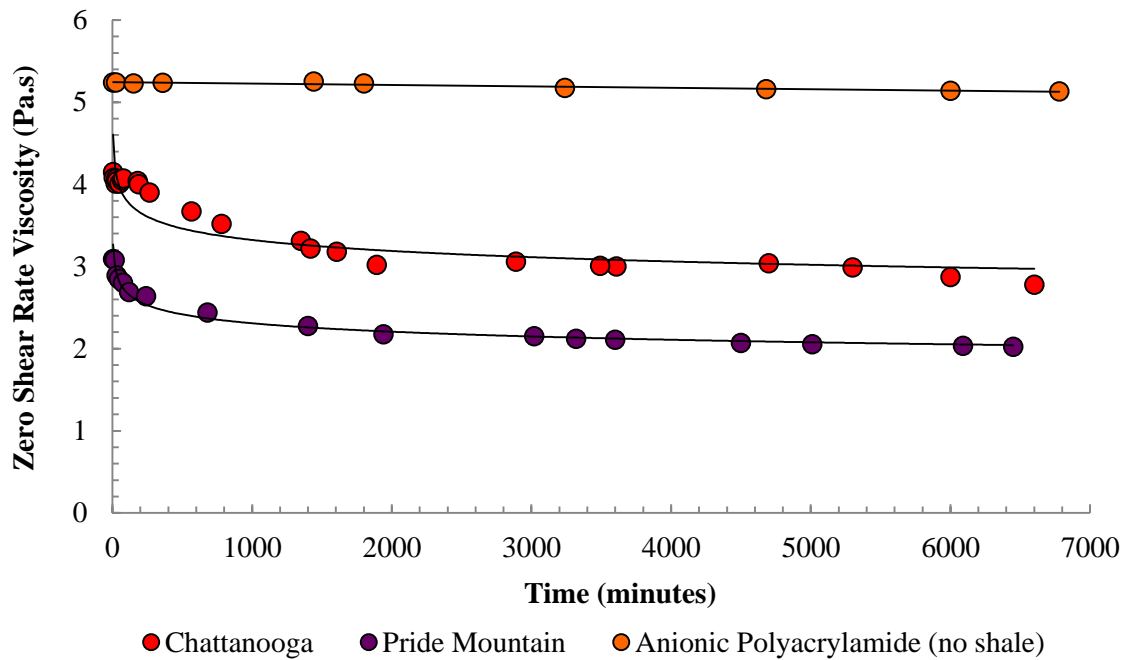


Figure 20: Change in zero shear rate viscosity with time of Chattanooga and Pride Mountain shale in anionic polyacrylamide

The viscosity curve (Figure 20) follows the same trend for both Pride Mountain and Chattanooga shale. After 2000 minutes the viscosity remains constant. This signifies the point at which the clay particles have reached saturation in the anionic polyacrylamide solution. The percentage of reduction of viscosity is approximately same for both the shale at the end of Day 5, which is ~ 34 %. The polyacrylamide is adsorbed onto the surface of shale particles, which leads to decreasing viscosity with time. Interestingly, the viscosity of the anionic polyacrylamide remains unchanged for the same experimental conditions, which proves that the anionic polyacrylamide remains stable over course of the experiment. In comparison with the zeta potential tests, rheological studies are easier to perform and the results are easier to interpret. Simple rheological methods like this can be used to assess shale-fluid interaction qualitatively.

CHAPTER III

3. Characterization of Shale-Fluid Interaction through a Series of Immersion Tests and Rheological Studies

3.1 Introduction

The interaction of shales with fluids used in drilling, completion, and stimulation of shale formations is an important and not well-understood aspect of the drilling, completion and production optimization process. Shale is a fine-grained sedimentary rock with high clay content (Huang, Azar, & Hale, 1998). Clay minerals have a great influence on the chemical and mechanical stability of shale. The common clay minerals present in shale are illite, montmorillonite, smectite, calcite and Kaolinite (Lu, 1988). Each clay mineral when present in abundance significantly changes the shale properties. For instance, mixed layer illite-smectite rich shale is reactive with water and smectite causes swelling of shale when in contact with water. Shale swelling is a primary cause of wellbore instability. When the shale absorbs water and ionic compounds from the injected fluid, it causes the clay layers to expand and the rock to swell (Zhang, Chenevert, Al-Bazali, & Sharma, 2004). Among the most important phenomena that cause shale to swell are osmotic effects associated with interaction of wellbore fluid with natural pore fluid during drilling and completion, as well as physio-chemical interactions between the reactive components of shale and the surrounding fluid (Chenevert, 1970; Steiger, 1993; Zhang et al., 2004).

Recent research demonstrates that each shale formation behaves uniquely when contacted with injected fluids (Gomez & He, 2012). Hence, formulations of these injected fluids have to be taken into account to minimize adverse effects. Interactivity between shale and wellbore fluid are measured by different means. Traditional tests, such as dispersion tests and swelling tests, do not fully account for the influence of fluid on rock structure and fracture development in shale (Junhao Zhou et al., 2013). Some of the commonly used methods use shale that is ground into fine particles and then reconstituted with water. These tests give completely different results that are often far from reality. Immersion tests give a visual confirmation of the effect of different types of fluid on rock structure (Rabe, da Fontoura, & dos Santos Antunes, 2002; Santos, Diek, Da Fontoura, & Roegiers, 1997). Immersion tests are used to evaluate the suitability of different drilling fluids for a particular shale formation. However, the absence of the confining pressure is a major limitation to the method (Santos et al., 1997). In this study, the interaction of wellbore fluids with shale was studied as a function of polymer concentration and salt type and concentration.

The common additives used in oilfield operations are friction reducers, acids, gellants, crosslinkers, clay control agents and other polymers. Polyacrylamide polymers are the most commonly used friction reducers and are also used as shale inhibitors albeit at higher concentrations. High molecular-weight polymers, such as polyacrylamide, provide effective shale inhibition by increasing the membrane efficiency of shale—they form a highly viscous isolation membrane on the shale that protects the rock from water (Mody et al., 2002). High molecular weight polyacrylamides also provide better friction reduction than the commonly used biopolymers such as guar and xanthan gum. High molecular weight polyacrylamides are thermally stable polymers that are stable at temperatures as high as 200°C (Carman & Cawiezel, 2007; Jia Zhou, Sun, Stevens, Qu, & Bai, 2011).

Potassium chloride (KCl), sodium chloride (NaCl) and TMAC are some of the common additives that are used to mitigate reaction of clay with process water. Salts such as NaCl and KCl are widely used in injected fluids for stabilization. Potassium salts are used as clay-swelling inhibitors, because the Potassium (K^+) ions penetrate into the porosity of the shale, creating a semi-permeable membrane, which prevents the water from entering the shale (Khodja et al., 2010). Simplified exposure tests were performed by (Horsrud et al., 1998) at simulated borehole conditions. They observed that exposure to KCl caused shrinkage of shale matrix and an increase of permeability. Shrinkage of shale is due to the K^+ ions replacing the previously adsorbed exchangeable cations on the clay surface leading to the compaction of clay structure (Horsrud et al., 1998; Okoro & Adewale, 2014). The rate of water inflow into the shale formation decreases with salt concentration due to the chemical potential of the process fluid being lower than that of the formation. This eventually leads to slower rate of pore pressure increase, thereby increasing shale stability (Tan et al., 1996). Shale exposed to salt solutions, such as KCl, NaCl and $CaCl_2$, dehydrates by transport of pore water into the contacting fluid (T. Al-Bazali, Zhang, Chenevert, & Sharma, 2008). Movement of ionic compounds from the shale to the fluid provides a reduction of intergranular friction that allows the grains to slip as stress is increased. This enhances shale strength (T. Al-Bazali et al., 2008; Tan et al., 1996). However, excessive dehydration can cause a decrease in the formation strength, thus reducing wellbore stability (Tan et al., 1996). KCl also offsets the friction reduction properties of polyacrylamide. Hence, the salt and polyacrylamide concentration should be carefully chosen to reduce viscosity reduction of polyacrylamides in the presence of salts.

Based on the immersion tests and rheological studies done in lab recommendations are provided for the four shale under study for the polymer and salt use. Additionally, based on the rheological

properties of the fluid mixtures used in this study an optimum salt and polyacrylamide system based on the rheological property of the fluid mixtures is determined.

3.2 *Materials and Methods*

3.2.1 Experimental Methods

This section is divided into two subsections. The first part focuses on characterizing shale samples in terms of mineralogy, porosity, total organic carbon (TOC) content, and pressure decay permeability. The second section focuses on immersion testing and analysis of the rheological properties of shale-fluid slurries to analyze the sensitivity of shale to wellbore fluids.

3.2.2 Shale Samples

To observe the effects of different wellbore fluid additives on shale, immersion testing was performed on shale samples from the Woodford Shale (Devonian, Anadarko Basin), Pride Mountain Formation (Mississippian, Black Warrior Basin), and Pottsville Formation (Pennsylvanian, Black Warrior Basin). Well-preserved core samples were used for the tests. Drying of the samples prior to the test causes a change in water content in the shale. A minimal change in water content dramatically changes the reactivity of the shale. Shale samples that were used in the tests were carefully preserved with large surface area that has had minimal exposure to coring fluids.

3.2.3 Shale Characterization

To characterize shale-fluid interaction it is imperative to characterize shale samples in terms of mineralogy, Total Organic Carbon (TOC) content, porosity and fluid saturation, and permeability to help understand shale-fluid interactions. Table 4 shows the various characterization methods used for the study.

Table 4: Shale characterization methods

Measurement	Equipment	Determination
Mineralogy	X- Ray Diffraction	Percentage composition of clay and non-clay minerals
TOC		Organic content of shale
Porosity and fluid saturation		Porosity of shale with respect to mobile pore fluid volume (water, oil, gas)
Pressure Decay Permeability		Clay matrix permeability
Surface Characteristics	Scanning Electron Microscopy	Mineral fabric, surface morphology of shale

Rock Mineralogy: X-Ray Diffraction (XRD) is used to determine the clay and non-clay content present in the shale samples quantitatively. XRD is a robust and powerful technique widely used in the characterization of shales. The quantitative analysis of clay, non - clay and expandable clay content is done using XRD. Table 5. Shows the clay content and the non-clay mineral content of the shale samples.

Table 5: Whole rock mineralogy of shale samples from different formations

Analysis	Woodford	Woodford	Chattanooga	Pride Mountain
Depth (ft)	10,372	10,382	9167	2,863
Clay Content (Wt. %)				
Smectite			0	1
Illite/Smectite	6	3	5	16
Illite+Mica	33	28	24	37
Kaolinite	Tr	Tr	0	12
Chlorite	1	Tr	0	4
Non Clay Mineral Content (Wt. %)				
Quartz	28	32	41	21
K Feldspar	5	4	16	3
Plagiocase	8	7	2	2
Calcite	Tr	Tr	0	1
Ankerite/Fe Dolomite	2	1	0	1
Dolomite			5	0
Pyrite	6	4	5	1
Fluorapatite	Tr	0	0	0
Barite	0	0	1	1
Siderite	Tr	Tr	0	1
Magnetite	0	0	0	0

Total Organic Content (TOC): The TOC is a crucial indicator of the development and behavior of shales. Many times TOC is determined in order to measure the kerogen content of the shale, but kerogen has sulfur, nitrogen, oxygen and hydrogen in addition to carbon. Organic rich shales have higher permeability and also are reactive compared to the less organic shales (Rickman, Mullen, Petre, Grieser, & Kundert, 2008). TOC, effective porosity and pressure-decay permeability are shown in Table 6.

Porosity: Determining the porosity of shale is important in understanding the mechanical behavior of shale at different stresses and in understanding shale stability and failure limit (Josh et al., 2012). The permeability of the shale is dependent on the pore sizes, which controls the elasticity and mechanical strength of shales (Khodja et al., 2010). Effective porosity is shown in Table 3.

Pressure Decay Permeability: The pressure decay permeability method is standard for measuring permeability in shale and other nano- to microdarcy rocks. Pressure decay takes a fraction of the time required for steady-state methods (Jones, 1997). Pressure decay permeability measurements are shown in Table 6.

Table 6: TOC, Effective Porosity, Pressure decay permeability and % Water Saturation

Parameters	Woodford (10372 ft)	Woodford (10382 ft)	Chattanooga (9167 ft)	Pride Mountain (2863 ft)
TOC (Wt. %)	4.68	3.76	3.33	0.80
Effective Porosity (% of BV)	4.8	4.8	2.32	12.30
Pressure Decay Permeability (μ D)	0.36	0.53	0.32	0.48
Water Saturation % of PV	40	29.7	8.13	76.56

Scanning Electron Microscopy: SEM techniques were used to study the surface properties and morphology of the shale under study. Cores were sliced to get 1 – 2 mm shale samples, parallel to the bedding plane. The sample was placed on the stub were sputter coated with conducting layers of gold. The surface of the shale was examined using different magnifications. In order to determine the elemental composition of shales, the shale samples were coated with layers of carbon and Energy Dispersive Spectroscopy (EDS) analysis of shale samples were done to determine elemental composition. Figures 21 through 23 show the morphology of the shale samples studies in this work.

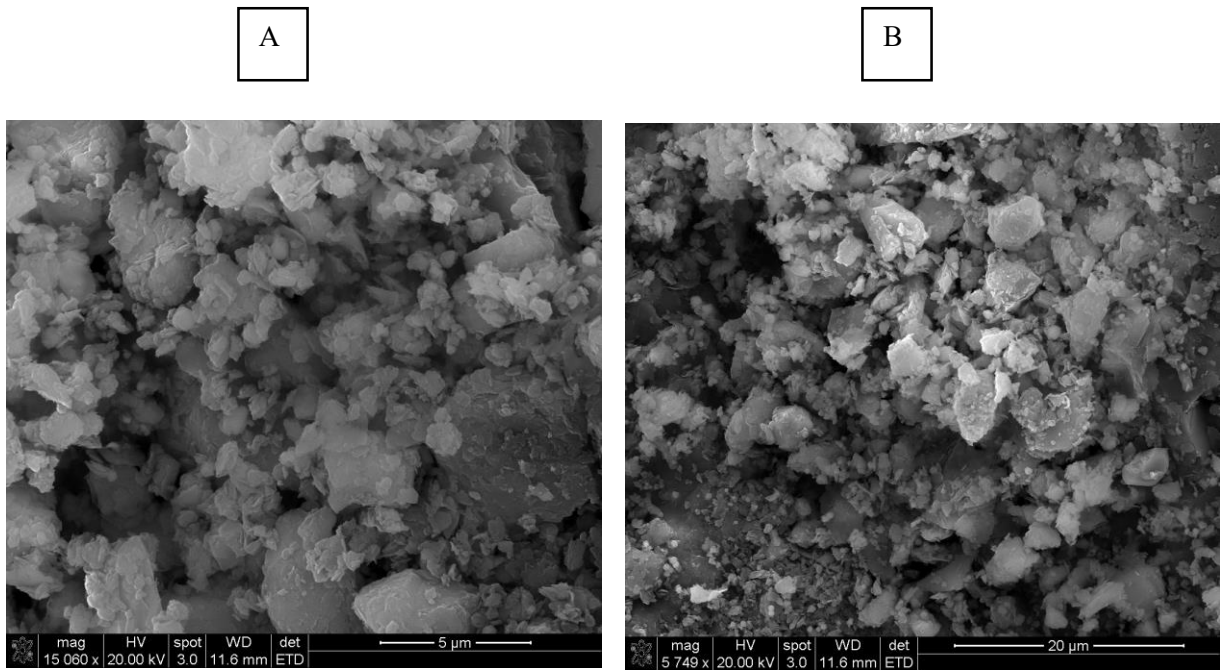


Figure 21: SEM images of Woodford Shale in Rother (10372.1 ft). Images A and B contain abundant randomly oriented clay platelets

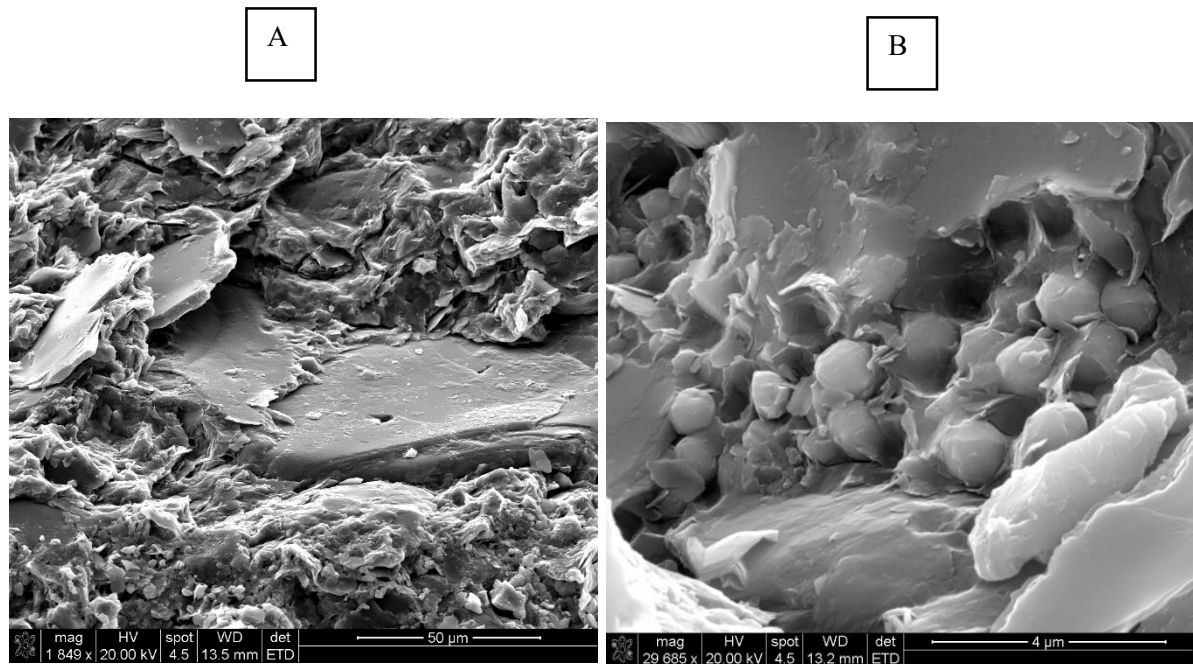


Figure 22: SEM images of pyrite in the Gorgas #1 well, Pride Mountain Formation (2864.4 ft) (A) Poorly aligned and folded clay platelets. (B) Clusters of pyrite crystals forming of spherical to oblate framboids

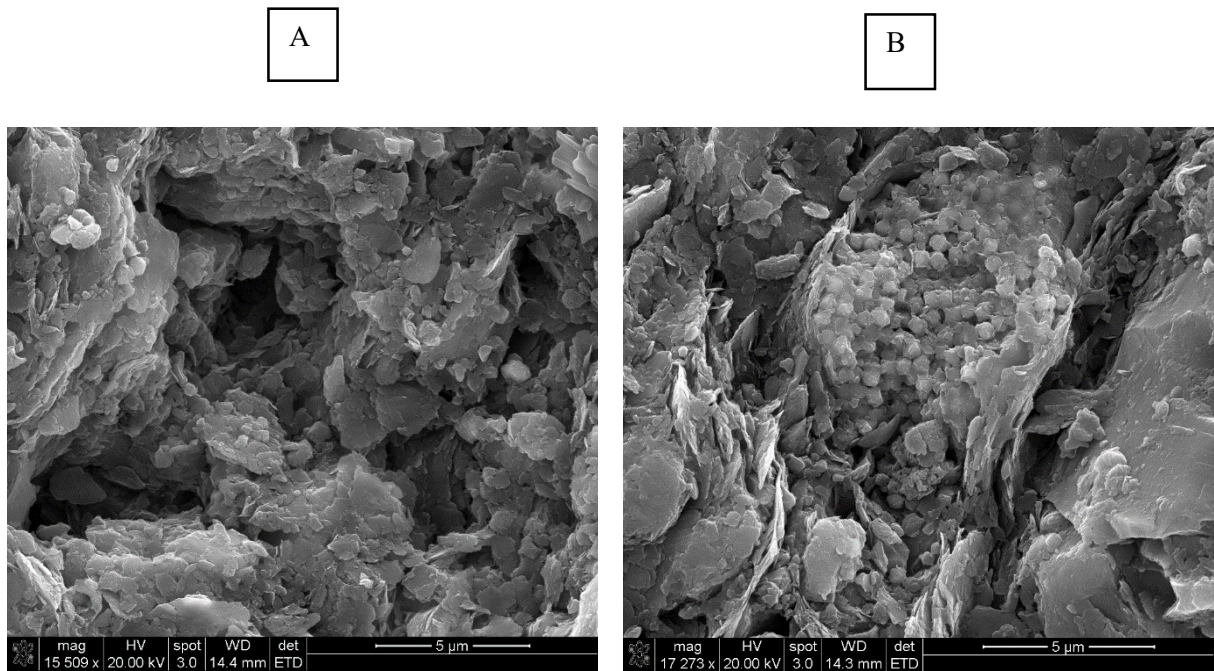


Figure 23: SEM images of Chattanooga Shale in Lamb 1 - 3 #1 well (9173.5 ft). (A) Randomly oriented clay platelets (B) Pyrite framboids in matrix of platy illite

3.3 *Formulation of Fluid Phase*

3.3.1 *Fluid Design*

One of the main objectives of this study was to study shale – fluid interaction. The fluids used are common oilfield fluids combined with additives, such as anionic and cationic polyacrylamide. Wyoming bentonite was used as the clay in this study. Other additives include KCl, NaCl and TMAC (Table 7).

Table 7: Composition of different fluid mixture used in the study

S/N	Fluid Mixture	Composition
1	Bentonite	2 lb/bbl bentonite + 0.2 wt.% anionic polyacrylamide 2 lb/bbl bentonite + 0.2 wt.% cationic polyacrylamide
2	KCl–Bentonite	2 lb/bbl bentonite + 0.2 wt.% anionic polyacrylamide + 2 % KCl 2 lb/bbl bentonite + 0.2 wt.% cationic polyacrylamide + 2 % KCl
3	NaCl–Bentonite	2 lb/bbl bentonite + 0.2 wt.% anionic polyacrylamide + 2 % NaCl 2 lb/bbl bentonite + 0.2 wt.% cationic polyacrylamide + 2 % NaCl
4	TMAC–Bentonite	2 lb/bbl bentonite + 0.2 wt.% anionic polyacrylamide + 2 % TMAC 2 lb/bbl bentonite + 0.2 wt.% cationic polyacrylamide + 2 % TMAC

Base Fluid used is DI Water (400 ml)

3.3.2 Equipment

A Discover DHR-3 controlled stress rheometer was used to make rheological measurements of the samples. Vane geometry was used for the polymer-shale samples; this geometry helps prevent wall slippage at higher shear rates, helps disrupt flow inhomogeneity while shearing, and also works well for samples containing suspended solids. For polymer solutions, the cone and plate geometry was used. Cone and plate is useful for solutions that have low viscosity and do not contain suspended solids > 64 μm in diameter. Cone and plate geometry (diameter: 60 mm and cone angle 2°) provide homogenous shear, shear rate and stress in the geometry gap. All experiments were performed at a temperature of 25 °C \pm 0.03 °C. The polymer-shale sample was pre-sheared at 200 s⁻¹ before the start of each experiment.

3.3.3 Immersion Tests

Preserved core samples were immersed in different fluid mixtures of varying compositions at 60°C. The samples were sealed and left in the fluid for five days for inert shale and two days for reactive shale. The change in weight of the shale samples before and after the test, linear swelling, and the change of hardness were measured. SEM images of the samples after exposure to characterize morphologic changes on the shale surface. The change in thickness of shale samples used in study was measured before and after the immersion tests using a Vernier caliper. This provides a qualitative measurement of the extent of sample expansion or shrinkage when in contact with the injected fluids. Additionally, change in weight of the shale samples was measured after immersion tests. The results were correlated with the linear swelling test results. In order to study the isolated effect of salt and polyacrylamides separately, immersion tests were performed with salts, polyacrylamides, and no additives.

3.4 Results and Discussion

The Woodford sample was immersed in salt solution to study the effectiveness of salt for preventing swelling. Figure 24 shows the percent expansion/shrinkage of Woodford Shale immersed in KCl, NaCl, TMAC and DI Water. The shale swells most in DI water. This is expected due to the water activity being highest in DI water, the water is driven towards the shale, which causes the swelling. This result is reflected in weight gain where DI water has the maximum weight gain. In the absence of other additives, TMAC causes maximum shrinkage. In many cases, shrinkage of shale by dehydration increases rock strength, and hence, wellbore stability (Horsrud et al., 1998; Mody & Hale, 1993; Zhang et al., 2004). However, in the previous studies, it has been shown that excessive shrinkage of shale can cause reduction in strength (Horsrud et al., 1998).

Figure 25 shows the percentage of expansion and shrinkage of Woodford shale immersed in anionic polyacrylamide and cationic polyacrylamide in comparison to DI water. Shale immersed in anionic polyacrylamide shrinks more than the cationic polyacrylamide. When compared with salt solutions, the polyacrylamides provide better inhibition of swelling. Polymers have been proven to be effective in bridging the interlayer spacing between the clay platelets, and they also form a stable isolation membrane that prevent the water from entering the shale.

To study the effectiveness of salts, TMAC, and polyacrylamides as shale inhibitors when mixed with bentonite mud, immersion tests were performed with fluid mixtures as shown in Table 7. When in contact with the medium, all of the Woodford samples shrunk. Shrinkage was greater in TMAC, and minimal with NaCl and cationic polyacrylamide. However, the samples showed considerable weight gain because of adsorption of the polyacrylamides on the shale surface.

The effect of salts, TMAC and polyacrylamides on the swelling behavior of Woodford Shale was studied separately (Figure 24 through Figure 26). As expected, the swelling was greatest for shale immersed in DI water. The shale immersed in a 2% NaCl solution swelled, whereas it shrunk in a 2% KCl solution. The hydrated radius of sodium is larger than that of potassium as a result of which a greater amount of water entered Woodford Shale after it was exposed to the NaCl solution (Junhao Zhou et al., 2013). Maximum weight gain was greatest for shale immersed in DI water followed by 2% NaCl, 2% KCl and 2% TMAC, respectively.

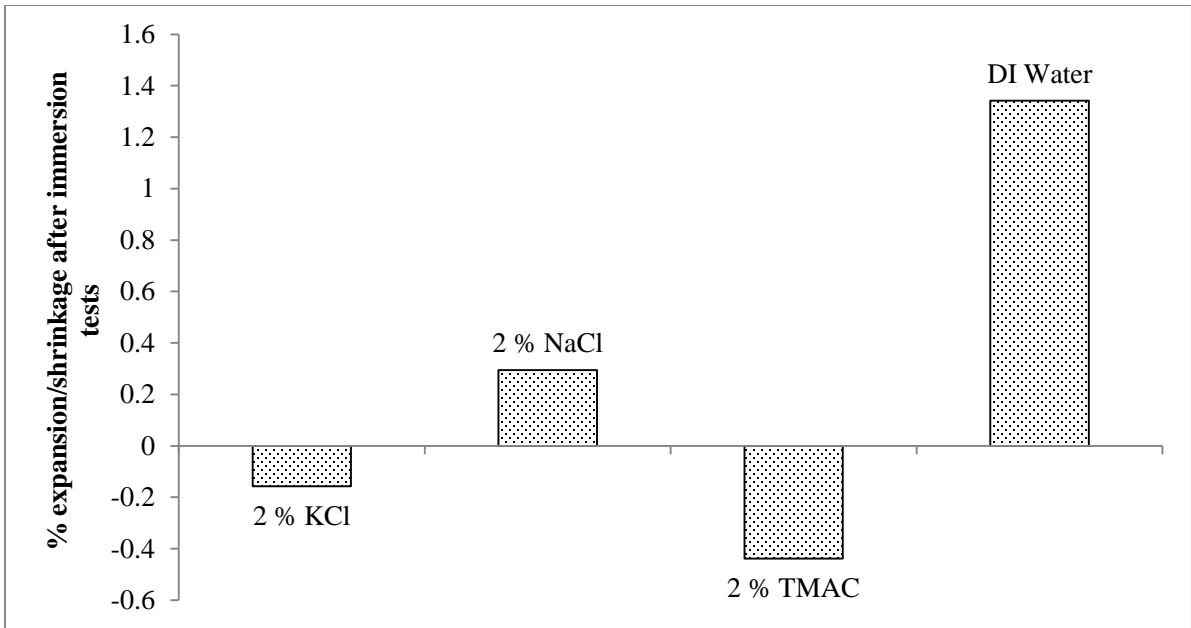


Figure 24: Percent expansion or shrinkage of Woodford Shale after immersion test

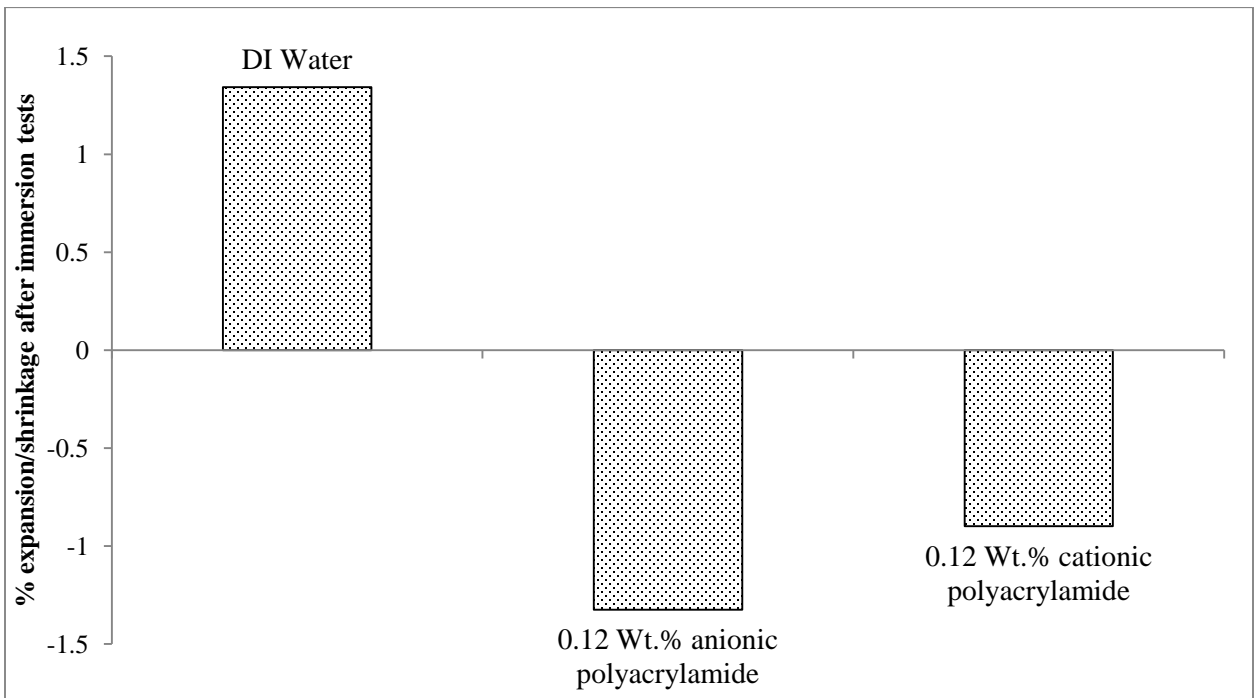


Figure 25: Percent expansion or shrinkage of Woodford Shale after immersion test

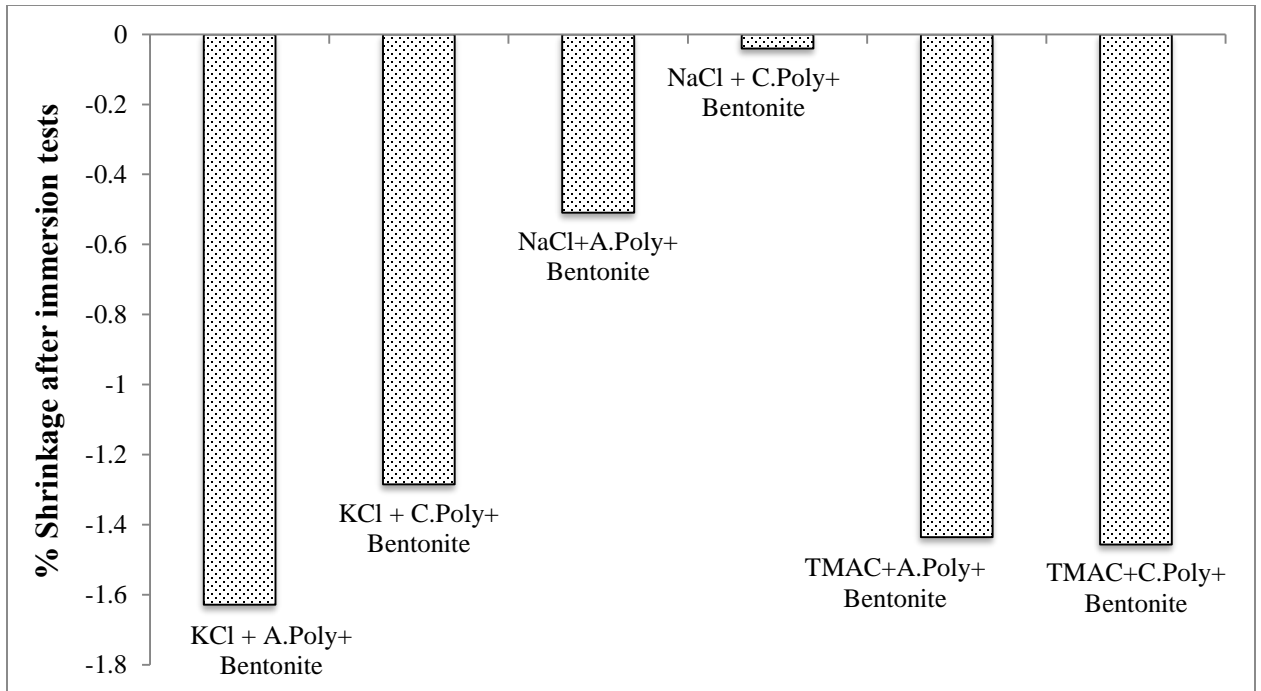


Figure 26: Percent expansion or shrinkage of Woodford Shale after immersion test

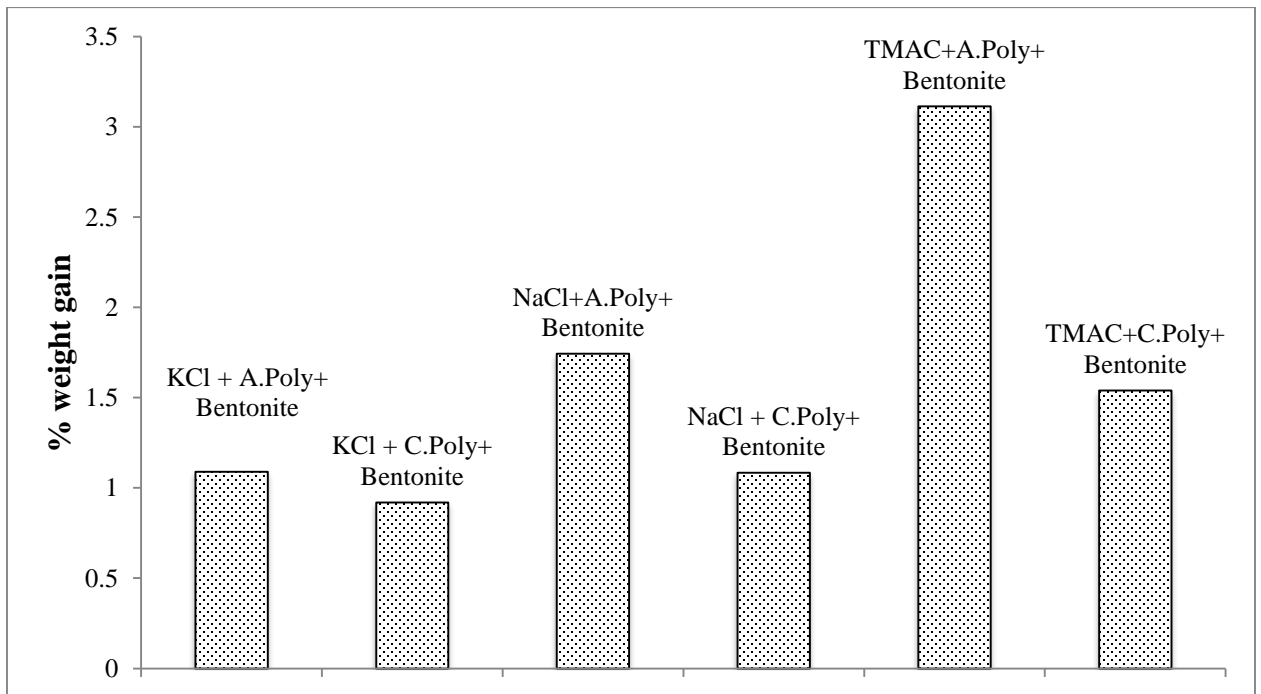


Figure 27: Percent weight gain of Woodford Shale after immersion test

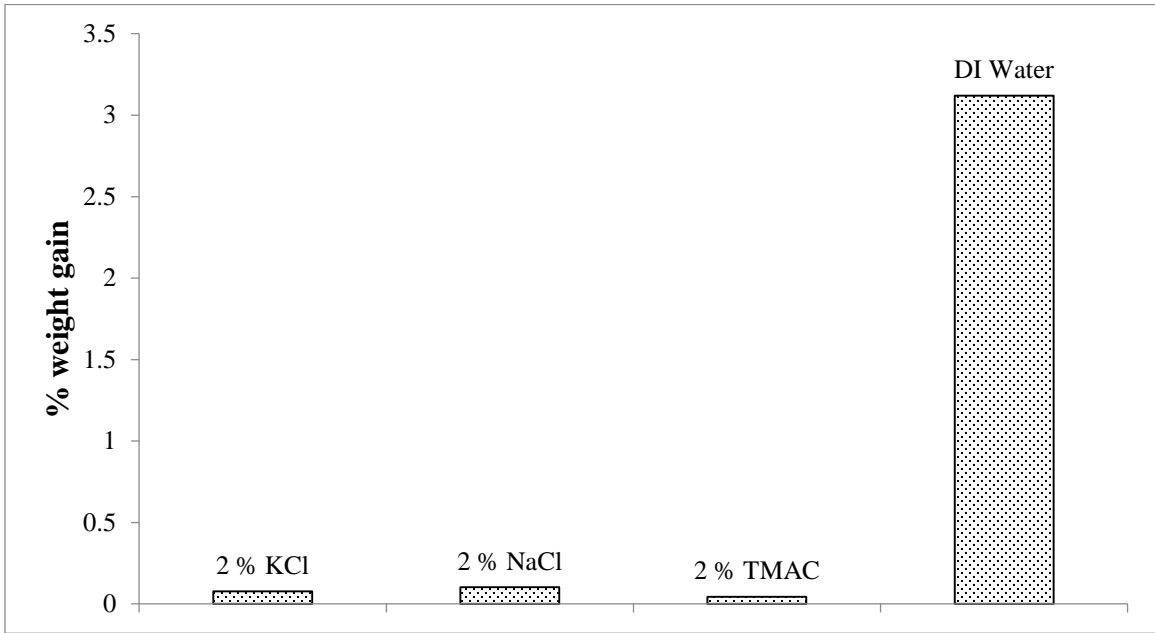


Figure 28: Percent weight gain of Woodford Shale after immersion test

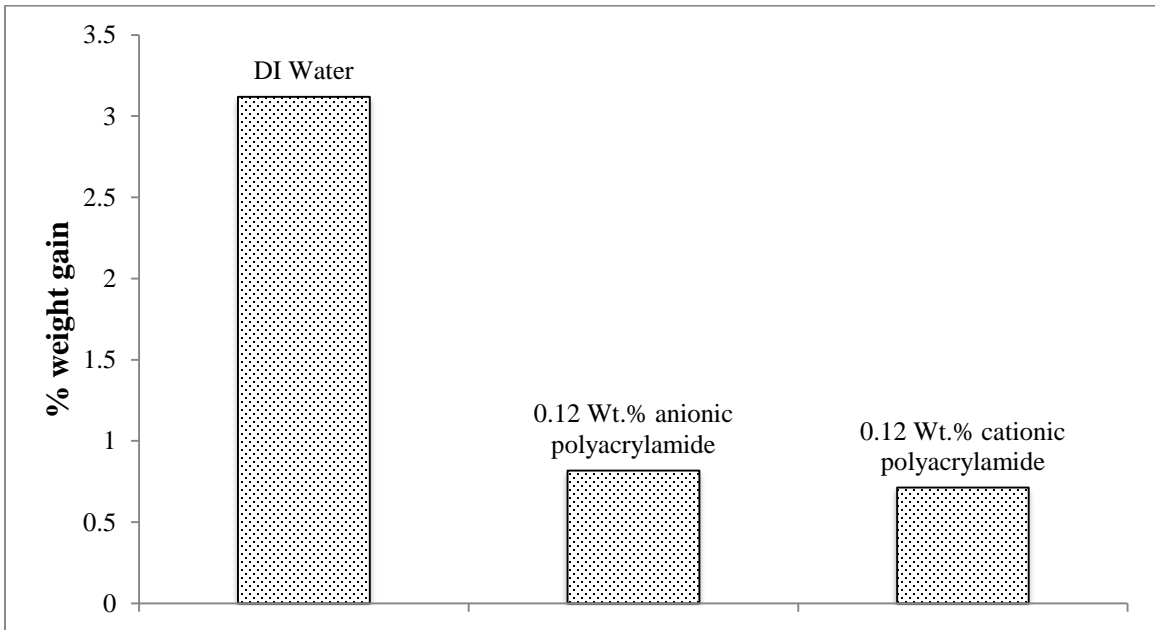


Figure 29: Percent weight gain of Woodford Shale after immersion test

Bentonite mud is commonly used when drilling shale wells and is proven to cause swelling and dispersion of shale formations. But when used with polyacrylamides and salts, the swelling can be minimized. The mechanism of shale inhibition investigated in this study is effective adsorption of polyacrylamide and salt on the shale, which prevents water from entering the shale. The surface of immersed shale was analyzed using SEM to see the nature of polyacrylamide-salt adsorption (Figure 30 through 33).

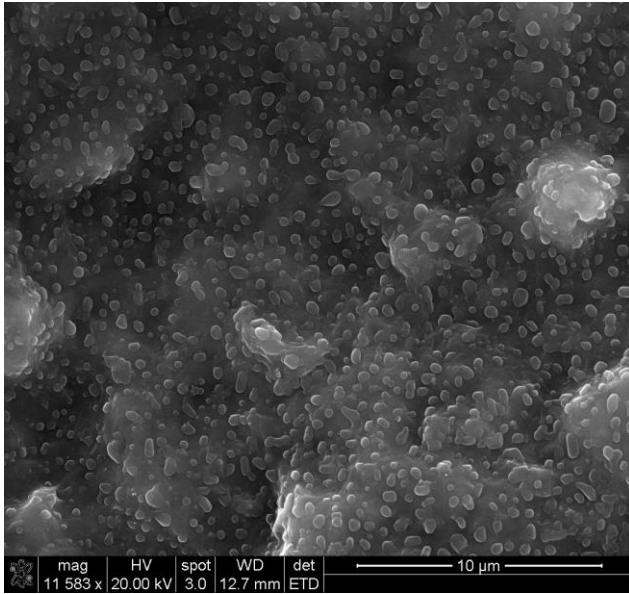


Figure 30: Surface of Woodford shale immersed in Bentonite + NaCl + Anionic Polyacrylamide

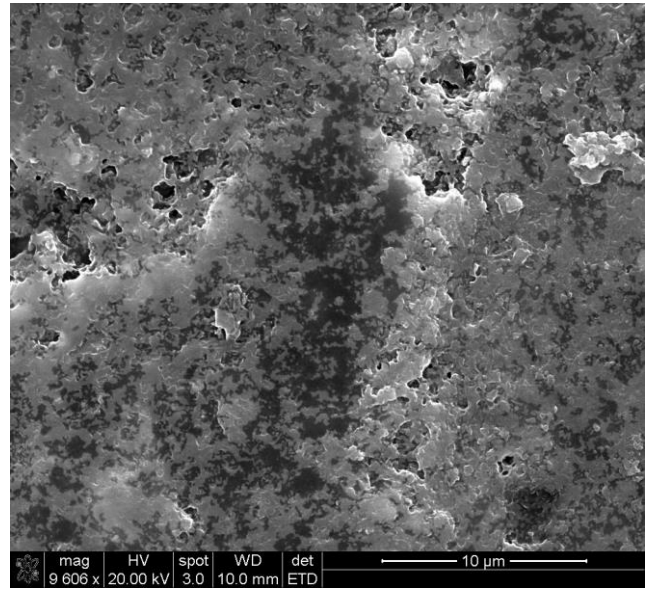


Figure 31: Surface of Woodford shale immersed in Bentonite + TMAC + Cationic Polyacrylamide

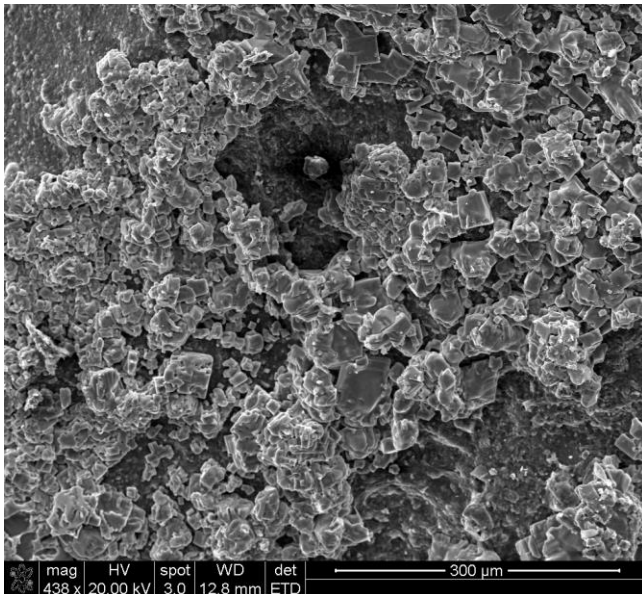


Figure 32: Surface of Woodford shale immersed in Bentonite + KCl + Cationic Polyacrylamide

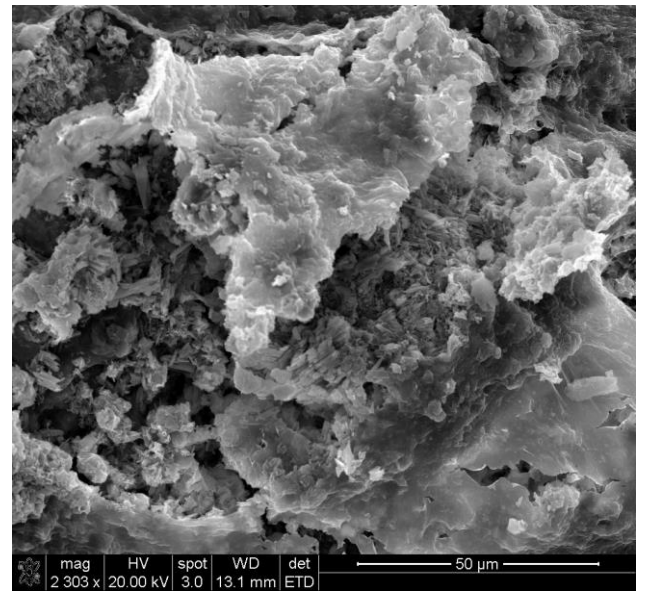


Figure 33: Surface of Woodford shale immersed in Bentonite + NaCl + Cationic Polyacrylamide

There was a significant change in the surface morphology of shale immersed in mud systems 2, 3 and 4 as observed using SEM. Bentonite with NaCl and anionic polyacrylamide forms a uniform membrane over the shale, which prevents the water from entering or leaving the shale, which explains the small percentage of shrinkage. As seen in Figure 31, there is minimal adsorption of polyacrylamide on the Woodford shale surface. TMAC has proven to effectively inhibit polymers from adsorbing onto the shale surfaces from the fracturing fluids (Himes & Simon, 1990). For shale immersed in cationic polyacrylamide with salts, salt and polyacrylamide precipitate on the surface of the shale. The KCl–cationic polyacrylamide system, in particular, provides a better inhibition due to the precipitation of salts on the surface which forms a thicker layer on the shale which prevents the shale from swelling or dispersing. The precipitation of the osmotic membrane on the exposed shale surface prevents the flow of water and ions into the shale, this membrane however allows water movement out of the shale, which leads to the shrinking of the shale (Fink, 2015).

The qualitative description of Woodford Shale samples is shown in Table 8 after the immersion tests. For most of the tests the Woodford sample remained intact and did not disperse or disintegrate during the test period. This could be attributed to less expandable clay, which promotes swelling, and higher quartz content, which imparts mechanical strength. Additionally, low porosity reduces the reactivity of the shale. The shale was comparatively softer when immersed in TMAC–bentonite mud. There are two possible reasons for this phenomenon. First, TMAC prevents the adsorption of polyacrylamide on the surface of the shale that leads to water and ions entering and leaving the shale. The second possibility is that the chemical potential difference between the fluid surrounding the shale and the pore fluid is higher, causing an osmotic potential difference that leads to shrinking of shale sample.

Table 8: Qualitative description of Woodford shale samples after immersion tests

Sample	Qualitative description
Anionic Polyacrylamide + Bentonite	Intact,Soft
Cationic Polyacrylamide + Bentonite	Intact,Firm
KCl + Anionic Polyacrylamide + Bentonite	Intact,Soft
KCl + Cationic Polyacrylamide + Bentonite	Intact,Hard
NaCl+Anionic Polyacrylamide + Bentonite	Intact,Hard
NaCl + Cationic Polyacrylamide + Bentonite	Intact,Hard
TMAC + Anionic Polyacrylamide+ Bentonite	Intact,Soft
TMAC + Cationic Polyacrylamide + Bentonite	Intact,Soft
2 % KCl	Intact,Hard
2 % NaCl	Intact,Hard
2 % TMAC	Intact,Hard
DI Water	Intact,Hard
0.12 Wt.% Anionic Polyacrylamide	Intact,Hard
0.12 Wt.% Cationic Polyacrylamide	Intact,Hard

The Chattanooga and Pride Mountain shale samples were chosen to study the effect of salt and polyacrylamides for limiting the swelling/dispersion of shales. Chattanooga shale has a lower expandable clay and higher quartz content, which makes it hard. Conversely, Pride Mountain shale is rich in mixed and expandable clays and is soft. The change in weight of both the shales was used as a measure of shale reactivity (Figures 34 through 37). The weight gain was maximum for TMAC in Pride Mountain and Chattanooga shale, which is indicative of TMAC entering the shale and causing it to swell.

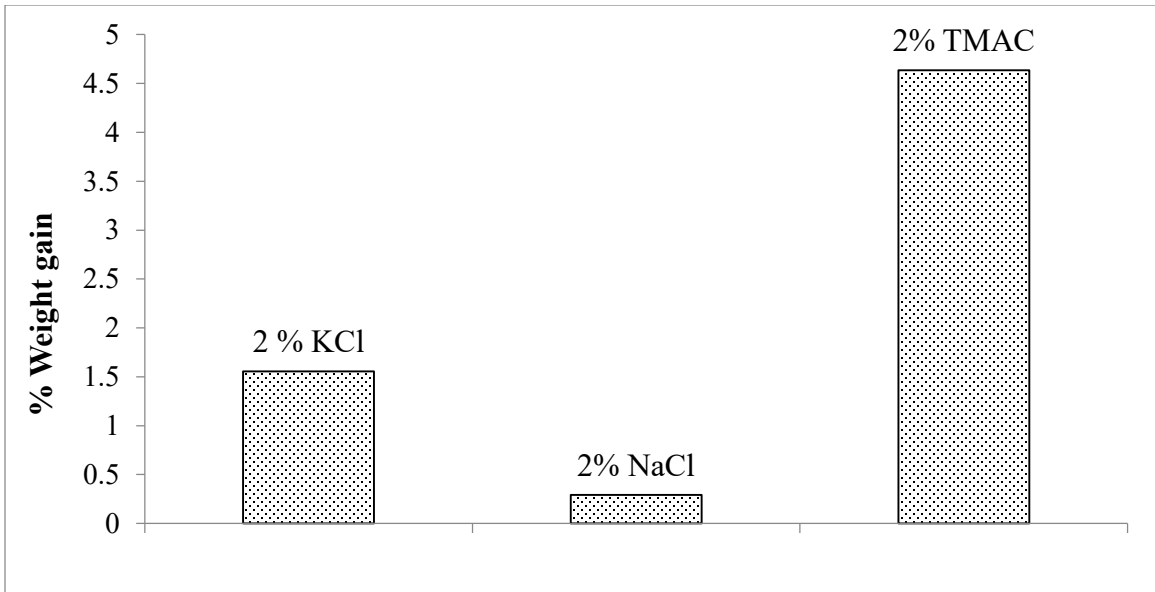


Figure 34: Percent weight gain of Chattanooga shale after immersion test

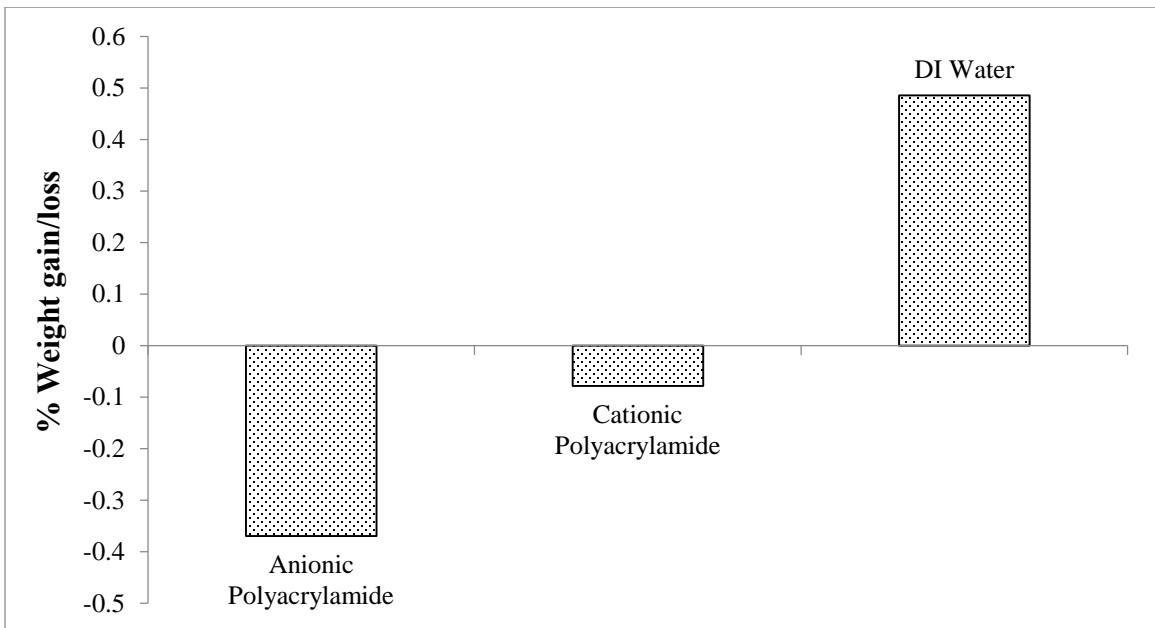


Figure 35: Percent weight gain or loss of Chattanooga shale after immersion test

Table 9: Qualitative description of Chattanooga shale samples after immersion tests

Sample	Qualitative Description
DI Water	Intact/Firm
2 % KCl	Intact/Firm
2% NaCl	Intact/Firm
2% TMAC	Intact/Soft
Anionic Polyacrylamide	Intact/Firm
Cationic Polyacrylamide	Intact/Firm

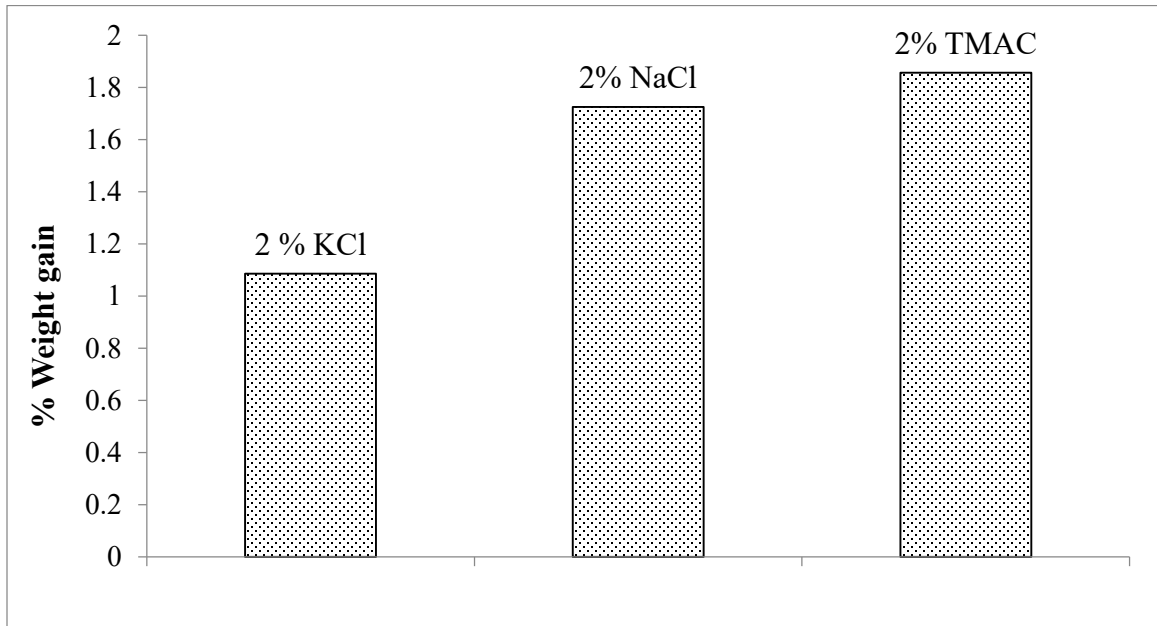


Figure 36: Percent weight gain of Pride Mountain Formation shale after immersion test

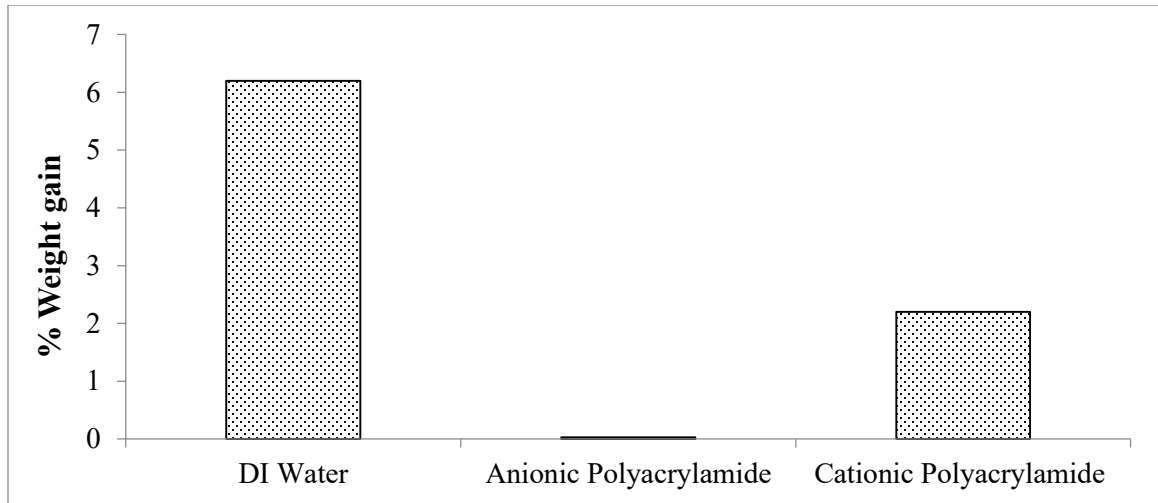


Figure 37: Percent weight gain of Pride Mountain Formation shale after immersion test

Table 10: Qualitative description of Pride Mountain Formation shale samples after immersion tests

Sample	Qualitative Description
DI Water	Disintegrated
2 % KCl	Intact/Firm
2% NaCl	Intact/Soft
2% TMAC	Intact/Firm
Anionic Polyacrylamide	Intact/Firm
Cationic Polyacrylamide	Intact/Firm

The transport of solutes to and from fluids to shales is caused by chemical potential gradient between the shale and the fluid (Van Oort, 2003). The surrounding fluid's ion content exceeds that of the pore fluid that causes the ions to diffuse from the fluid to the shale. Also, ionic compounds in the interplatelet spaces cause swelling due to repulsion of ions of similar charge. TMAC in the absence of other additives adsorbs onto the shale surface, thereby causing repulsion of the $N(CH_3)_4^+$ ions, which leads to an increase in swelling pressure. However, TMAC when

used with other fluid additives such as polyacrylamides and bentonite can prove to be good at inhibiting swelling of the shale. It is recommended not to use high concentration of TMAC for Chattanooga and Pride Mountain shale even in the presence of other additives. The anionic and cationic polyacrylamides are efficient in preventing shale dispersion and swelling for both the Pride Mountain and Chattanooga shale. The qualitative description of the shale after the immersion tests is given in Tables 9 and 10. The recommendations for the type of salt to be used for the 3 shales are given in Tables 11 through 13.

Table 11: Application of KCl based fluids for the shales under study

Shale	Shale Type	Dispersion limiting ability of KCl	Swelling limiting ability of KCl	Is the use of KCl suggested
Woodford	Medium Hard, high in illite, with expandable clays, less dispersion shale	Fair	Good	Yes
Chattanooga	Hard, high in quartz, less expandable clays	Good	Fair	Yes
Pride Mountain	Soft, high expandable, interlayer mixed clays and highly dispersible	Good	Good	Yes

Table 12: Application of NaCl based fluids for studied shale formations

Shale	Shale Type	Dispersion limiting ability of NaCl	Swelling limiting ability of NaCl	Is the use of NaCl suggested
Woodford	Medium Hard, high in illite,with expandable clays, less dispersion shale	Good	Fair	Yes
Chattanooga	Hard, high in quartz, less expandable clays	Good	Good	Yes
Pride Mountain	Soft, high expandable, interlayer mixed clays and highly dispersible	Fair	Fair	No

Table 13: Application of TMAC-based fluids for the studied shale samples

Shale	Shale Type	Dispersion limiting ability of TMAC	Swelling limiting ability of TMAC	Is the use of TMAC suggested
Woodford	Medium Hard, high in illite,with expandable clays, less dispersion shale	Fair	Good	Yes
Chattanooga	Hard, high in quartz, less expandable clays	Good	Fair	No
Pride Mountain	Soft, high expandable, interlayer mixed clays and highly dispersible	Good	Good	Yes

3.4.1 *Rheological Studies*

The effect of salts on the rheological properties of the fluid mixtures used in the study is discussed in this section (Figure 38 and 39). Salts were found to be detrimental to the rheology of the fluids containing anionic polymer. The K^+ ions form a strong bond between the smectite layers in the bentonite, thereby leading to clay aggregates and reduction in the fluid viscosity (Güven, Panfil, & Carney, 1988). The addition of potassium salts in anionic fluids leads to reduction in viscosity, whereas in cationic fluid systems, salts improve the rheology of the system. This is because apparent viscosity is higher in saline fluids containing cationic polymers. Addition of salt to the cationic polyacrylamide system leads to polyacrylamide-bentonite aggregates that result from the interaction of polyacrylamide with the negative face charge of bentonitic clay. Bentonite is sodium montmorillonite clay, which is major expandable clay in many North American shales. Additionally, the rheological results can be used to correlate the interaction of sodium montmorillonite, with polyacrylamides and salt. Higher apparent viscosity indicates stronger interactions between the clay and the bulk fluid. For both the cationic and anionic polyacrylamide, the viscosity is higher in the presence of TMAC. This corroborates with our immersion tests and SEM results. With TMAC, the bulk fluid adsorbs/sticks to the shale surface more preventing the water from entering the shale.

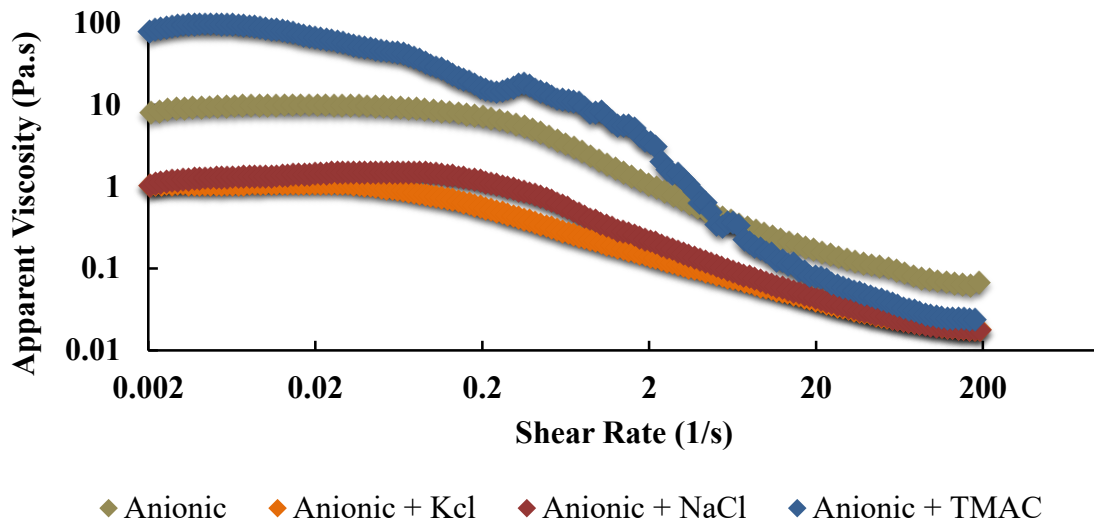


Figure 38: Change in apparent viscosity of an anionic polyacrylamide system with shear rate

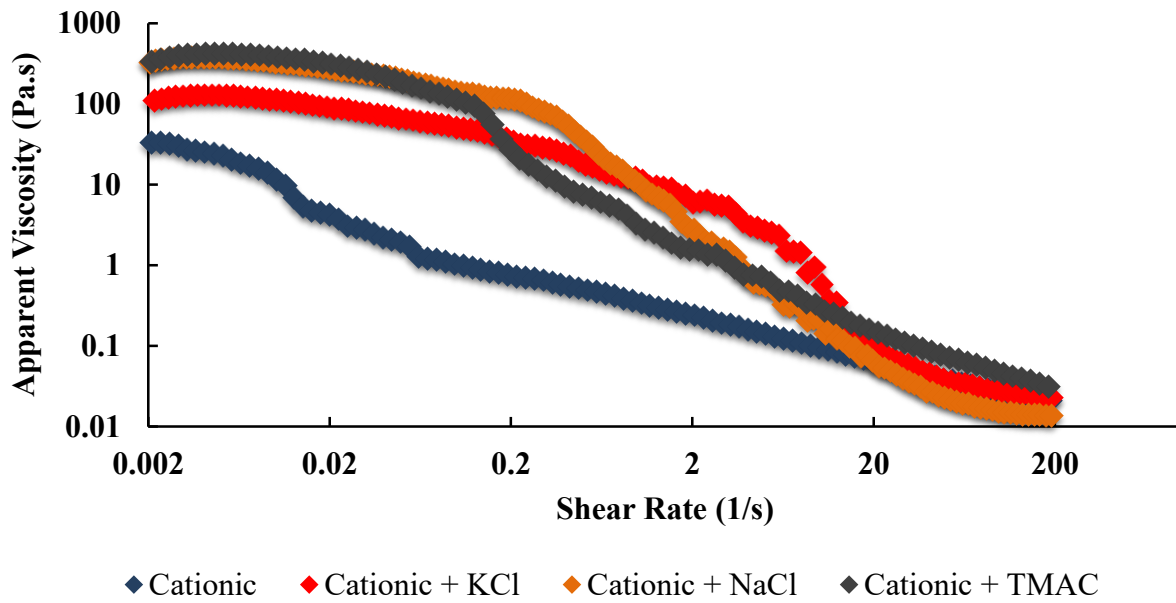


Figure 39: Change in apparent viscosity of a cationic polyacrylamide system with shear rate

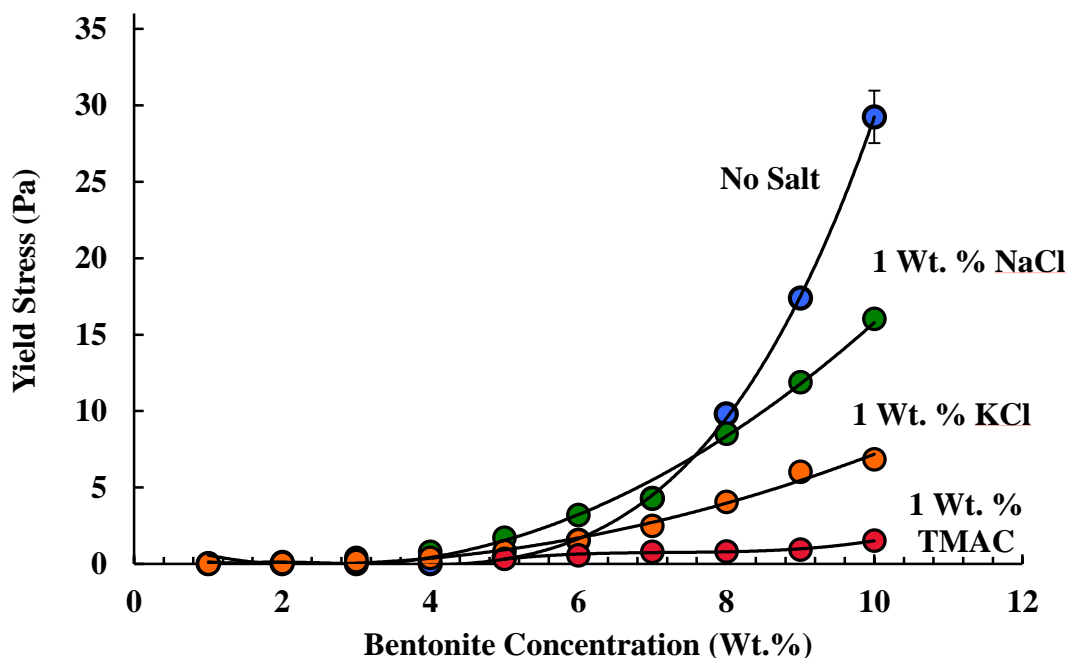


Figure 40: Change in zero shear-rate viscosity of a bentonite salt system with shear rate

The effect of salt on the rheology of bentonite was studied separately (Figure 40). Bentonite forms an important constituent of the drilling fluid and is used in the production of high density drilling fluids having shear-thinning flow behavior (Goh et al., 2011). Yield stress was determined for the bentonite-salt dispersions. Rheology of bentonite in presence of salts and TMAC is indicative of the clay to swell in presence of additives such as salt and TMAC, Addition of KCl and TMAC leads to a reduction of the yield stress. In absence of salts the yield stress of the bentonite increases, due to strong swelling and interparticle interactions between the clay particles. Additionally, this rheological method is easy and reliable in determining the swelling ability of clays in different fluids. The K^+ and $N(CH_3)_4^+$ ions exchange with the more swellable

Na^+ ions in the bentonite, thereby reducing the swelling of the clay, which leads to reduction in the yield stress and the apparent viscosity. Whereas, in the presence of NaCl, the swelling is increased due to the larger hydration radius of Na^+ . Hence, it is recommended for shales rich in expandable clays, such as montmorillonite, to use KCl instead of NaCl when formulating fluids.

CHAPTER IV

4. Studying the Effect of Stripping Lighter Hydrocarbons from Shale Oil by Probing the Rheology of a Model Oil System

4.1 Introduction

The offshore and subsea petroleum production deals with various flow assurance problems on a regular basis. With the advent of onshore shale-oil production, which is often rich in high molecular weight wax, flow assurance, transportation, and storage of shale oils becomes a problem due to wax deposition. Some of the most common flow assurance problems are wax deposition, hydrates formation, asphaltenes, corrosion and scale deposition (Raman et al., 2016). Most of the crude oils contain heavy paraffinic compounds that precipitate below the wax appearance temperatures (WAT) and cause complicated non-Newtonian behavior due to the wax formation and gelation at lower operating temperatures. Wax formation is a major flow assurance problem especially in pipeline transportation where the temperatures can be lower than the WAT and the pour point of the crude oil. Wax deposition is also a big problem in the production and storage of the waxy crude oils. Wax structures start developing below the WAT and these structures entrap the oil in it giving rise a 3-D gel network that resembles a polymer gel (Kriz & Andersen, 2005; Singh, Youyen, & Fogler, 2001). When the temperature falls below the pour point or otherwise called the gelation temperature, the viscosity of the oil increases several folds

due to continuous wax aggregation and behaves like a viscoelastic solid (Visintin, Lapasin, Vignati, D'Antona, & Lockhart, 2005). Understanding the rheology of waxes in oil is imperative to address the wax deposition problems, especially at lower temperatures.

The increasing production of oil from shale formations pose a particularly difficult problem. These oils tend to have high concentrations of waxes coupled with a high vapor pressure. To meet transportation requirements, it is necessary to strip the oil to lower the vapor pressure. This results in an increased tendency for the waxes to precipitate and cause flow assurance, transportation, and storage problems.

The rheology of waxy oils is dependent on the composition of the crude oil and the thermal and shear history of the oil (Cheng, Boger, & Nguyen, 2000; Li & Zhang, 2003; Mendes, Vinay, Ovarlez, & Coussot, 2015; Rønningsen, 1992; Wardhaugh, Boger, & Tonner, 1988; Webber, 1999). The composition of the wax might be low molecular weight n-alkanes or high molecular weight iso-paraffins and cyclic alkanes (Roenningsen, Bjoerndal, Baltzer Hansen, & Batsberg Pedersen, 1991). Asphaltenes and resins also affect wax precipitation, with numerous studies proving that both asphaltenes and resins prevent wax precipitation and act as pour point depressants (Kriz & Andersen, 2005; Rønningsen, 1992; Vos & Van den Haak, 1980). Depending on the wax composition, the nature of wax crystals formed changes. (Roenningsen et al., 1991) showed that waxes predominant in n-alkanes form crystals that are large needle or plate like and higher molecular weight isoparaffins and cyclic alkanes form microcrystalline waxes. Simple model oil systems consider only the effect of n-alkanes, whereas in reality crude oils contain varying proportions of iso-alkanes and cyclic alkanes that could significantly alter the gelation behavior of the waxy oils (Visintin et al., 2005).

Over the years many studies have been done to determine wax deposition mechanisms, and now it is well established that molecular diffusion is the predominant wax deposition mechanism (Aiyejina, Chakrabarti, Pilgrim, & Sastry, 2011; Zheng, Zhang, Huang, & Fogler, 2013). When the temperatures at the wall is below the WAT, the wax starts to crystalize which leads to a concentration difference between the wax at the wall and the bulk fluid. This leads the diffusion of wax components from the bulk fluid towards the wall to form a wax layer (Zheng et al., 2013). Due to the existing thermal driving force and also the concentration gradient the wax build-ups until equilibrium is reached (Aiyejina et al., 2011; Azevedo & Teixeira, 2003). The mass flux of the diffused wax can be estimated using the Fick's law (Azevedo & Teixeira, 2003)

$$\frac{dm_m}{dt} = \rho_D D_m A \frac{dC}{dr}$$

Where m_m is the mass of deposited wax, ρ_D is the density of the solid wax deposit, D_m is the diffusion coefficient of liquid wax in the oil, A is the area of deposition, C is the volume fraction concentration of wax in solution and r is the radial coordinate.

Depending on the composition of the wax components the solubility and diffusivity of the each wax component changes. Higher molecular weight components such as long chain n-alkanes, aromatic hydrocarbons have less solubility and precipitate faster than the lower molecular weight wax components. The carbon number of the n-alkanes play an important role in the extent of wax deposition. This has been studied in detail by (Zheng et al., 2013). The effect of carbon number

C-15 and higher on the wax deposition and yield stress properties have been widely studied through modeling and rheological experiments. But the effect of lower molecular weight n-alkanes and cyclic alkanes on the rheological properties of the wax-oil system is seldom researched. In this work, the isolated effect of C-5, C-6, C-7 alkanes, cyclopentane and cyclohexane on the rheological properties and morphology of the waxes formed is analyzed using a model-oil system.

Numerous studies have been done to ascertain the effect of mechanical or shear history and cooling rates on the rheology of crude oil systems (Chang, Boger, & Nguyen, 1998; Cheng et al., 2000; Li & Zhang, 2003). There are contradicting results in the literature on the effect of the cooling rates on the yielding nature of the waxy oils. Most of these studies have used crude oils as the carrier fluid to determine the effect of cooling rate on the rheological properties of the oil. Failure to erase the thermal and stress history of the oil before each study can lead to erroneous results or reproducibility problems. In the past, researchers have tried to relate morphology of wax formed to cooling rates using optical and polarized light microscopy. Ronningsen studied the effect of cooling rates on gel strength. The effect of cooling rates on the wax crystallization and dissolution temperature, yield stress properties and the activation energy of viscosity-temperature dependence region was studied in detail by Richard M. Webber using two mineral oil samples from Exxon and Chevron RLOP (Webber, 1999). Webber found that the viscosity of the oil increased with increase in cooling rate at low temperatures and the average wax crystal size decreased with increasing cooling rate, which leads to increase in the apparent viscosity and the yield stress of the oil. These findings were in contrast to the studies done by Cheng Chang et al., where they used dynamic oscillatory measurements and optical microscopy to measure the effect of cooling rate on the static yield stress of the oil and the wax crystal sizes respectively using the Daihung crude oil and Beatrice crude oil. Additionally, in this work the effect of cooling rates on

the yield stress and the viscoelastic properties of the wax-oil system is probed and correlated to the experimental findings of the polarized light microscope.

4.2 *Materials and Methods*

Model waxy oil is prepared using a light mineral oil as the base and 5 Wt.% paraffin wax a model system similar to the one used by (Magda et al., 2008). The light mineral oil, hydrocarbon solvents and paraffin wax samples were obtained from Sigma Aldrich. The hydrocarbons used were pentane, hexane, heptane, cyclopentane and cyclohexane in equimolar quantities equivalent to 5 Wt % of pentane. The samples were prepared by adding melted paraffin wax to light oil at 60 °C, stirring it on a hot plate till the waxes mix homogenously and adding the hydrocarbon at the end. The sample is sealed and let to cool quiescently at room temperature for at least 24 h before using it in the experiments. The WAT was measured using a cross polarized microscopy and the WAT values are shown in Table 14 for each system.

Table 14: WAT for all the model oil samples used

Sample	WAT (°C)
Model Oil	29 ± 0.5
Model Oil + Cyclohexane	27.4 ± 0.7
Model Oil + Cyclopentane	27.5±0.3
Model Oil + Heptane	27.5 ± 0.5
Model Oil + Hexane	26.5 ± 0.8
Model Oil + Pentane	26 ± 0.2

4.2.1 *Rheometer*

A DHR-3 stress controlled rheometer (TA instruments) was used for all the rheological measurements. The temperature and cooling rate was controlled using a peltier system connected to a cooling water bath. The temperature could be varied from – 40 °C to 150 °C and at cooling rate of up to 5 °C/min. The rheometer used in this research is shown in Figure 41.

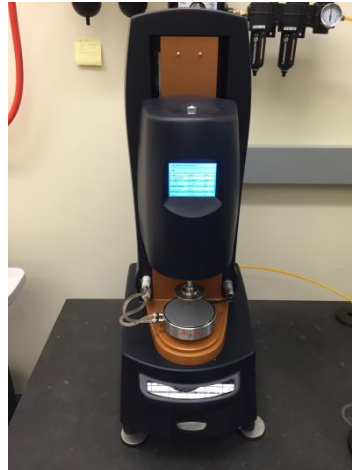
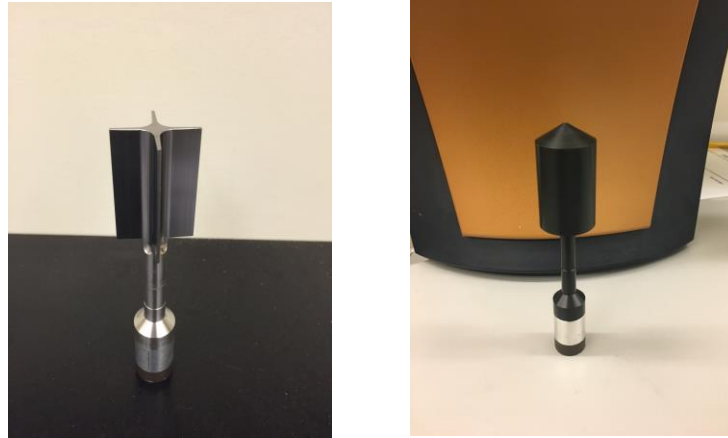


Figure 41: DHR-3 Rheometer

4.2.2 *Rheometer Geometry*

Vane geometry was used for the study. Vane geometry has been proven effective for measuring yield stresses and hence was used in this study. Vane geometry helps prevent wall slippage at higher shear rates, helps disrupt flow inhomogeneity while shearing, and also works well for samples with suspended solids (Goh et al., 2011). To measure the rheological properties of the light mineral oil, a bob and cup geometry was used. Bob and cup setup measures the rheological properties of a low-medium viscous solution with good accuracy and hence it was used for the light mineral oil viscosity and dynamic oscillatory measurements. The vane and bob geometry used is shown in Figure 42.



(a)

(b)

Figure 42: (a) Vane Geometry (b) Bob Geometry

4.2.3 Rheological measurements

The instrument and geometry was calibrated before loading the sample. Before loading the sample in the rheometer, the sample is heated to 80 °C and loaded to the rheometer at 80 °C and left at that temperature for 1 h before each experiment to remove the previous thermal and stress history. For samples containing hydrocarbon solvents, the samples were loaded at 40 °C, which is still 12 °C higher than the WAT of these samples to prevent the solvent from evaporating. The hydrocarbons used in the study were used on a molar basis, equivalent to 5 Wt.% of pentane. A cover was used to minimize losses due to evaporation during the course of all the experiments. All the yield stress, creep and recovery, oscillatory measurements were done at 4 °C, at least 20 °C less than the pour point of the system. After the desired temperature was reached the sample was left at that temperature for 15 minutes before the start of each experiment. All the rheological experiments were performed within 5 days of preparing the sample.

4.2.4 Microscopy

A polarized optical microscope (Olympus BX53) equipped with a Linkam temperature controlled shear stage and a high-speed camera was used to study the crystallization process. Temperature

and shear rate were controlled using the Linkam stage, the wax – model oil sample was pre-heated to 80 °C and loaded onto the stage at 80 °C, where step-wise cooling was used to cool the sample to 2 °C. Images were acquired at regular intervals using the attached camera.

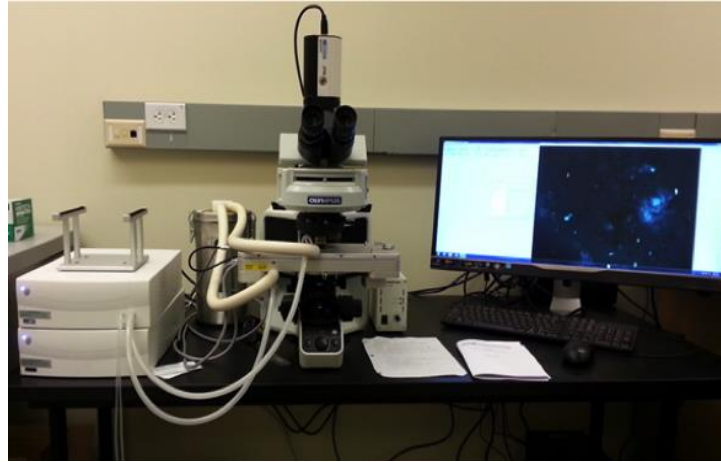


Figure 43: Olympus microscope and the linkam stage

4.3 Results and Discussion

4.3.1 Yield stress measurements

Numerous methods have been developed to determine yield stress. This is the stress limit between flow and non-flow condition. Many indirect methods use the extrapolation of the shear stress – shear rate data using the rheological models. In this study a direct measurement of yield stress is done using the vane geometry, where the stress at which fluid starts to flow is measured as the yield stress (Nguyen & Boger, 1992; Yoshimura, Prud'homme, Princen, & Kiss, 1987). A controlled stress test was done where the stress was increased from zero to a maximum value and the strain % is recorded as a function of stress. Before yield stress the strain remains constant and after the yield stress is exceeded the strain increases sharply. Figure 44 shows the yield stress measurements using stress sweep experiment performed by (Cheng et al., 2000). Point A indicated the static yield stress (ζ_s), the start of fracture whereas point B indicates the end of

fracture (Cheng et al., 2000). The static yield stress of the samples was measured at 5 °C, with careful stress sweep and temperature control.

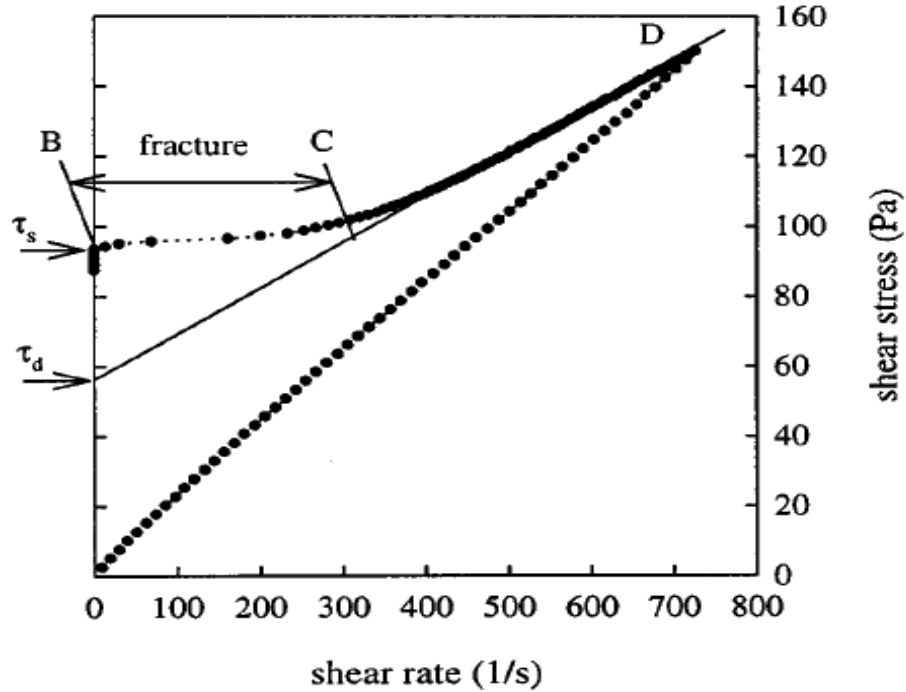


Figure 44: Static yield stress and dynamic yield stress measured using stress sweep experiment

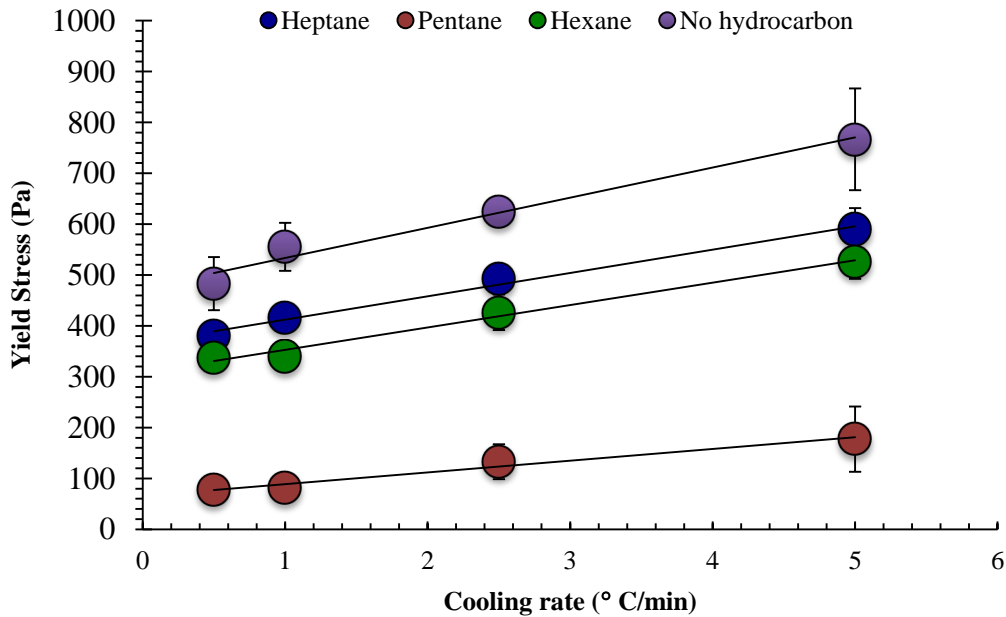
The yield stress values were compared for different model oil system (Figure 45 (a) and (b)). A minimum value of the yield stress is associated with the presence of pentane. Waxes have higher solubility in the lower molecular weight solvents such as pentane (Jennings & Weispfennig, 2005). The differences in yield stress values were significant between the model oil system containing pentane and hexane. The reason for this is lower alkane solvents more effectively contact and solvate the solute (wax) leading to an increase in the solubility of the solute in the solvent. The yield stress values were compared with straight chain alkanes and cyclic compounds. For hexane and cyclohexane the yield stress values were about the same, whereas the cyclopentane values were higher when compared to cyclohexane and pentane in model oil. Odd and even alkanes have proven to exhibit different solubility trends. This is a result of different

crystal packing structures, arising from different alignment of end groups in the packed structure of molecules (Jennings & Weispfennig, 2005). Odd carbon molecules show lower heats of fusion than the even carbon molecules. The heats of fusion can be related to solubility using the following equation

$$\delta_i^S = \frac{(\Delta H_v + \Delta H_f - RT)_i^{0.5}}{V}$$

Where δ_i^S solubility parameter of component i in solid solutions, ΔH_v is heat of fusion, T is the absolute temperature and R is universal gas constant. So when the heat of fusion is lower, the solubility is low, which explains heptane and cyclopentane having higher yield stress values due to their low solubility values.

(a)



(b)

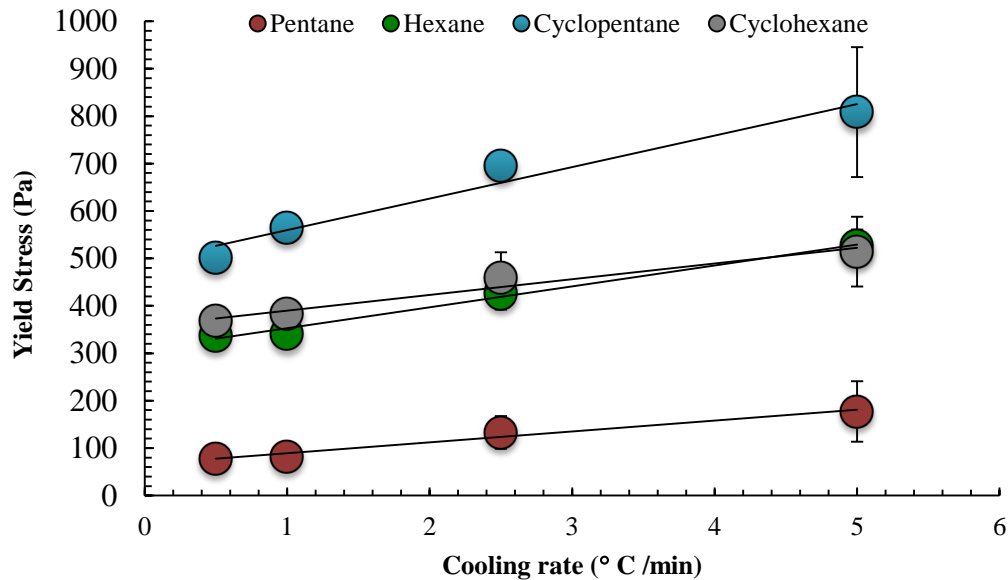


Figure 45: Effect of cooling rate on yield stress of (a) straight chain alkanes (b) cyclic alkane

4.3.2 Small Amplitude Oscillatory Measurements

Small amplitude oscillatory measurements were used to characterize the rheology and gel characteristics of the wax — model oil system. These viscoelastic measurements are useful for characterizing changes like crystallization and gel formation. The small amplitude measurements are made to make sure the frequency values chosen do not cause the wax crystals to deform and become time dependent. Storage modulus is a measure of stored energy, indicative of elastic nature of the gel and loss modulus is a measure of dissipated energy in the form of heat, indicative of the viscous nature of the gel. At the pour point the waxes ideally transition to a solid like region and cease to flow. In traditional gel transition studies for polymers, this is considered as the point at which the storage modulus exceeds or crosses over the loss modulus. The loss modulus is indicative of steady shear viscosity as shown by the equation below

$$\eta' = \frac{G''}{\omega}$$

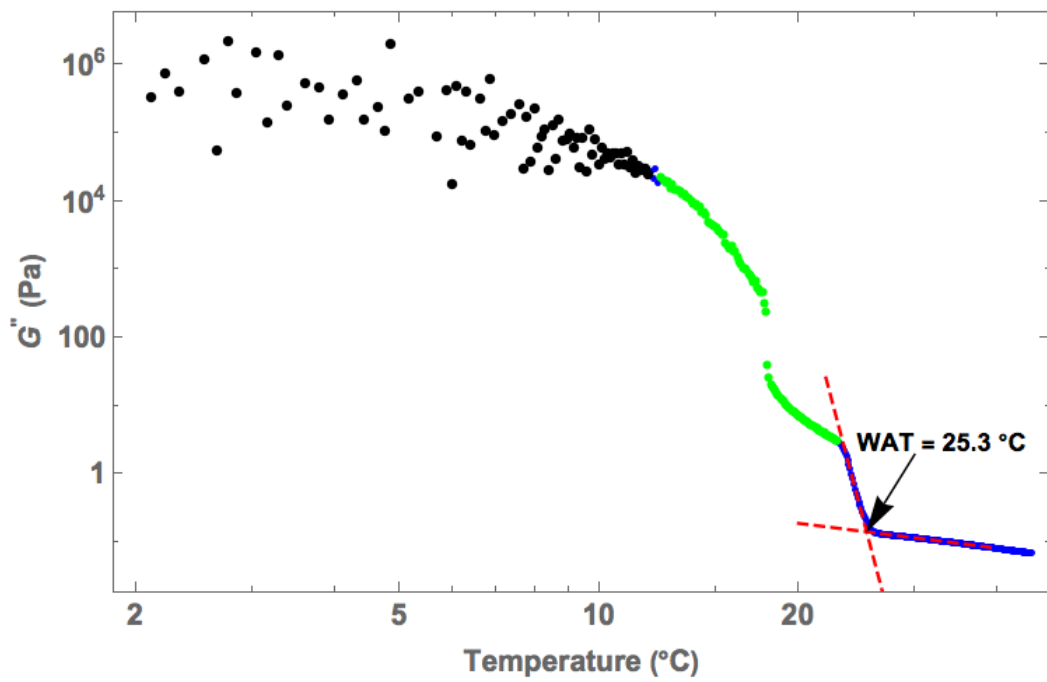
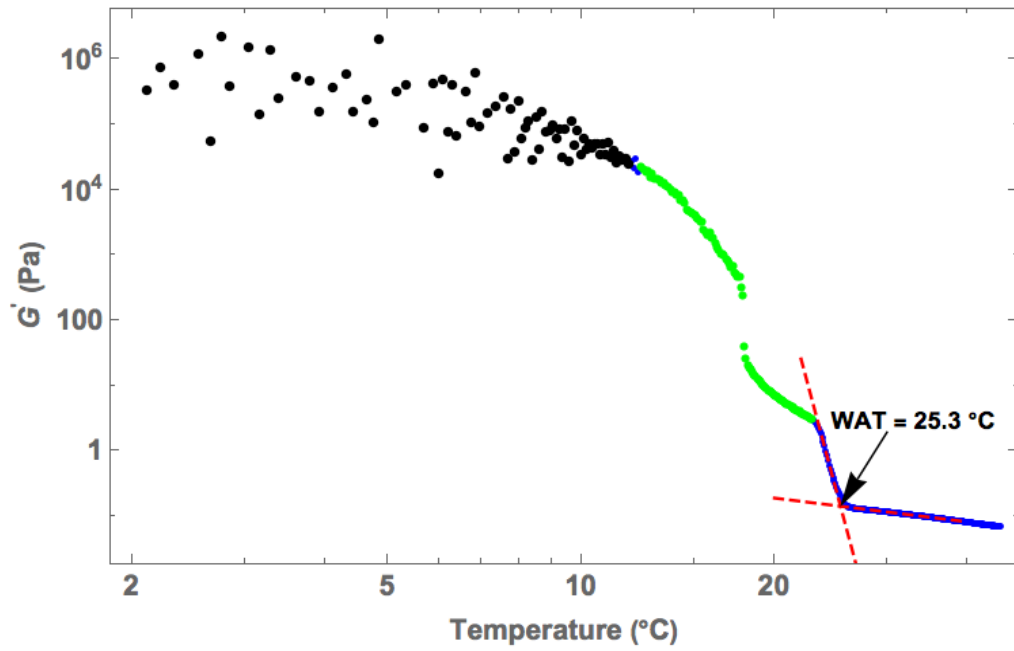


Figure 46: G' and G'' change with temperature

where η' is the steady shear viscosity G'' is the loss modulus, ω is the angular frequency. So as the material approaches a solid like state the viscous dissipation should be zero i.e., the loss modulus is expected to decrease (Power, Rodd, Paterson, & Boger, 1998). In this study, the pour point is the inflection point of a storage modulus, loss modulus vs. temperature cooling curve. Figure 46 shows storage modulus, loss modulus vs. temperature for the model oil system. The sample is heated to 80 °C and held there for 120 minutes and cooled at 1 °C/min to 2 °C with an angular frequency of 1 Hz. With decrease in temperature the storage modulus and the loss modulus decrease simultaneously, till it reaches a temperature where the storage modulus increases more than the loss modulus. This point is considered the gelation point and indicates the formation of a rigid network and a structural transition to the gel state. The viscoelastic properties of the wax crystals become obvious from this point onwards with the elasticity of the structures becoming more prevalent at lower temperatures. Comparing Table 14 and Table 15, it is clear that the pour point values are much lower than the WAT. Table 15 shows the pour point values measured for all the samples used in this work.

Table 15: Pour point of all the wax - model oil samples used

Sample	Pour Point (°C)
Model Oil	22.35
Model Oil + Cyclohexane	20.80
Model Oil + Cyclopentane	21.04
Model Oil + Heptane	18.57
Model Oil + Hexane	18.70
Model Oil + Pentane	17.94

The storage modulus is used to evaluate gel strength of each system as a function of temperature and is compared with different system. The linear viscoelastic properties of the model-oil system

are studied. A strain of 2% (within LVR) and an angular frequency of 1 HZ were used for all dynamic rheological studies. Four cooling rates were chosen (0.5 °C/min, 1 °C/min, 2.5 °C/min, 5 °C/min) and the change in storage modulus by varying the angular frequency from 0.1 rad/s to 100 rad/s and by varying the oscillatory stress from 1 Pa to 200 Pa is studied.

Measuring storage modulus (G') of a system can be used to determine the degree of network formation and strength. A higher storage modulus is representative of strong network between the wax particles. When the storage modulus was measured with respect to the oscillatory strain for the wax-model oil hydrocarbon system (Figure 47) at 4 different cooling rates, the storage modulus is highest for the higher cooling rate and remains constant throughout the stress range. Whereas for the lowest cooling rate the storage modulus is least, and with increasing stress the modulus decreases indicative of network weakening due to weak interactions between the wax particles. A wax gel is formed when the wax crystals start to form and trap the oil in the structures as the temperature is lowered forming a 3-D network of wax crystal network. In presence of the oscillatory stress when the gel is weak, as the stress is increases the wax crystal network collapses and this leads to the release of entrapped oil. As shown in previous studies, this leads to mixture having two layers, the released oil layer and the weak wax – oil layer (Singh, Fogler, & Nagarajan, 1999). When the wax-oil system is cooled rapidly the gel network forms at a faster rate leading to a stronger gel, which the application of stress does not break to release the oil trapped in the gel structure. Application of stress significantly alters the morphology of the wax crystals and the bonding interactions, which causes the gel to dissipate energy and become weaker at higher stresses.

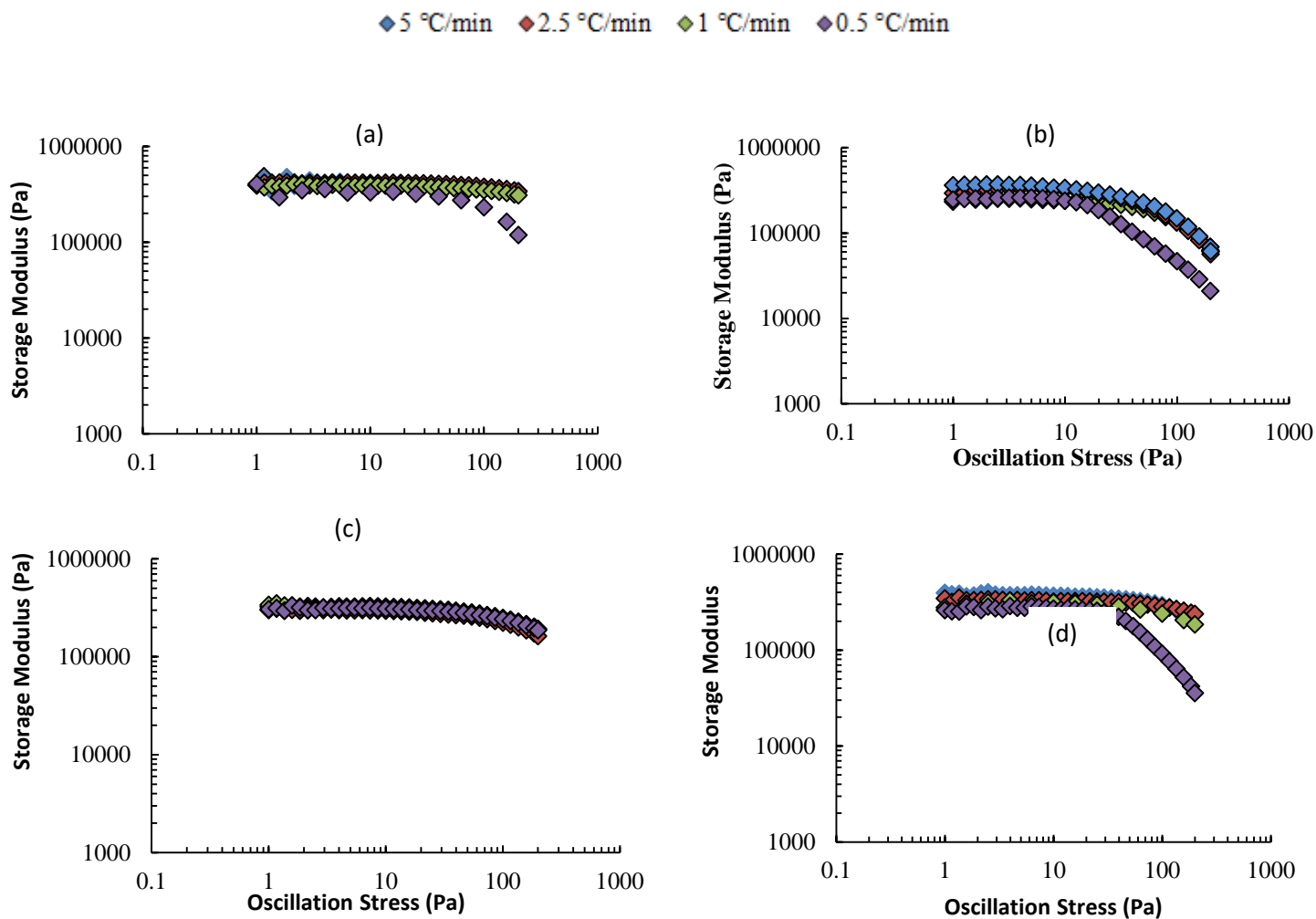


Figure 47: Storage Modulus vs. Oscillation stress for different cooling rate (a) wax in model oil system (b) wax in model oil with solvent hexane (c) wax in model oil with solvent pentane (c) wax in model oil with solvent heptane

The effect of cooling rate on gelation is studied using isothermal time cure tests performed at a constant frequency of 1 Hz and at 20 °C for model wax oil system with heptane (Figure 48). The sample was loaded at 40 °C and cooled statically to the test temperature at 1° C/min. The sample is held at 20 °C for 30 minutes before performing the test. The change in G' and G'' is measured

over time. There is a greater increase in storage modulus for a higher cooling rate due to more extended gel network and aggregated crystal formation at higher cooling rates.

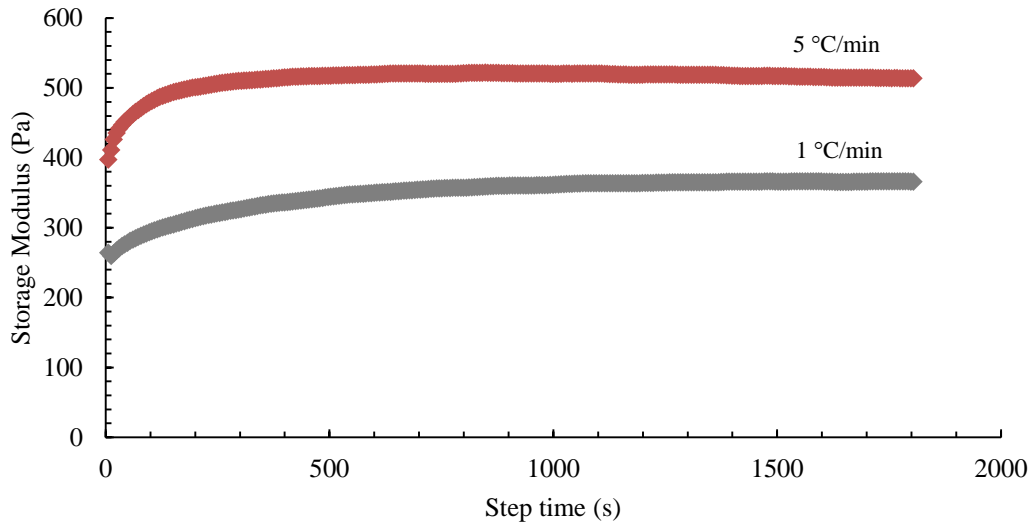


Figure 48: Storage modulus as a function of time for different cooling rates for wax in model oil system with heptane in solvent

The strain sweep is done to characterize the viscoelastic behavior of the gel (Figure 49). The region marked in the graph marks the linear viscoelastic region (LVR). The strain at which the LVR ends called the linearity stress (γ_0) is characteristic of the interactions between the crystal and crystal aggregates. In the dynamic rheological studies performed by (da Silva & Coutinho, 2004) they assumed that the colloidal aggregates fractal sizes are much larger compared to the primary crystal size and hence the storage modulus and linearity stress is a function of the particle volume fraction (ϕ) and can be related by power law models as previously done by (Buscall, Mills, Goodwin, & Lawson, 1988).

$$G' \sim \phi^A$$

$$\gamma_0 \sim \phi^B$$

Where A and B are related to the fractal dimension of the system. So, as the temperature is decreased, the particle volume fraction increases with more oil being trapped within the crystals instead of being in the bulk fluid and dominant interactions between the crystal aggregates, which leads to the system being more rigid at lower temperatures and less viscoelastic in nature.

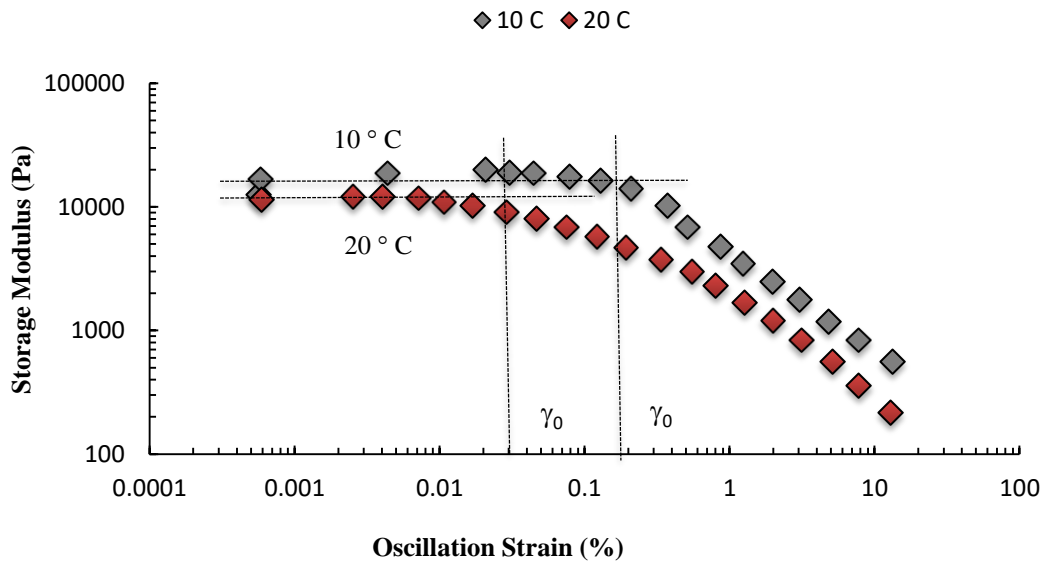


Figure 49: The storage modulus as a function of oscillation strain showing the LVR for wax model oil system at 10 °C and 20 °C

Figure 50 show the storage modulus and loss modulus of wax in model oil for temperature range from 5 °C to 30 °C. As the temperature is decreased below the gelation point, the elastic character of the network increase and hence the storage modulus increases. The storage modulus increases with decrease in the temperature due to the increased density of the junction zones between the wax crystals (da Silva & Coutinho, 2004). At higher temperatures due to weaker structures the moduli are weak.

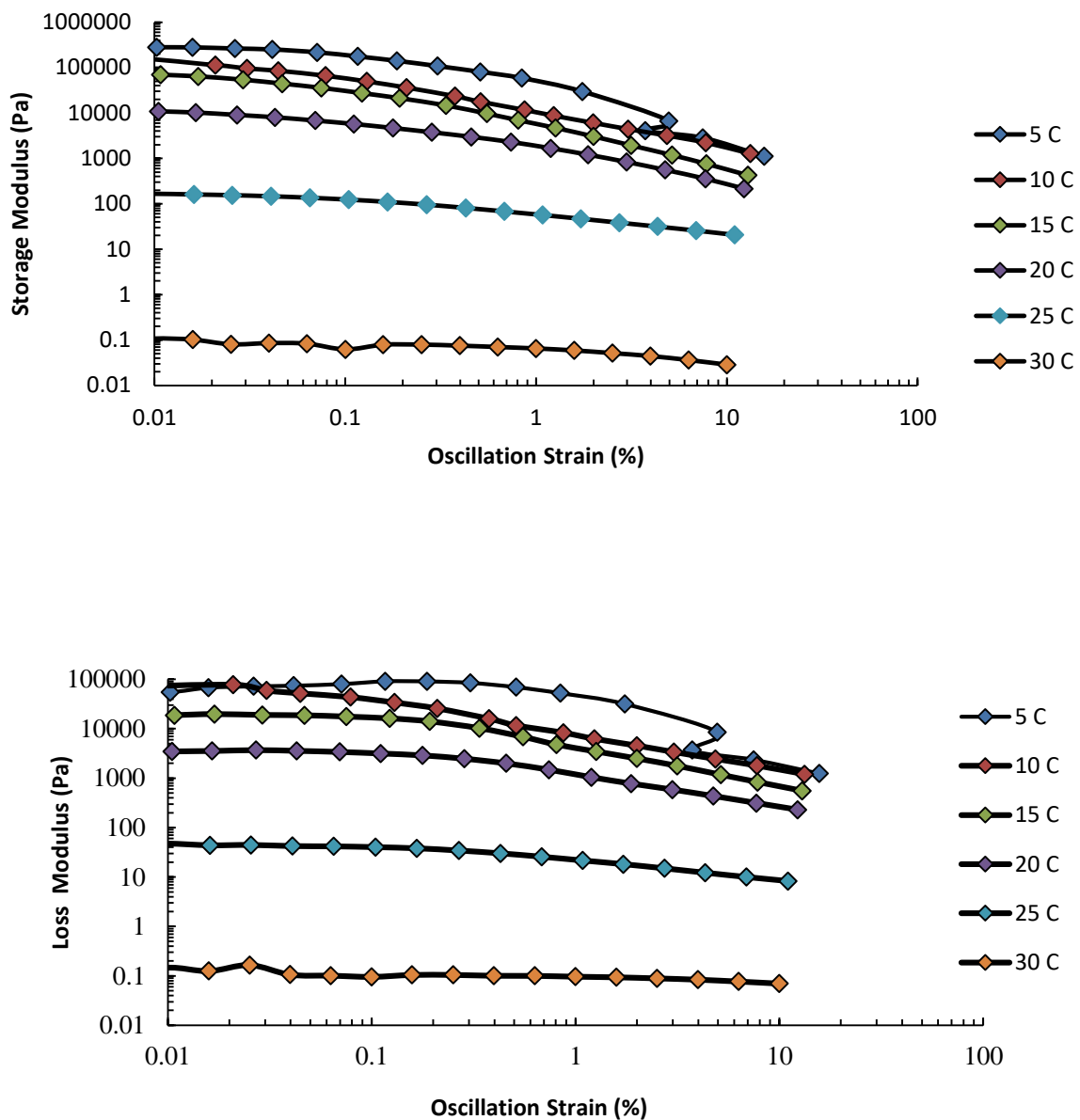


Figure 50: (a) Storage modulus vs. oscillation strain at different temperatures (b) Loss modulus vs. oscillation strain at different temperatures

4.3.3 Creep and recovery of gels with varying cooling rates

Creep tests are done to study the elastic response of the gel under constant imposed stress. A stress of 40 Pa was selected for these tests. The stress was imposed for 600 s and then released. The gel was left to recover for 600 s. When a stress is imposed on the material, it

deforms continuously and proceeds at 3 stages. The first or the primary stage where the creep rate is decreasing, followed by the second stage where the creep rate is constant and the final stage terminates in a fracture (Findley & Davis, 2013). After the load is removed the material tries to recoil back to its original state and this recoverable strain is time dependent (Magda et al., 2008).

Figure 51 shows the creep and recovery of model oil systems. For creep and then recovery the gels were made at different cooling rates and no shear conditions and were submitted to high stresses. The chosen stress was such that it was less than the static yield stress but slightly higher than the elastic limit yield stress. With application of stress there is immediate deformation, which can be seen with the sudden increase in the strain % values and after the removal of the stress there is partial recovery of the stress, which can be related to the storage modulus of the system. A steep and sudden increase in the strain % is indicative of large deformations and weaker gel structures. The system with highest cooling rate deformed the least and the effect is profound as it can be seen in Figure 51 a where when cooled at 0.5 °C/min the strain % is 0.35 %. To show the comparison of presence of more volatile lower hydrocarbons in the system, creep test results for model wax oil system with hexane is shown in Figure 51 b. In presence of hexane, for the same experimental conditions the deformation is much higher compared to the model oil system with no hydrocarbons. This result correlates to the observation that low volume fraction of crystals is present in gel state in presence of hydrocarbons and hence weaker gel structures are formed that leads to stronger deformation.

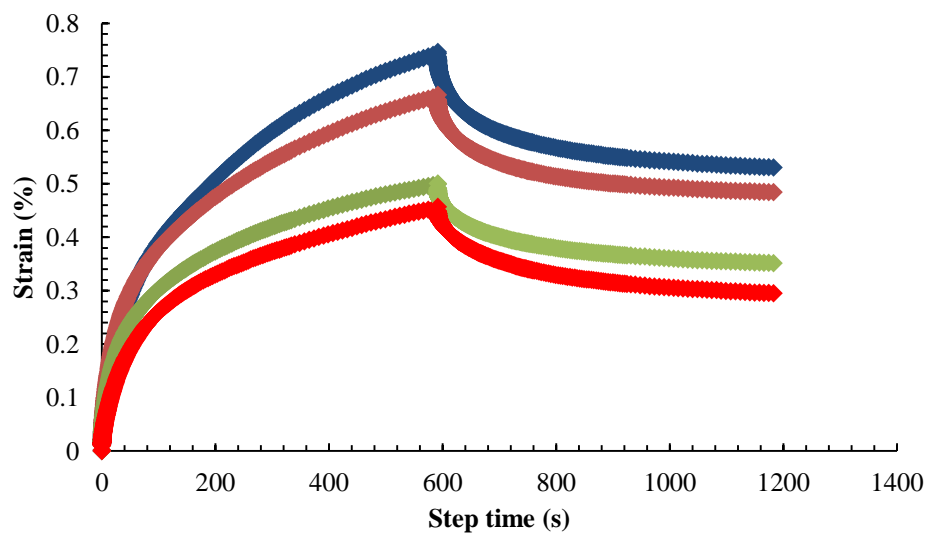
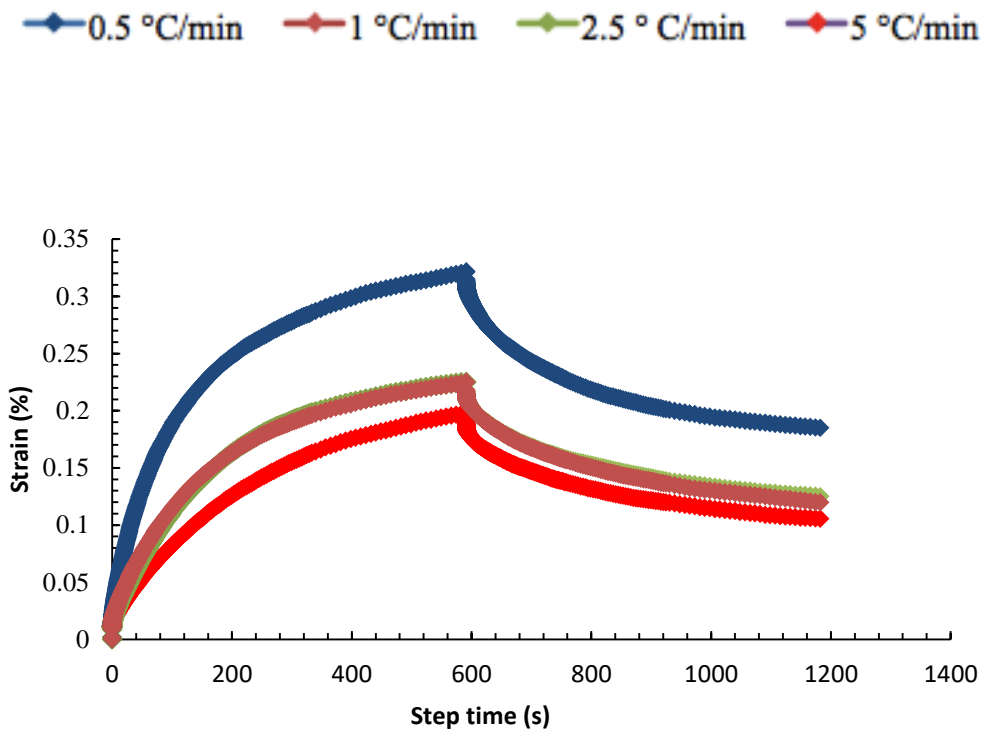


Figure 51: Creep and recovery experiments at various cooling rates for (a) wax in model oil (b) wax in model oil with hexane in solvent

4.3.4 Effect of cooling rate on morphology and particle size distribution of wax crystal

Polarized light microscopy was used to observe wax morphology at different cooling rate for model oil system with and without lighter hydrocarbons. Crystals appear in micrograph as needles, which is in agreement with the commonly reported crystal morphology of waxes. As the sample is cooled, the wax crystals grow in size, but the growth of individual crystals as such has a smaller effect compared to the increase in density of the crystallites. With slower cooling rates, there is enough time for the crystals to grow extensively, but at higher cooling rates the smaller crystals tend to nucleate, leading to larger number density of wax crystals which causes a decrease in the average crystal size. At higher cooling rates the increase in viscosity is due to the wax cluster networks trapping more oil, which makes the gel stronger and more viscous in nature.

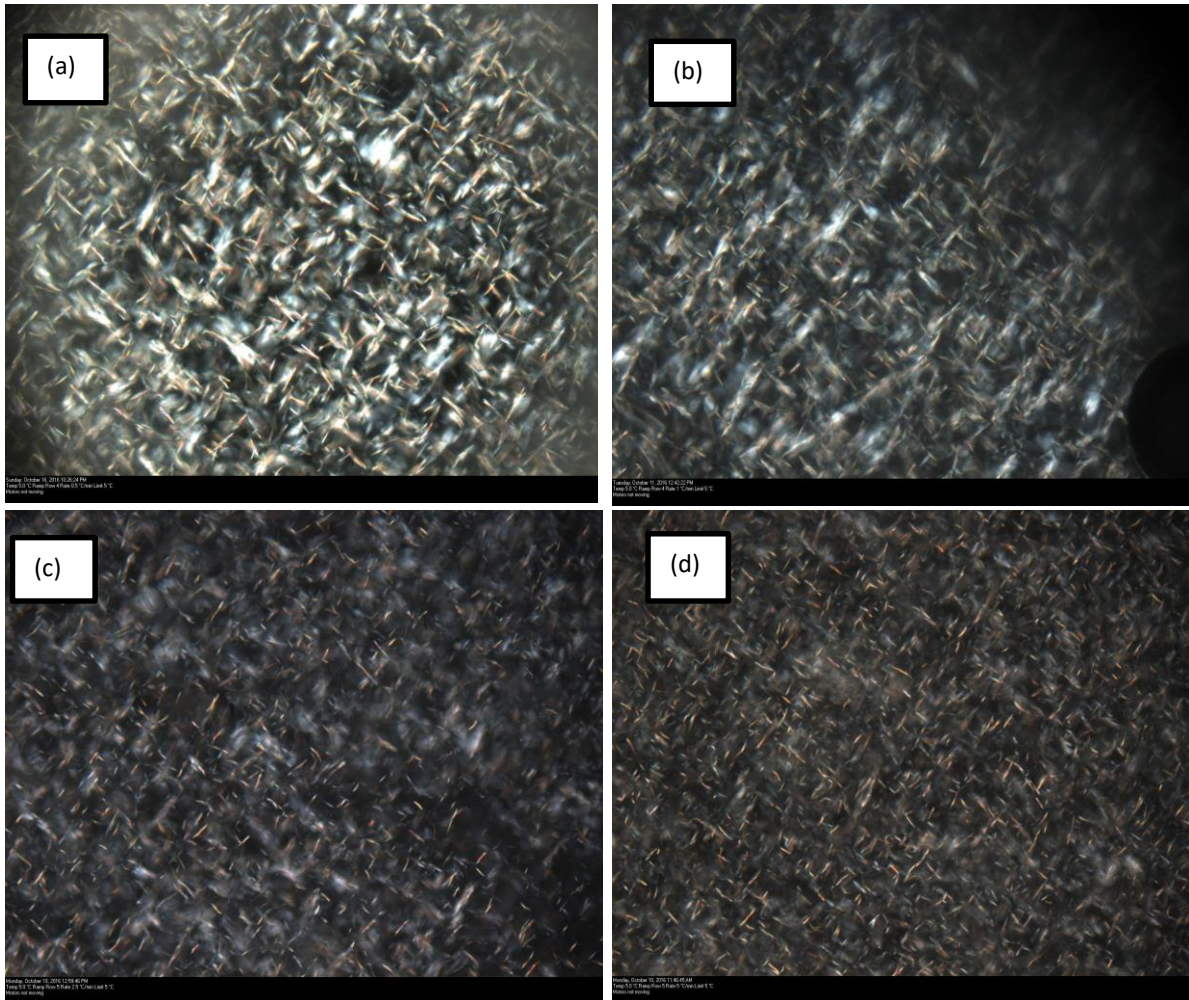


Figure 52: Images of wax crystals in wax model oil system at 5 C after cooling at different rates (a) 0.5 °C/min (b) 1 °C/min (c) 2.5 °C/min (d) 5 °C/min

From Figure 52 it can be observed that with increasing in cooling rate the particle size decreased. When the particle size distribution curve is drawn (Figure 53), with increasing cooling rate the particle size distribution becomes narrower. The particle size distribution had a major effect on the suspension viscosity. The decrease in viscosity with a broader particle size distribution is characterized by smaller hydrodynamically interacting clusters (Webber, 1999).

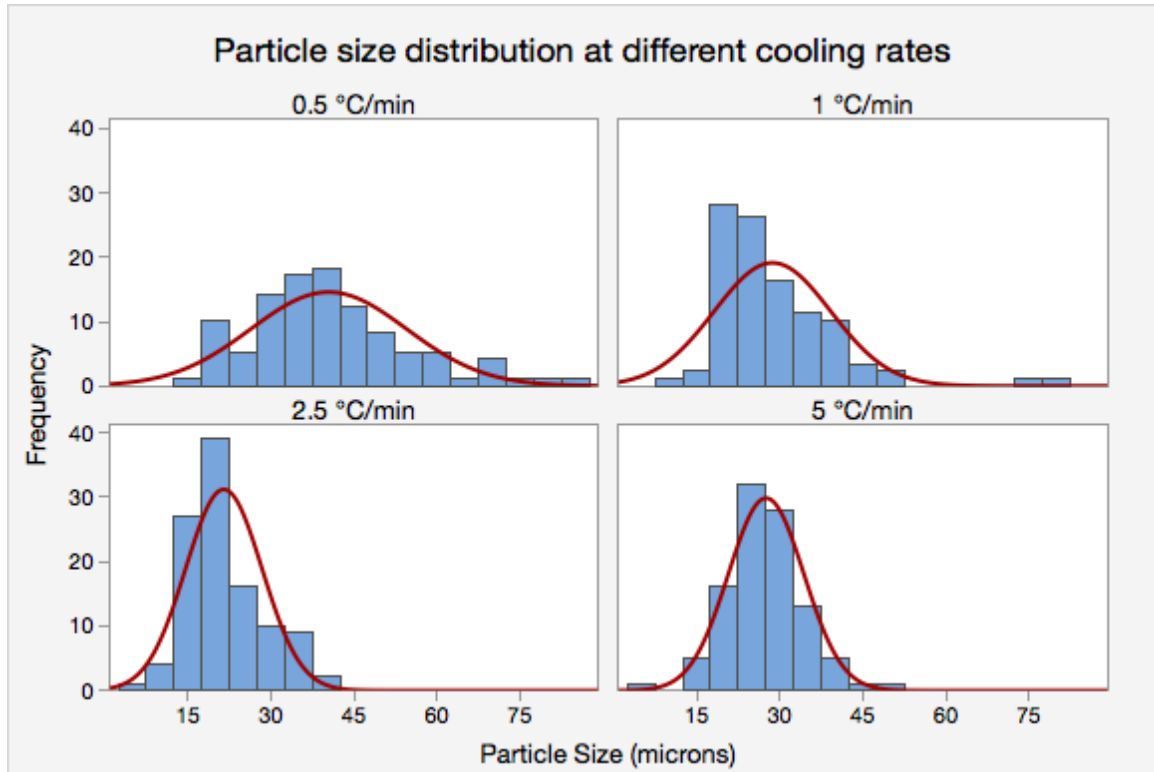


Figure 53: Particle size distribution at different cooling rates for wax in model oil system at 5 °C

4.3.5 *Effect of lighter hydrocarbons on WAT and total volume fraction of wax-oil system*

The rheological measurement gives qualitative effect of absence of lighter hydrocarbons and the effective of cooling rates. In order to quantify the effect of stripping lighter hydrocarbons, the effective volume fraction of particles was measured using the equation derived by Toda et. al This equation gives the phenomenological relation between viscosity of the suspension and the volume fraction.

$$\eta_r = \frac{1 - 0.5 \Phi}{(1 - \Phi)^3}$$

Where η_r is relative viscosity and was measured for each system Φ is the particle volume fraction. The volume fraction was determined using the equation proposed by Toda et al., for varying stress at 20 °C, statically cooled for all the systems used in the study. This equation has disadvantages such as not accounting for maximum volume fraction and this equation was derived for spherical particles. But this equation helps us get a rough estimate of the particle volume fraction and make a comparison for the different systems under study. The relative viscosity here is the viscosity of the system relative to before the appearance of solid i.e. wax crystals. The viscosity was measured rheologically using temperature ramp experiment.

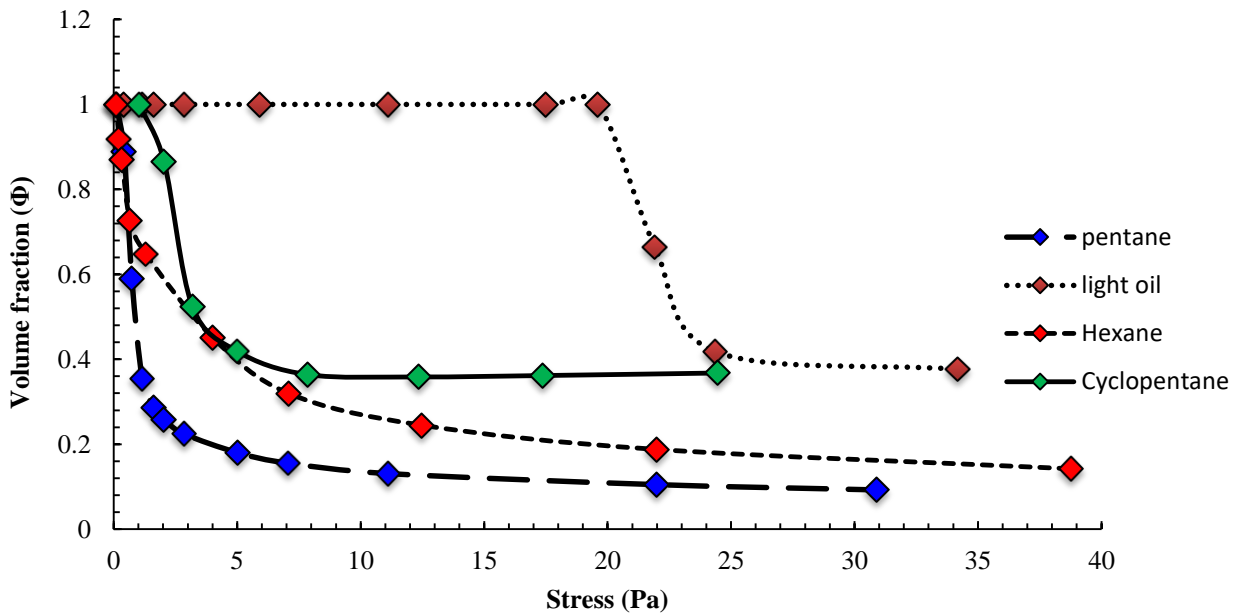
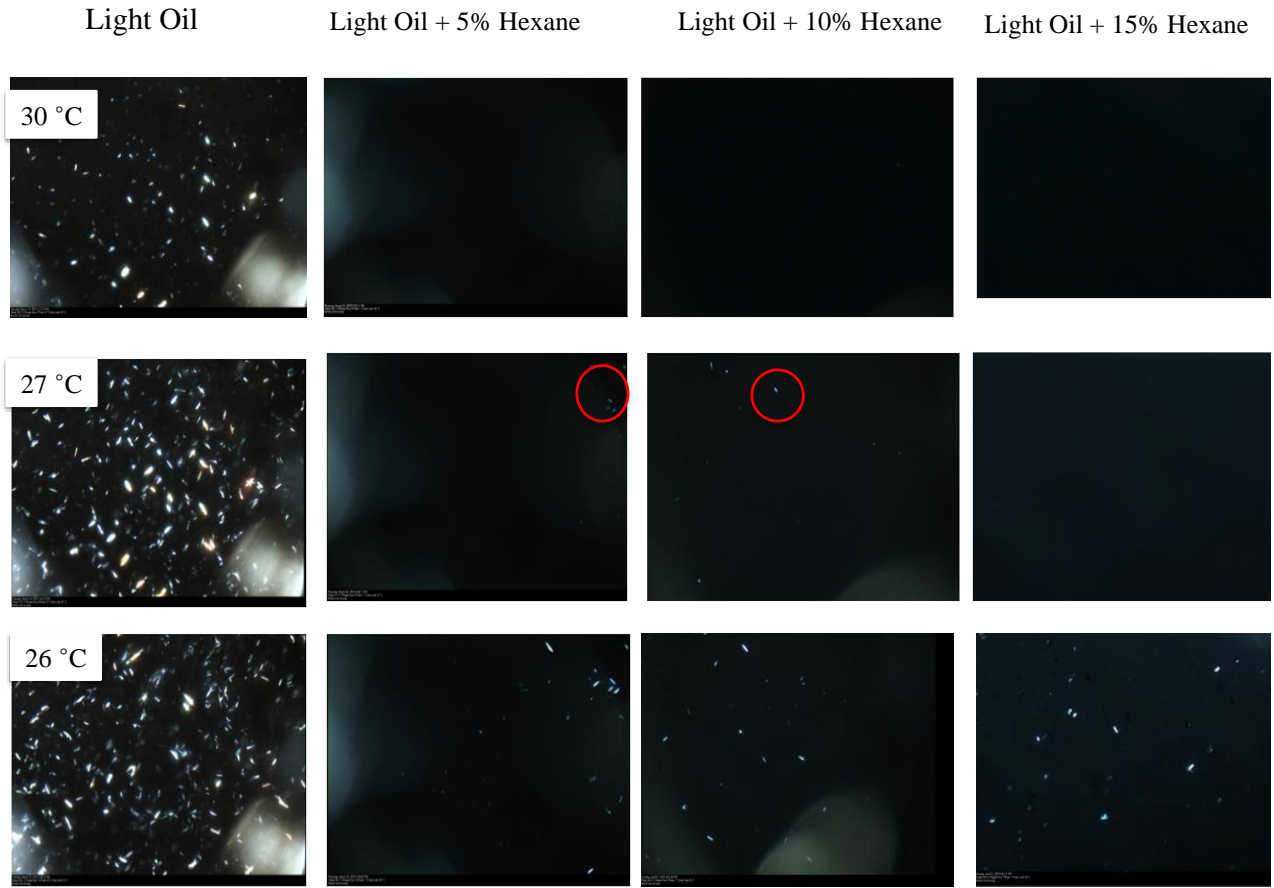


Figure 54: Volume fraction vs. the shear stress for wax in model oil system with different solvents

In Figure 54 it can be seen that as the stress is increased the particle volume fraction decreases. This is a widely studied and observed phenomena. At lower stresses, the wax crystals are bigger in size and have more entrapped oil in them and as they are subject to higher stresses the aggregates break releasing the oil leading to a decrease in volume fraction. In absence of

hydrocarbons the volume fraction is highest and remains constant before 20 Pa. This behavior is indicative of highly rigid gel structures that require higher stress to deform. When the critical stress is overcome there is a significant breakdown of the structural network. This critical stress is higher in absence of the lighter hydrocarbons. In presence of pentane, the volume fraction is least. Lighter ends keep the waxes dissolved, i.e. lighter the hydrocarbons higher is the solubility of the waxes in the solvent.

The effect of hydrocarbons on the model-oil system was studied extensively using rheological methods as shown in sections 4.1.1 to 4.3.3. In the following section, hexane was used to show the how removal of lighter ends affects the WAT. From Figure 55 it can be seen that in absence of hexane (i.e. the light oil system) the wax crystals appear at 30 °C and with visual inspection the number density of wax crystals formed is higher in absence of hexane. The WAT is significantly higher in absence of hexane, and addition of 5 Wt. % and 15 Wt. % hexane did not alter the WAT significantly (Table 16).



10

Figure 55: Effect of solvent concentration on WAT

Table 16: WAT measured as an effect of solvent concentration

Sample	WAT (°C)
Light Mineral Oil	30 ± 0.6
Light Mineral Oil + 5 Wt. % Hexane	27 ± 0.7
Light Mineral Oil + 10 Wt.% Hexane	27 ± 0.6
Light Mineral Oil + 15 Wt.% Hexane	26 ± 0.5

With addition of lighter hydrocarbons, the average particle size of the wax particle decreased (Figure 56). The wax remains dissolved when the hydrocarbons are present in the solvent, which prevents it from forming larger crystals. As shown in the previous section when the particle size decreases the viscosity should increase, but in this case the effect of solvent viscosity on enhancing the overall viscosity of the system offsets the effect of particle size. If the viscosity ratio/relative viscosity $[\frac{\eta_{gel}}{\eta_{sol}}]$ is considered, the relative viscosity is higher for solvents containing lighter hydrocarbons, so the contribution of wax crystal aggregates to the overall viscosity of the system is less.

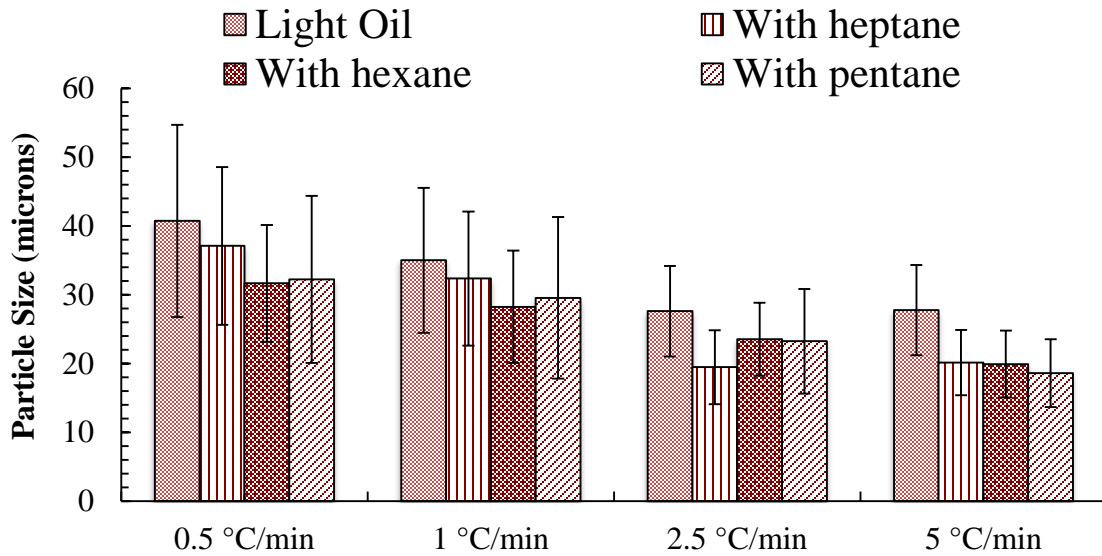


Figure 56: Average particle size for the wax in model oil in presence of solvents measured at different cooling rates

Chapter V

5. Conclusion and Recommendations

5.1 Quantitative Characterization of Polyacrylamide – Shale Interaction

A method was developed to characterize polyacrylamide-shale interaction. Zeta potential and rheological measurements were made to semi-quantify these interactions. Based on the studies, cationic polyacrylamides interact with both the shales strongly even in presence of salt and TMAC, whereas anionic polyacrylamide interacts less with the shales. Each type of shale analyzed interacts differently with polyacrylamide. All samples interact strongly with cationic polyacrylamide because of the negative surface charge on clay platelets. It is recommended to use anionic polyacrylamide because of its minimal interaction and also compatibility with other fluid additives. Due to the cationic polyacrylamides interacting strongly with shale and it can potentially cause formation damage. Both the rheological studies and the zeta potential tests gave the same results. Rheological methods are easier to use and require less time than zeta potential experiments and can be used for qualitative understanding of shale - fluid interaction. Whereas zeta potential tests can be used for semi-quantitative understanding alterations to shale surface when in contact with different fluids. It is imperative to understand fluid-rock interaction extensively, and this is especially true for polyacrylamide. Additives that are widely used as good shale inhibitors for one formation need not necessarily work well for another formation. For instance, in this study TMAC was effective inhibitor for Chattanooga shale but increased swelling in Pride Mountain shale. This study reiterates the importance of testing shale for additives that

can cause wellbore instability before injecting the fluids. Further studies are being performed to model the polymer - shale interaction and to identify additives that would facilitate effective friction reduction while minimizing these interactions.

5.2 Characterization of Shale-Fluid Interaction through a Series of Immersion Tests and Rheological Studies

In this work the role of salts, TMAC and polyacrylamides as shale inhibitors is investigated through simple immersion tests and by using rheology as a means of measuring clay-fluid interaction. The following conclusions are drawn from the experimental results

1. Polyacrylamides (anionic and cationic) prevent swelling in all the three shale formations studied by forming an isolation membrane on the shale and preventing the water and ions from entering the shale.
2. Using high concentrations of TMAC is not recommended. TMAC prevents the adsorption of polyacrylamides and also causes excessive shrinkage of shale matrix, which can lead to a loss of mechanical strength in the wellbore.
3. NaCl increases swelling in montmorillonite-rich shale. Instead, salts like KCl and TMAC are better inhibitors to use in shale formations rich in expandable clay.
4. Polyacrylamide with salts and TMAC is very effective in preventing swelling and dispersion of all three shale formations.
5. Salts are inimical to the rheology of polyacrylamides. Salts reduce the viscosity of the fluid system and hence can increase fluid loss.

5.3 Studying the Effect of Stripping Lighter Hydrocarbons from Shale Oil

This work intends to establish the effect of stripping lighter hydrocarbons on the rheology and the WAT using a model wax oil system. When removing lighter hydrocarbons from oil, the solubility of waxes is decreased. As a result of which the waxes start appearing at higher temperatures and also favors structural build up due to extensive crystal formation. Additionally, the structure and rheology of the model-oil system is probed with different cooling rates. The effect of cooling rate has widely been studied before and there are many conflicting results. Hence a simple model oil system was used to study the effect of cooling rate with well-controlled cooling rates and thermal history of the system. In comparison with the contradicting results existent in the literature, this work concludes that the effect of cooling rate on the rheological properties and the morphology of wax crystals formed is dependent on the base oil and solvent. Researchers who have concluded that with decreasing cooling rates the viscosity and the yield stress nature of the system increases have used crude oil in their study compared to the study done by Webber with a simple lubricating mineral oil. Even with careful temperature control and after erasing the thermal history, with decreasing cooling rates the wax - oil system formed weaker gels and had lower yield stresses.

5.4 Recommendations for Future Work

Following recommendations can be considered for the possible continuation of this work

1. pH of the polyacrylamide-salt samples can be changed to study the effect of pH on aiding/preventing polyacrylamides from adsorbing on the shale surface.
2. Ion movement in and out of the shale samples can be measured using electrodes, to assess the complete effect of shale inhibitors in preventing ions from entering the shale.

3. Prepare a simple setup in order to vary confining pressure while doing immersion tests.
4. Use crude oil of varying compositions from heavy crudes to light crudes and study the effect of cooling rate on the rheological properties.
5. Compare these results to the results obtained using the model wax oil system.

6. REFERENCE

1. Aften, C., & Watson, W. P. (2009). Improved friction reducer for hydraulic fracturing. Paper presented at the SPE Hydraulic Fracturing Technology Conference.
2. Aiyejina, A., Chakrabarti, D. P., Pilgrim, A., & Sastry, M. K. S. (2011). Wax formation in oil pipelines: A critical review. *International journal of multiphase flow*, 37(7), 671-694.
3. Al-Bazali, T., Zhang, J., Chenevert, M. E., & Sharma, M. M. (2008). Factors controlling the compressive strength and acoustic properties of shales when interacting with water-based fluids. *International Journal of Rock Mechanics and Mining Sciences*, 45(5), 729-738.
4. Al-Bazali, T. M. (2005). Experimental study of the membrane behavior of shale during interaction with water-based and oil-based muds.
5. Al-Bazali, T. M. (2011). The consequences of using concentrated salt solutions for mitigating wellbore instability in shales. *Journal of Petroleum Science and Engineering*, 80(1), 94-101.
6. Anderson, R. L., Ratcliffe, I., Greenwell, H. C., Williams, P. A., Cliffe, S., & Coveney, P. V. (2010). Clay swelling—a challenge in the oilfield. *Earth-Science Reviews*, 98(3), 201-216.
7. Azevedo, L. F. A., & Teixeira, A. M. (2003). A critical review of the modeling of wax deposition mechanisms. *Petroleum Science and Technology*, 21(3-4), 393-408.

8. Brooks, D. E., & Seaman, G. V. F. (1973). The effect of neutral polymers on the electrokinetic potential of cells and other charged particles: I. Models for the zeta potential increase. *Journal of Colloid and Interface Science*, 43(3), 670-686. doi:[http://dx.doi.org/10.1016/0021-9797\(73\)90413-X](http://dx.doi.org/10.1016/0021-9797(73)90413-X)
9. Buscall, R., Mills, P. D. A., Goodwin, J. W., & Lawson, D. W. (1988). Scaling behaviour of the rheology of aggregate networks formed from colloidal particles. *Journal of the Chemical Society, Faraday Transactions 1: Physical Chemistry in Condensed Phases*, 84(12), 4249-4260.
10. Carman, P. S., & Cawiezel, K. (2007). Successful breaker optimization for polyacrylamide friction reducers used in slickwater fracturing. Paper presented at the SPE Hydraulic Fracturing Technology Conference.
11. Chang, C., Boger, D. V., & Nguyen, Q. D. (1998). The yielding of waxy crude oils. *Industrial & engineering chemistry research*, 37(4), 1551-1559.
12. Chenevert, M. E. (1970). Shale alteration by water adsorption. *Journal of petroleum technology*, 22(09), 1,141-141,148.
13. Cheng, C., Boger, D. V., & Nguyen, Q. D. (2000). Influence of thermal history on the waxy structure of statically cooled waxy crude oil. *SPE Journal*, 5(02), 148-157.
14. Clark, P., Pashin, J., Carlson, E., Goodliffe, A., McIntyre-Redden, M., Mann, S., & Thompson, M. (2012). Site Characterization for CO₂ Storage from Coal-fired Power Facilities in the Black Warrior Basin of Alabama. Retrieved from

15. da Silva, J. A. L., & Coutinho, J. A. P. (2004). Dynamic rheological analysis of the gelation behaviour of waxy crude oils. *Rheologica acta*, 43(5), 433-441.
16. Delgado, Á. V., González-Caballero, F., Hunter, R. J., Koopal, L. K., & Lyklema, J. (2007). Measurement and interpretation of electrokinetic phenomena. *Journal of colloid and interface science*, 309(2), 194-224.
17. Ewy, R. T., & Stankovich, R. J. (2002). Shale-fluid interactions measured under simulated downhole conditions. Paper presented at the SPE/ISRM Rock Mechanics Conference.
18. Findley, W. N., & Davis, F. A. (2013). Creep and relaxation of nonlinear viscoelastic materials: Courier Corporation.
19. Fink, J. (2015). *Water-Based Chemicals and Technology for Drilling, Completion, and Workover Fluids*: Gulf Professional Publishing.
20. Friedheim, J., Guo, Q., Young, S., & Gomez, S. (2011). Testing and evaluation techniques for drilling fluids-shale interaction and shale stability. Paper presented at the 45th US Rock Mechanics/Geomechanics Symposium.
21. Ghassemi, A., & Diek, A. (2003). Linear chemo-poroelasticity for swelling shales: theory and application. *Journal of Petroleum Science and Engineering*, 38(3), 199-212.
22. Gholizadeh-Doonechaly, N., Tahmasbi, K., & Davani, E. Development of High-Performance Water-Based Mud Formulation Based on Amine Derivatives.
23. Goh, R., Leong, Y.-K., & Lehane, B. (2011). Bentonite slurries—zeta potential, yield stress, adsorbed additive and time-dependent behaviour. *Rheologica acta*, 50(1), 29-38.

24. Gomez, S. L., & He, W. Fighting Wellbore Instability: Customizing Drilling Fluids Based on Laboratory Studies of Shale-Fluid Interactions.
25. Gomez, S. L., & He, W. (2012). Fighting wellbore instability: customizing drilling fluids based on laboratory studies of shale-fluid interactions. Paper presented at the IADC/SPE Asia Pacific Drilling Technology Conference and Exhibition.
26. Gupta, P., Elkins, C., Long, T. E., & Wilkes, G. L. (2005). Electrospinning of linear homopolymers of poly (methyl methacrylate): exploring relationships between fiber formation, viscosity, molecular weight and concentration in a good solvent. *Polymer*, 46(13), 4799-4810.
27. Guven, N., Panfil, D. J., & Carney, L. L. (1988). Comparative Rheology of Water-Based Drilling Fluids With Various Clays. Paper presented at the International Meeting on Petroleum Engineering.
28. Harris, P. C. (1988). Fracturing-fluid additives. *Journal of petroleum technology*, 40(10), 1,277-271,279.
29. He, W., Gomez, S. L., Leonard, R. S., & Li, D. T. (2014). Shale-fluid interactions and drilling fluid designs. Paper presented at the IPTC 2014: International Petroleum Technology Conference.
30. Heurtault, B., Saulnier, P., Pech, B., Proust, J.-E., & Benoit, J.-P. (2003). Physico-chemical stability of colloidal lipid particles. *Biomaterials*, 24(23), 4283-4300.
31. Himes, R. E., & Simon, D. E. (1990). Fluid additive and method for treatment of subterranean formations: Google Patents.

32. Horsrud, P., Bostrom, B., Sonstebo, E. F., & Holt, R. M. (1998). Interaction between shale and water-based drilling fluids: Laboratory exposure tests give new insight into mechanisms and field consequences of KCl contents. Paper presented at the SPE Annual Technical Conference and Exhibition.
33. Huang, H., Azar, J. J., & Hale, A. H. (1998). Numerical simulation and experimental studies of shale interaction with water-base drilling fluid. Paper presented at the IADC/SPE Asia Pacific Drilling Technology.
34. Hunter, R. J. (2013). Zeta potential in colloid science: principles and applications (Vol. 2): Academic press.
35. Jennings, D. W., & Weispfennig, K. (2005). Experimental solubility data of various n-alkane waxes: effects of alkane chain length, alkane odd versus even carbon number structures, and solvent chemistry on solubility. Fluid phase equilibria, 227(1), 27-35.
36. Jia, X., & Williams, R. A. (1990). Particle deposition at a charged solid/liquid interface. Chemical Engineering Communications, 91(1), 127-198.
37. Jiang, L., Gao, L., & Sun, J. (2003). Production of aqueous colloidal dispersions of carbon nanotubes. Journal of colloid and interface science, 260(1), 89-94.
38. Johnson, J. D., Schoppa, D., Garza, J. L., Zamora, F., Kakadjian, S., & Fitzgerald, E. (2010). Enhancing Gas and Oil Production With Zeta Potential Altering System. Paper presented at the SPE International Symposium and Exhibiton on Formation Damage Control.

39. Josh, M., Esteban, L., Delle Piane, C., Sarout, J., Dewhurst, D. N., & Clennell, M. B. (2012). Laboratory characterisation of shale properties. *Journal of Petroleum Science and Engineering*, 88, 107-124.
40. Kaya, A., Oren, A. H., & Yukselen, Y. (2003). Settling behavior and zeta potential of kaolinite in aqueous media. Paper presented at the The Thirteenth International Offshore and Polar Engineering Conference.
41. Khodja, M., Canselier, J. P., Bergaya, F., Fourar, K., Khodja, M., Cohaut, N., & Benmounah, A. (2010). Shale problems and water-based drilling fluid optimisation in the Hassi Messaoud Algerian oil field. *Applied Clay Science*, 49(4), 383-393.
42. Kriz, P., & Andersen, S. I. (2005). Effect of asphaltenes on crude oil wax crystallization. *Energy & Fuels*, 19(3), 948-953.
43. Kulshrestha, P., Giese, R. F., & Aga, D. S. (2004). Investigating the molecular interactions of oxytetracycline in clay and organic matter: insights on factors affecting its mobility in soil. *Environmental Science & Technology*, 38(15), 4097-4105.
44. Labenski, F., Reid, P., & Santos, H. (2003). Drilling fluids approaches for control of wellbore instability in fractured formations. Paper presented at the SPE/IADC Middle East Drilling Technology Conference and Exhibition.
45. Lal, M. Shale Stability: Drilling Fluid Interaction and Shale Strength.
46. Lal, M. (1999). Shale stability: drilling fluid interaction and shale strength. Paper presented at the SPE Asia Pacific Oil and Gas Conference and Exhibition.

47. Lane, R. H., & Aderibigbe, A. A. (2013). Rock/Fluid Chemistry Impacts on Shale Fracture Behavior. Paper presented at the SPE International Symposium on Oilfield Chemistry.
48. Lee, L., Patel, A. D., & Stamatakis, E. (2001). Glycol based drilling fluid: Google Patents.
49. Li, H., & Zhang, J. (2003). A generalized model for predicting non-Newtonian viscosity of waxy crudes as a function of temperature and precipitated wax☆. *Fuel*, 82(11), 1387-1397.
50. Lu, C.-F. (1988). A new technique for the evaluation of shale stability in the presence of polymeric drilling fluid. *SPE production engineering*, 3(03), 366-374.
51. Luckham, P. F., & Rossi, S. (1999). The colloidal and rheological properties of bentonite suspensions. *Advances in colloid and interface science*, 82(1), 43-92.
52. Magda, J. J., El-Gendy, H., Oh, K., Deo, M. D., Montesi, A., & Venkatesan, R. (2008). Time-Dependent Rheology of a Model Waxy Crude Oil with Relevance to Gelled Pipeline Restart†. *Energy & Fuels*, 23(3), 1311-1315.
53. Mahto, V., & Sharma, V. P. (2004). Rheological study of a water based oil well drilling fluid. *Journal of Petroleum Science and Engineering*, 45(1–2), 123-128.
doi:<http://dx.doi.org/10.1016/j.petrol.2004.03.008>
54. McBride, M. B. (1997). A critique of diffuse double layer models applied to colloid and surface chemistry. *Clays and Clay Minerals*, 45(4), 598-608.
55. Mendes, R., Vinay, G., Ovarlez, G., & Coussot, P. (2015). Modeling the rheological behavior of waxy crude oils as a function of flow and temperature history. *Journal of Rheology (1978-present)*, 59(3), 703-732.

56. Menon, V. B., & Wasan, D. T. (1987a). Adsorption of maltenes on sodium montmorillonite. *Colloids and Surfaces*, 25(2–4), 387-392. doi:[http://dx.doi.org/10.1016/0166-6622\(87\)80316-5](http://dx.doi.org/10.1016/0166-6622(87)80316-5)
57. Menon, V. B., & Wasan, D. T. (1987b). Particle—fluid interactions with applications to solid-stabilized emulsions Part III. Asphaltene adsorption in the presence of quinaldine and 1,2-dimethylindole. *Colloids and Surfaces*, 23(4), 353-362. doi:[http://dx.doi.org/10.1016/0166-6622\(87\)80276-7](http://dx.doi.org/10.1016/0166-6622(87)80276-7)
58. Mody, F. K., & Hale, A. H. (1993). Borehole-stability model to couple the mechanics and chemistry of drilling-fluid/shale interactions. *Journal of petroleum technology*, 45(11), 1,093-091,101.
59. Mody, F. K., Tare, U. A., Tan, C. P., Drummond, C. J., & Wu, B. (2002). Development of novel membrane efficient water-based drilling fluids through fundamental understanding of osmotic membrane generation in shales. Paper presented at the SPE Annual Technical Conference and Exhibition.
60. Mueller, S., Llewelin, E. W., & Mader, H. M. (2010). The rheology of suspensions of solid particles. *Proceedings: Mathematical, Physical and Engineering Sciences*, 466(2116), 1201-1228. doi:10.1098/rspa.2009.0445
61. Muniz, E. S., Fontoura, S. A. B., & Lomba, R. F. T. (2005). Rock-drilling fluid interaction studies on the diffusion cell. Paper presented at the SPE Latin American and Caribbean Petroleum Engineering Conference.
62. Nguyen, Q. D., & Boger, D. V. (1992). Measuring the flow properties of yield stress fluids. *Annual Review of Fluid Mechanics*, 24(1), 47-88.

63. Okoro, E. E., & Adewale, D. (2014). EXPERIMENTAL ANALYSIS OF SHALE FOR 3 EVALUATING SHALE DRILLING FLUID 4 INTERACTION IN AGBADA FORMATION 5. *British Journal of Applied Science & Technology*, 4(35), 4878.
64. Patel, A. D. (2009). Design and development of quaternary amine compounds: shale inhibition with improved environmental profile. Paper presented at the SPE International Symposium on Oilfield Chemistry.
65. Patel, A. D., Stamatakis, E., & Davis, E. (2001). Shale hydration inhibition agent and method of use: Google Patents.
66. Petersen, P. B., & Saykally, R. J. (2008). Is the liquid water surface basic or acidic? Macroscopic vs. molecular-scale investigations. *Chemical Physics Letters*, 458(4), 255-261.
67. Power, D. J., Rodd, A. B., Paterson, L., & Boger, D. V. (1998). Gel transition studies on nonideal polymer networks using small amplitude oscillatory rheometry. *Journal of Rheology (1978-present)*, 42(5), 1021-1037.
68. Rabe, C., da Fontoura, S. A. B., & dos Santos Antunes, F. (2002). Experimental study of interaction shale-fluid through immersion tests. *Revista de Engenharia Térmica*, 1(2).
69. Raman, A. K. Y., Koteeswaran, S., Venkataramani, D., Clark, P., Bhagwat, S., & Aichele, C. P. (2016). A comparison of the rheological behavior of hydrate forming emulsions stabilized using either solid particles or a surfactant. *Fuel*, 179, 141-149.

70. Rao, M. A. (2014). Flow and functional models for rheological properties of fluid foods Rheology of Fluid, Semisolid, and Solid Foods (pp. 27-61): Springer.
71. Rickman, R., Mullen, M. J., Petre, J. E., Grieser, W. V., & Kundert, D. (2008). A practical use of shale petrophysics for stimulation design optimization: All shale plays are not clones of the Barnett Shale. Paper presented at the SPE Annual Technical Conference and Exhibition.
72. Roenningsen, H. P., Bjoerndal, B., Baltzer Hansen, A., & Batsberg Pedersen, W. (1991). Wax precipitation from North Sea crude oils: 1. Crystallization and dissolution temperatures, and Newtonian and non-Newtonian flow properties. *Energy & Fuels*, 5(6), 895-908.
73. Rønningesen, H. P. (1992). Rheological behaviour of gelled, waxy North Sea crude oils. *Journal of Petroleum Science and Engineering*, 7(3), 177-213.
74. Santos, H., Diek, A., Da Fontoura, S., & Roegiers, J. C. (1997). Shale Reactivity test: a novel approach to evaluate shale-fluid interaction. *International Journal of Rock Mechanics and Mining Sciences*, 34(3), 268. e261-268. e211.
75. Singh, P., Fogler, H. S., & Nagarajan, N. (1999). Prediction of the wax content of the incipient wax-oil gel in a pipeline: An application of the controlled-stress rheometer. *Journal of Rheology*, 43(6), 1437-1459.
76. Singh, P., Youyen, A., & Fogler, H. S. (2001). Existence of a critical carbon number in the aging of a wax-oil gel. *AIChE journal*, 47(9), 2111-2124.
77. Steiger, R. P. (1993). Advanced triaxial swelling tests on preserved shale cores. Paper presented at the International journal of rock mechanics and mining sciences & geomechanics abstracts.

78. Street, N., & Wang, F. D. (1966). Surface potentials and rock strength. Paper presented at the 1st ISRM Congress.
79. Tan, C. P., Richards, B. G., & Rahman, S. S. (1996). Managing physico-chemical wellbore instability in shales with the chemical potential mechanism. Paper presented at the SPE asia pacific Oil and Gas Conference.
80. Van Olphen, H. (1977). Introduction to clay colloid chemistry: Wiley.
81. Van Oort, E. (1994). A novel technique for the investigation of drilling fluid induced borehole instability in shales. Paper presented at the Rock Mechanics in Petroleum Engineering.
82. Van Oort, E. (2003). On the physical and chemical stability of shales. *Journal of Petroleum Science and Engineering*, 38(3), 213-235.
83. Van Oort, E., Hale, A. H., & Mody, F. K. (1995). Manipulation of coupled osmotic flows for stabilisation of shales exposed to water-based drilling fluids. Paper presented at the SPE Annual Technical Conference and Exhibition.
84. van Oort, E., Hale, A. H., Mody, F. K., & Roy, S. (1996). Transport in shales and the design of improved water-based shale drilling fluids. *SPE drilling & completion*, 11(03), 137-146.
85. Van Oss, C. J., Giese, R. F., & Costanzo, P. M. (1990). DLVO and non-DLVO interactions in hectorite. *Clays Clay Miner*, 38(2), 151-159.
86. Vane, L. M., & Zang, G. M. (1997). Effect of aqueous phase properties on clay particle zeta potential and electro-osmotic permeability: Implications for electro-kinetic soil remediation processes. *Journal of Hazardous Materials*, 55(1-3), 1-22.
doi:[http://dx.doi.org/10.1016/S0304-3894\(97\)00010-1](http://dx.doi.org/10.1016/S0304-3894(97)00010-1)

87. Visintin, R. F. G., Lapasin, R., Vignati, E., D'Antona, P., & Lockhart, T. P. (2005). Rheological behavior and structural interpretation of waxy crude oil gels. *Langmuir*, 21(14), 6240-6249.
88. Vos, B., & Van den Haak, K. (1980). Wax interaction modifiers for waxy crude oils.
89. Wardhaugh, L. T., Boger, D. V., & Tonner, S. P. (1988). Rheology of waxy crude oils. Paper presented at the International Meeting on Petroleum Engineering.
90. Webber, R. M. (1999). Low temperature rheology of lubricating mineral oils: effects of cooling rate and wax crystallization on flow properties of base oils. *Journal of Rheology (1978-present)*, 43(4), 911-931.
91. Werner, C., Zimmermann, R., & Kratzmüller, T. (2001). Streaming potential and streaming current measurements at planar solid/liquid interfaces for simultaneous determination of zeta potential and surface conductivity. *Colloids and Surfaces A: Physicochemical and Engineering Aspects*, 192(1), 205-213.
92. Yalçın, T., Alemdar, A., Ece, Ö. I., & Güngör, N. (2002). The viscosity and zeta potential of bentonite dispersions in presence of anionic surfactants. *Materials Letters*, 57(2), 420-424. doi:[http://dx.doi.org/10.1016/S0167-577X\(02\)00803-0](http://dx.doi.org/10.1016/S0167-577X(02)00803-0)
93. Yoshimura, A. S., Prud'homme, R. K., Princen, H. M., & Kiss, A. D. (1987). A comparison of techniques for measuring yield stresses. *Journal of Rheology (1978-present)*, 31(8), 699-710.
94. Yu, M., Chenevert, M. E., & Sharma, M. M. (2003). Chemical–mechanical wellbore instability model for shales: accounting for solute diffusion. *Journal of Petroleum Science and Engineering*, 38(3), 131-143.

95. Zhang, J., Al-Bazali, T. M., Chenevert, M. E., & Sharma, M. M. Factors Controlling the Membrane Efficiency of Shales When Interacting with Water-Based and Oil-Based Muds. doi:10.2118/100735-PA
96. Zhang, J., Chenevert, M. E., Al-Bazali, T., & Sharma, M. M. (2004). A new gravimetric-swelling test for evaluating water and ion uptake in shales. Paper presented at the SPE Annual Technical Conference and Exhibition.
97. Zheng, S., Zhang, F., Huang, Z., & Fogler, H. S. (2013). Effects of operating conditions on wax deposit carbon number distribution: Theory and experiment. *Energy & Fuels*, 27(12), 7379-7388.
98. Zhong, H., Qiu, Z., Huang, W., & Cao, J. (2011). Shale inhibitive properties of polyether diamine in water-based drilling fluid. *Journal of Petroleum Science and Engineering*, 78(2), 510-515. doi:<http://dx.doi.org/10.1016/j.petrol.2011.06.003>
99. Zhou, J., Jung, C. M., Pedlow, J. W., Chenevert, M. E., & Sharma, M. M. (2013). A New Standardized Laboratory Protocol to Study the Interaction of Organic-Rich Shales with Drilling and Fracturing Fluids. Paper presented at the SPE Annual Technical Conference and Exhibition.
100. Zhou, J., Sun, H., Stevens, R. F., Qu, Q., & Bai, B. (2011). Bridging the gap between laboratory characterization and field applications of friction reducers. Paper presented at the SPE Production and Operations Symposium.

VITA

SAMYUKTA KOTEESWARAN

Candidate for the degree of

Doctor of Philosophy

Thesis: RHEOLOGICAL CHARACTERIZATION OF CHARGED POLYACRYLAMIDES USED IN FRACTURING FLUIDS WITH EMPHASIS ON SHALE – POLYACRYLAMIDE INTERACTION

Major Field: Chemical Engineering

Biographical:

Education

1. Doctor of Philosophy in Chemical Engineering, at Oklahoma State University, Stillwater, Oklahoma, USA in May, 2017.
2. Bachelor of Technology in Chemical Engineering, at Anna University, Chennai, India in May, 2012.

Experience:

1. Graduate Teaching Assistant – Rate Operations (Separations), School of Chemical Engineering, Oklahoma State University, Stillwater, OK, USA
January 2017 – Present
2. Graduate Teaching Assistant - Transport Phenomena, School of Chemical Engineering, Oklahoma State University, Stillwater, OK, USA August 2016 – December 2016
3. Graduate Teaching Assistant – Unit Operations Laboratory, School of Chemical Engineering, Oklahoma State University, Stillwater, OK, USA
January 2016 – May 2016

Professional Memberships

1. Society of Petroleum Engineers
2. International Society of Automation
3. American Institute of Chemical Engineers